AD_____

Award Number: DAMD17-98-1-8223

TITLE: Developing Strategies to Block Beta-Catenin Action in Signaling and Cell Adhesion during Carcinogenesis

PRINCIPAL INVESTIGATOR: Mark A. Peifer, Ph.D.

CONTRACTING ORGANIZATION: University of North Carolina
Chapel Hill, North Carolina 27599-1350

REPORT DATE: July 2000

TYPE OF REPORT: Annual

PREPARED FOR: U.S. Army Medical Research and Materiel Command
Fort Detrick, Maryland 21702-5012

REPORT DOCUMENTATION PAGE

Form Approved
OMB No. 074-0188

1. AGENCY USE ONLY (Leave blank)	2. REPORT DATE	3. REPORT TYPE AND DATES COVERED
	July 2000	Annual (1 Jul 99 - 30 Jun 00)

4. TITLE AND SUBTITLE
Developing Strategies to Block Beta-Catenin Action in Signaling and Cell Adhesion during Carcinogenesis

5. FUNDING NUMBERS
DAMD17-98-1-8223

6. AUTHOR(S)
Mark A. Peifer, Ph.D.

7. PERFORMING ORGANIZATION NAME(S) AND ADDRESS(ES)
University of North Carolina
Chapel Hill, North Carolina 27599-1350

E-MAIL:
peifer@unc.edu

8. PERFORMING ORGANIZATION REPORT NUMBER

9. SPONSORING / MONITORING AGENCY NAME(S) AND ADDRESS(ES)
U.S. Army Medical Research and Materiel Command
Fort Detrick, Maryland 21702-5012

10. SPONSORING / MONITORING AGENCY REPORT NUMBER

11. SUPPLEMENTARY NOTES
This report contains colored photographs

12a. DISTRIBUTION / AVAILABILITY STATEMENT
Approved for public release; distribution unlimited

12b. DISTRIBUTION CODE

13. ABSTRACT *(Maximum 200 Words)*

To understand cancer, we must first understand normal cell behavior. *Drosophila* Armadillo (Arm) and its human homolog ß-catenin are key players in adhesive junctions and in transduction of Wingless (Wg)/Wnt signals. Our working hypotheses are: 1) Several protein partners compete to bind Arm, and 2) Arm:dTCF activates Wg-responsive genes, while dTCF alone represses the same genes. Aim 1 is to understand how different partners compete with one another for binding Arm. Aim 2 focuses on how Arm and dTCF positively and negatively regulate Wg-responsive genes. In the past year we made significant progress. Aim 1. We used the two-hybrid system to further define the Arm binding site on DE-cadherin and extended our analysis of the effect of point mutations on binding. Our collaborators at the Weizmann Institute nearly completed a parallel analysis in mammalian cells, assessing the ability of cadherin-derived peptides to compete ß-catenin from its endogenous partners. Aim 2. Our analysis of the role of Arm's C-terminus was published in Genetics. We extended our study of Wg-responsive genes by examining the role of the chromatin remodeling protein Brahma: human Brahma was identified as a two-hybrid interactor with ß-catenin. Our preliminary data suggest that Brahma and Osa repress Wg-target genes.

14. SUBJECT TERMS	15. NUMBER OF PAGES
Breast Cancer	47
	16. PRICE CODE

17. SECURITY CLASSIFICATION OF REPORT	18. SECURITY CLASSIFICATION OF THIS PAGE	19. SECURITY CLASSIFICATION OF ABSTRACT	20. LIMITATION OF ABSTRACT
Unclassified	Unclassified	Unclassified	Unlimited

FOREWORD

Opinions, interpretations, conclusions and recommendations are those of the author and are not necessarily endorsed by the U.S. Army.

___ Where copyrighted material is quoted, permission has been obtained to use such material.

___ Where material from documents designated for limited distribution is quoted, permission has been obtained to use the material.

___ Citations of commercial organizations and trade names in this report do not constitute an official Department of Army endorsement or approval of the products or services of these organizations.

N/A In conducting research using animals, the investigator(s) adhered to the "Guide for the Care and Use of Laboratory Animals," prepared by the Committee on Care and use of Laboratory Animals of the Institute of Laboratory Resources, national Research Council (NIH Publication No. 86-23, Revised 1985).

X For the protection of human subjects, the investigator(s) adhered to policies of applicable Federal Law 45 CFR 46.

N/A In conducting research utilizing recombinant DNA technology, the investigator(s) adhered to current guidelines promulgated by the National Institutes of Health.

N/A In the conduct of research utilizing recombinant DNA, the investigator(s) adhered to the NIH Guidelines for Research Involving Recombinant DNA Molecules.

N/A In the conduct of research involving hazardous organisms, the investigator(s) adhered to the CDC-NIH Guide for Biosafety in Microbiological and Biomedical Laboratories.

7/10/00

PI - Signature Date

Table of Contents

(5) Introduction:

To understand abnormal cell behavior in cancer, we must first understand normal cell behavior. We focus on *Drosophila* Armadillo (Arm); Arm and its human homolog ß-catenin are critical for normal embryonic development (reviewed in (1). Both are key players in two separable biological processes: 1) They are components of cell-cell adhesive junctions, and 2) they act in transduction of Wingless/Wnt (Wg/Wnt) family cell-cell signals. Mutations in ß-catenin or its regulators are early steps in colon cancer and melanoma (reviewed in (2). We use the fruit fly as our model, combining classical and molecular genetics with cell biology and biochemistry. We take advantage of the speed and ease of the fly system and of its synergy with vertebrate cell biology. As one avenue to reveal Arm's roles in adherens junctions and transduction of Wg signal, we are identifying and examining the function of proteins with which Arm physically and/or functionally interacts. Our goal is to precisely define Arm/ß-catenin's dual roles, ultimately allowing the design of drugs inhibiting oncogenic ß-catenin. Our working hypotheses are: 1) Several protein partners compete to bind to the same site on Arm; the affinity of Arm for different partners is adjusted via phosphorylation of these partners, and 2) The Arm:dTCF complex activates Wg-responsive genes; dTCF represses the same genes in the absence of Arm. We will integrate approaches at all levels from combinatorial chemistry to studying gene function in intact animals, using fruit flies to carry out a functional genomics approach to understanding Arm function, and then transferring this knowledge directly to the mammalian system. Our first Aim is to understand how different partners interact with and compete with one another for binding Arm, and how phosphorylation regulates this. Our second Aim focuses on how the Arm and its partner dTCF positively and negatively regulate Wg responsive genes.

Specific Aim 1. Identify the sequence determinants mediating the binding of Armadillo/ß-catenin's protein partners to Armadillo/ß-catenin.

Specific Aim 2. Explore the mechanism of action of dTCF, a Wg/Wnt effector.

We have made significant progress on both of these Specific Aims, which we have outlined below.

(6) Body:

Aim 1.

Our statement of work stated:

Year 1

1. Minimize interacting regions of all three partners and begin mutagenesis.
2. Carry out two-hybrid screen for random peptides that interact with Arm.
3. Mutagenize & test in two-hybrid system potential phosphorylation sites.

Year 2

1. Complete mutational analysis of Arm targets in two hybrid system and test peptides in vivo.
2. Mutate potential phosphorylation sites in peptide models and test effects of GSK.

We previously found that dAPC, DE-cadherin , and dTCF all can bind to a ~260 amino acid fragment comprising Arm's Arm repeats 3-8 (3) (4). In our earlier work under this grant, we had defined a 30 amino acid region of the DE-cadherin cytoplasmic tail that was sufficient for binding to Arm (using the yeast two-hybrid system as an assay).. We have extended these findings, in pursuit of task 1 in the statement of work. We now have found that a 22 amino acid region of the cadherin tail can mediate binding (Fig. 1). We further extended these observations by beginning to examine the sequence requirements for Arm binding, beginning our examination by focusing on the DE-cadherin target. We based these experiments on both the enrichment of acidic amino acids in all of the targets of Arm, and on a slight but intriguing sequence similarity between Arm's partners. In particular, the motif SLSSL is conserved in APC and cadherin. This is of special interest because vertebrate E-cadherin and APC are phosphorylated in this region, most likely on these serines. In APC, phosphorylation of these serines by GSK-3 enhances ß-catenin binding (5). In E-cadherin, serines in the region are phosphorylated by an unknown kinase; mutation of the serines to alanine blocks ß-catenin binding (6) . We thus made an extensive series of site-directed mutations of conserved residues (focusing in particular on acidic amino acids and on serines) within the minimal Arm binding region, including a small deletion and clustered point mutations, as outlined in parts one and three of the statement of work (Fig. 2A). To our surprise, many of these mutations do not block binding to Arm when tested in the context of the full length cadherin tail (Fig. 2B,C). This suggests that multiple points of contact may underlie binding and that changes in individual contact sites may not be sufficient to block the interaction. However, the more extensive changes do abolish binding, and some of the lesser changes reduce binding detectably, beginning to reveal key

residues.

To supplement this work using the yeast two-hybrid system, we are carrying out a collaboration with Avri Ben'Zeev of the Weizmann Institute in Israel. Using a series of assays which they have developed for examining the ability of the E-cadherin cytoplasmic tail to block ß-catenin action (7), they have nearly completed testing our wild-type and mutant DE-cadherin constructs for their ability to bind to ß-catenin in mammalian cells, when expressed as GFP-fusion proteins. They are examining the localization of these fusion proteins, as well as their ability to block destruction of endogenous ß-catenin or to block activation by the ß-catenin LEF complex. We are currently preparing a manuscript describing this work. We have not yet begun the work outlined in part two of the statement of work, as the work on the other sections has gone well and we have chosen to focus our effort on these sections.

Aim 2. Armadillo:dTCF, a bipartite transcription factor

We made significant progress in our work on the role of Arm and dTCF in regulating Wg/Wnt responsive genes. We explored in more detail the role of Arm's C-terminus in Wg signaling (Part 1 of the Statement of Work above). We found that C-terminally truncated mutant Armadillo has a deficit in Wg signaling activity, even when corrected for reduced protein levels. However, we also found that Armadillo proteins lacking all or part of the C-terminus retain some signaling ability if overexpressed, and that mutants lacking different portions of the C-terminal domain differ in their level of signaling ability. Finally, we found that the C-terminus plays a role in Armadillo protein stability in response to Wingless signal, and that the C-terminal domain can physically interact with the Arm repeat region. These data suggest that the C-terminal domain plays a complex role in Wingless signaling, and that Armadillo recruits the transcriptional machinery via multiple contact sites, which act in an additive fashion. These data were published in Genetics, with partial support from our Army grant ((8); reprints are included).

We extended our work on the role of Arm and TCF in transcriptional regulation by looking at a novel partner which may act as a repressor of Wg-responsive genes (part 2 of the Statement of Work above). This partner, the chromatin remodeling protein Brahma (9), was initially identified by our collaborators in the Clevers lab in a two-hybrid screen for interactors with human ß-catenin. We have examined whether Brahma plays a role in Wg signaling in vivo. We have found that while zygotic mutations in *brahma* alone do not affect the cuticular pattern, animals doubly heterozygous for both *brahma* and *osa* (which encodes a putative partner of Brahma in the SWI/SNF complex) exhibit a phenotype consistent with an activation of Wg signaling. We are currently extending this analysis to determine whether this is the case and to characterize this role in more detail.

Career Development Award

The Career Development Award component of this grant pays a substantial portion of my salary (i.e., the PI, Mark Peifer). This has substantially reduced the amount of time I have to devote to teaching and service, and has thus allowed me to focus on research, both that funded by the Army and other research ongoing in my lab. I have thus acknowledged this support in several additional publications produced during this period, which are listed in Section 8, and included reprints (where available) in the Appendix.

(7) Key research accomplishments.

a) A 22 amino acid piece of DE-cadherin is sufficient for Armadillo binding in the yeast two-hybrid system.
b) Clusters of 3-4 point mutations in conserved sequence motifs in DE-cadherin do not block Armadillo binding in the two hyrbid system, while a subset of more extensive amino acid substitutions in this region do so.
c) The minimal cadherin peptides can compete for interaction with ß-catenin, displacing its endogenous partners.
d) The effect of mutations in the core binding region parallels that assessed in yeast, with a few exceptions.
e) Binding to TCF/LEF is more easily competed than that to cadherin or APC/Axin.
f) Armadillo's C-terminus plays multiple roles in Armadillo function.

(8) Reportable outcomes.

Publications supported in part by the IDEA grant:

Cox, R.T., Pai,L.-M., Kirkpatrick, C., Stein,J., and Peifer, M. (1999). Roles of the C-terminus of Armadillo in Wingless signaling in *Drosophila* . Genetics 153, 319-332 (copy included in appendix).

Publications acknowledging partial salary support for Mark Peifer via the CDA:

McEwen, D.G., Cox, R.T., and Peifer, M. (2000). The canonical Wg and JNK signaling cascades collaborate to promote both dorsal closure and ventral patterning. Development 127, in press (reprint not yet available).

Cox, R.T., McEwen, D.G., Myster, D.G., Duronio, R.J., Loureiro, J., and Peifer, M. (2000). A screen for mutations that suppress the phenotype of *Drosophila armadillo*, the ß-catenin homolog. Genetics 155, in press (reprint not yet available).

Peifer, M., and Polakis, P. (2000). Wnt signaling in oncogenesis and embryogenesis: A look outside the nucleus. Science 287, 1606-1609 (copy included in the appendix).

McCartney, B., Dierick, H.A., Kirkpatrick, C., Moline, M.M., Baas, A., Peifer, M., and Bejsovec, A. (1999). *Drosophila* APC2 is a cytoskeletally-associated protein that regulates Wingless signaling in the embryonic epidermis. J. Cell Biol. 146, 1303-1318 (copy included in the Appendix).

Presentations by Mark Peifer discussing this work.

"Cell adhesion, signal transduction and cancer: the Armadillo Connection.", Biological Structure and Gene Expression Gordon Conference, Meriden NH August, 1999.

"Cell adhesion, signal transduction and cancer: the Armadillo Connection.", Batsheva Conference on "The dialogue between Cell Adhesion, Protein Degradation, and Transcriptional Regulation in Cancer", Weizmann Institute, Rehovot ISRAEL, November, 1999.

"Cell adhesion, signal transduction and cancer: the Armadillo Connection.", Keynote address at Keystone Conference on Intercellular Junctions, Keystone CO, February 2000.

"Cell adhesion, signal transduction and cancer: the Armadillo Connection.", at "Cell Communication", the Annual CMB Symposium, Duke University, Durham NC, March 2000.

"A Drosophila model system for examining ß-catenin function in cell adhesion and transcriptional activation.", Era of Hope, the DOD Breast Cancer Research Program Meeting, Atlanta GA June, 2000.

"Cell adhesion, signal transduction, and cancer: the Armadillo Connection." Cancer Genetics Group, Lineberger Comprehensive Cancer Center, University of North Carolina-Chapel Hill NC, July 1999.

"Cell adhesion, signal transduction, and cancer: the Armadillo Connection." Department of Genetics, Cell and Developmental Biology, University of Minnesota, Minneapolis MN, August 1999.

"Cell adhesion, signal transduction, and cancer: the Armadillo Connection." First Annual Novartis-UNC Biology Joint Retreat, University of North Carolina, Chapel Hill NC, August 1999.

"Cell adhesion, signal transduction, and cancer: the Armadillo Connection." Dept. of Biological Chemistry, Johns Hopkins University, Baltimore MD, September, 1999.

"Cell adhesion, signal transduction, and cancer: the Armadillo Connection." Dept. of Genetics, University of Georgia, Athens GA, October, 1999.

"Cell adhesion, signal transduction, and cancer: the Armadillo Connection." Institute Of Molecular Biology, University of Oregon, Eugene OR, January, 2000

"Cell adhesion, signal transduction, and cancer: the Armadillo Connection." Sphinx Pharmaceuticals/Eli Lilly, Research Triangle Park, NC, May 2000.

"Cell adhesion, signal transduction, and cancer: the Armadillo Connection." Division of Clinical Sciences Seminar Series, National Cancer Institute/NIH, Bethesda MD May 2000.

(9) Conclusions.

We have made significant progress on each of the specific aims. We have focused in on the binding site for Arm on DE-cadherin, identifying a very small region that is sufficient for binding in the yeast two-hybrid system and identifying within that region the key amino acids required for biding. We have nearly completed an analysis of binding of wild-type and mutant peptides in mammalian cells, in collaboration with our colleagues at the Weizmann Institute. We are currently writing up this work for publication. These data should provide a basis for understanding the interaction between the protein product of the oncogene ß-catenin and its mammalian partners in both normal development and physiology, and during oncogenesis.

Our work on the roles of Arm's C-terminus in Wg signaling resulted in a publication in Genetics (included in the Appendix). We have also initiated work on Brahma, which our collaborators identified as a two-hybrid interactor with ß-catenin. Our preliminary data suggest that the Brahma-Osa chromatin remodeling complex may act in repression. Understanding the mechanism by which Wnt target genes are repressed will provide insight into the normal and abnormal regulation of the genes responsible for oncogenesis in tumors resulting from activation of the Wnt pathway.

(10) References.

1. M. Peifer, *Science* **275**, 1752-1753 (1997).
2. M. Peifer, P. Polakis, *Science* **287**, 1606-1609 (2000).
3. L.-M. Pai *et al.*, *Journal of Biological Chemistry* **271**, 32411-32420 (1996); M. van de Wetering *et al.*, *Cell* **88**, 789-799 (1997).
4. B. M. McCartney *et al.*, *Journal of Cell Biology* **146**, 1303-1318 (1999).
5. B. Rubinfeld *et al.*, *Science* **272**, 1023-1026 (1996).
6. J. Stappert, R. Kemler, *Cell Adhesion and Communication* **2**, 319-327 (1994).
7. E. Sadot, I. Simcha, M. Shtutman, A. Ben-Ze'ev, B. Geiger, *Proc Natl Acad Sci U S A* **95**, 15339-44 (1998).
8. R. T. Cox, L.-M. Pai, C. Kirkpatrick, J. Stein, M. Peifer, *Genetics* **153**, 319-332 (1999).
9. J. W. Tamkun, *Curr Opin Genet Dev* **5**, 473-7 (1995).

Appendix I-- Figures

Figure 1. Minimal binding site on DE-cadherin for Armadillo

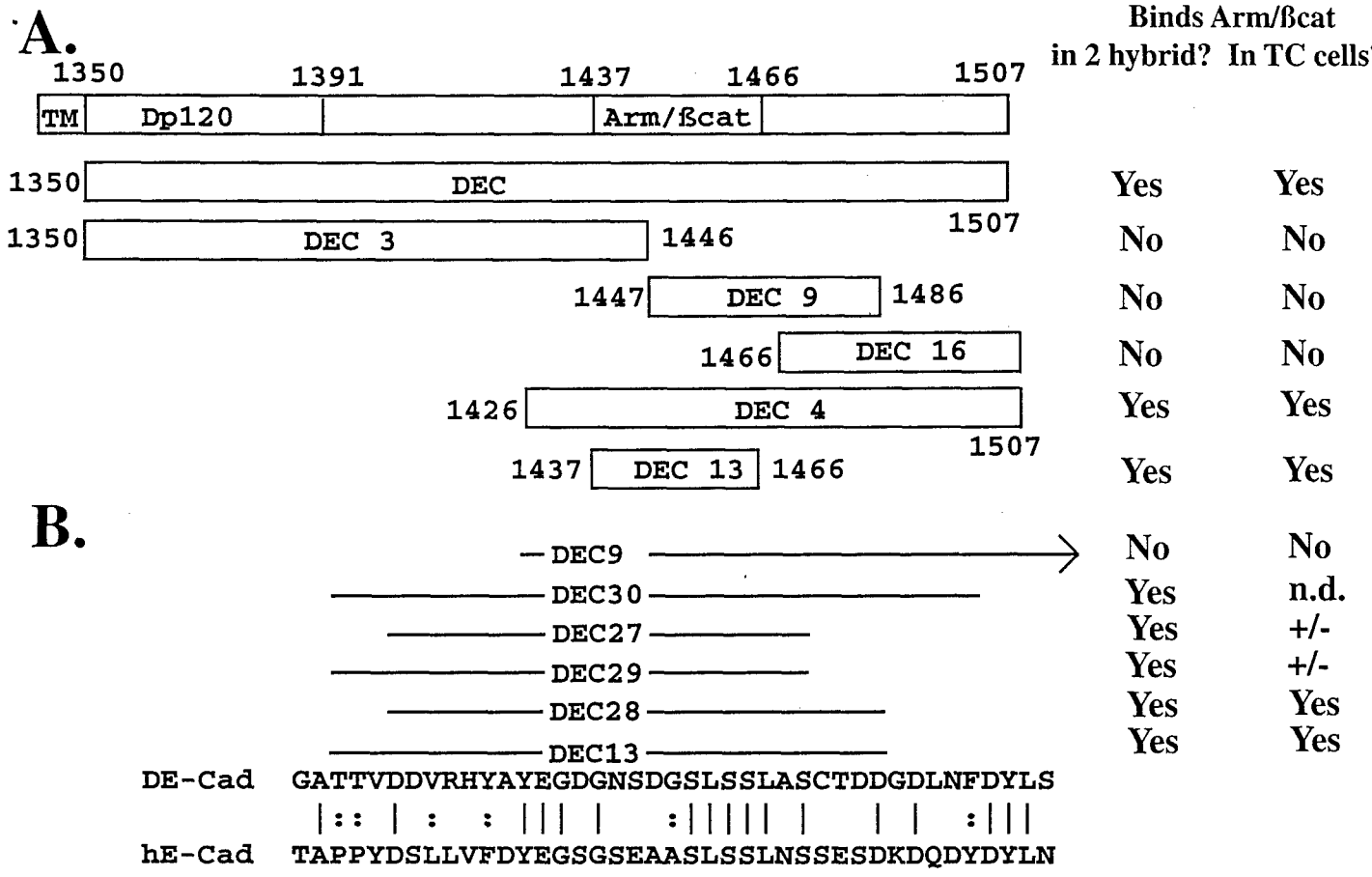

Figure 2. **Defining the Arm binding site on DE-cadherin.** A. Diagram of mutations induced in DE-cadherin. All were tested in the context of the full length cytoplasmic tail of DE-cadherin. B. Interactions with the full Arm repeat regions of Armadillo (armR1-13) and of murine beta-catenin (MbcatR1-13). The Y-axis indicates the construct tested. pCK4, the empty vector, is the negative control, and pCK4-DEC, the full length DE-cadherin tail, is the positive control. The X axis indicates the results of ß-galactosidase assays, in units. C. Similar tests of interactions with the central Arm repeats of Armadillo (armR2-ins) and of murine beta-catenin (MbcatR2-ins).

A.

```
M3                                        AA A
M9                          E EE   E
M1                          A AA   A
M2                  AAA A
DE-Cad   DDVRHYAYEGDGNSDGSLSSLASCTDD
hE-Cad   DSLLVFDYEGSGSEAASLSSLNSSESD
M7                  AAA A     A AA   A
M8                          A   A AA   A A
M10 deletion   (--------------------)
```

B.

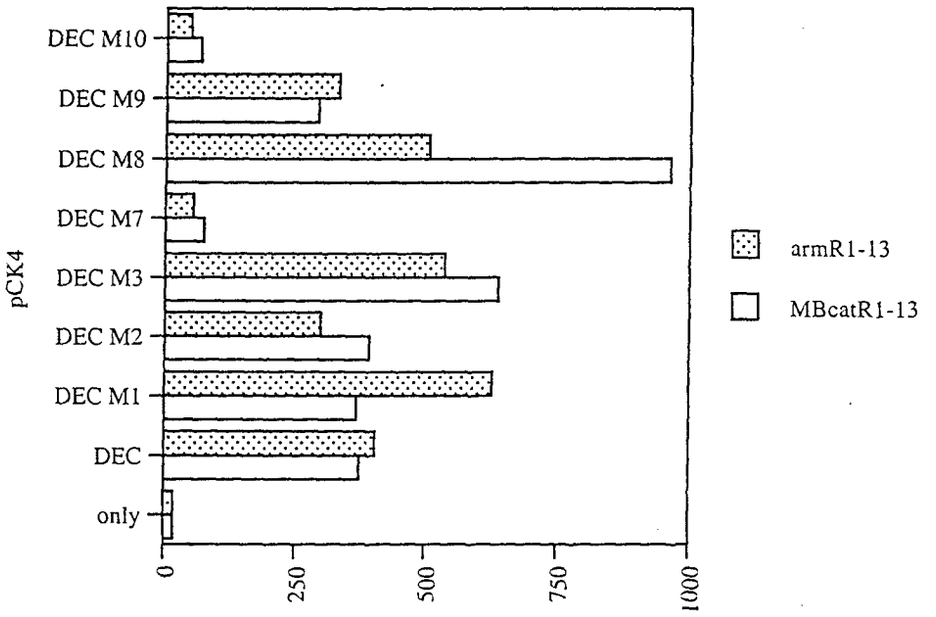
DEC M10
DEC M9
DEC M8
DEC M7
DEC M3
DEC M2
DEC M1
DEC
only
pCK4
0
250
500
750
1000
armR1-13
MBcatR1-13

C.

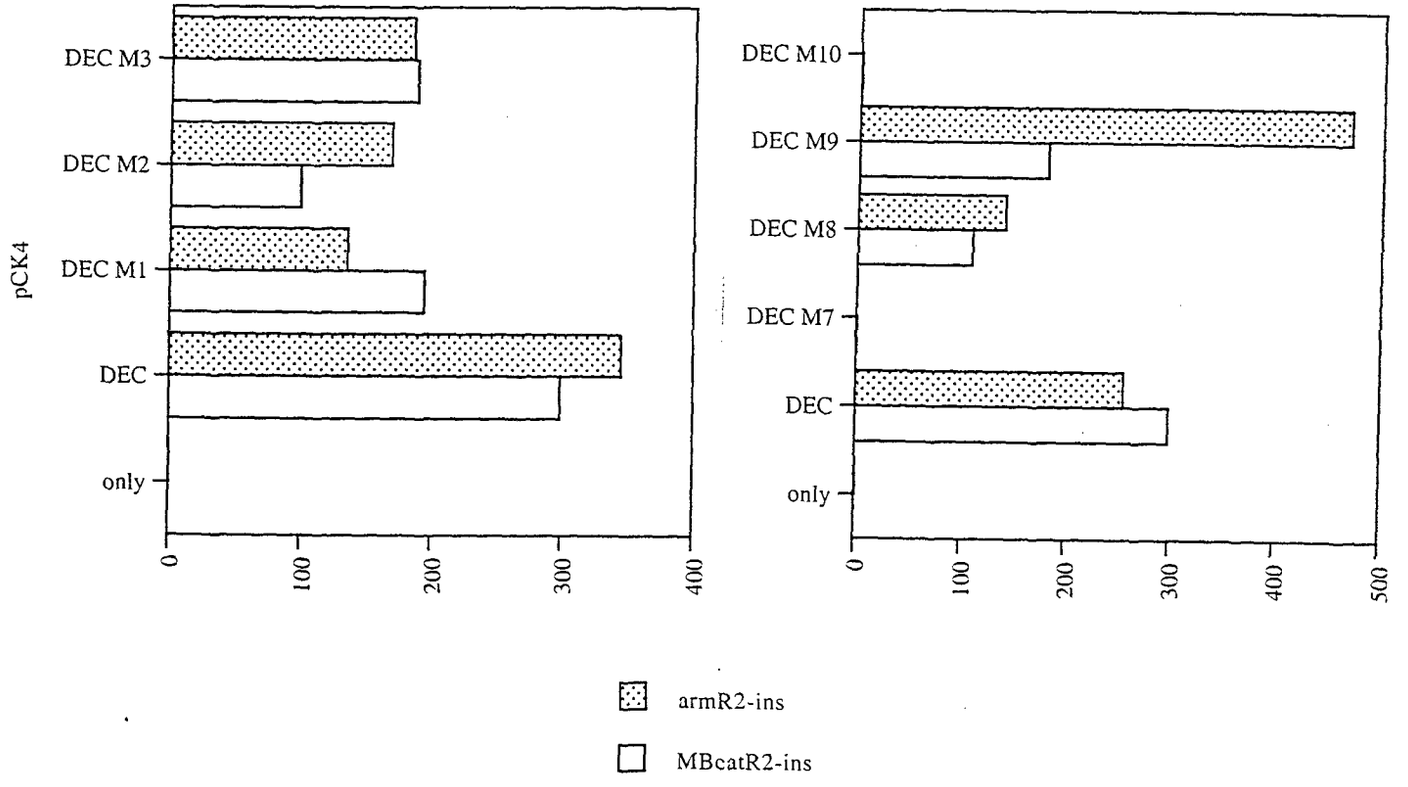
DEC M3
DEC M2
DEC M1
DEC
only
pCK4
0
100
200
300
400
DEC M10
DEC M9
DEC M8
DEC M7
DEC
only
0
100
200
300
400
500
armR2-ins
MBcatR2-ins

Appendix II—Reprints of publications supported in part by this grant

Publications supported in part by the IDEA grant:

Cox, R.T., Pai,L.-M., Kirkpatrick, C., Stein,J., and Peifer, M. (1999). Roles of the C-terminus of Armadillo in Wingless signaling in *Drosophila* . Genetics 153, 319-332

Publications acknowledging partial salary support for Mark Peifer via the CDA:

Peifer, M., and Polakis, P. (2000). Wnt signaling in oncogenesis and embryogenesis: A look outside the nucleus. Science 287, 1606-1609 (copy included in the appendix).

McCartney, B., Dierick, H.A., Kirkpatrick, C., Moline, M.M., Baas, A., Peifer, M., and Bejsovec, A. (1999). *Drosophila* APC2 is a cytoskeletally-associated protein that regulates Wingless signaling in the embryonic epidermis. J. Cell Biol. 146, 1303-1318

Roles of the C Terminus of Armadillo in Wingless Signaling in Drosophila

Rachel T. Cox,[†,1] Li-Mei Pai,[*,1] Catherine Kirkpatrick,[*] Joel Stein[*] and Mark Peifer[*,†]

[*]Department of Biology and [†]Curriculum in Genetics and Molecular Biology, University of North Carolina, Chapel Hill, North Carolina 27599-3280

Manuscript received April 6, 1999
Accepted for publication May 24, 1999

ABSTRACT

Drosophila melanogaster Armadillo and its vertebrate homolog β-catenin play multiple roles during development. Both are components of cell-cell adherens junctions and both transduce Wingless (Wg)/Wnt intercellular signals. The current model for Wingless signaling proposes that Armadillo binds the DNA-binding protein dTCF, forming a bipartite transcription factor that activates Wingless-responsive genes. In this model, Armadillo's C-terminal domain is proposed to serve an essential role as a transcriptional activation domain. In Xenopus, however, overexpression of C-terminally truncated β-catenin activates Wnt signaling, suggesting that the C-terminal domain might not be essential. We reexamined the function of Armadillo's C terminus in Wingless signaling. We found that C-terminally truncated mutant Armadillo has a deficit in Wg-signaling activity, even when corrected for reduced protein levels. However, we also found that Armadillo proteins lacking all or part of the C terminus retain some signaling ability if overexpressed, and that mutants lacking different portions of the C-terminal domain differ in their level of signaling ability. Finally, we found that the C terminus plays a role in Armadillo protein stability in response to Wingless signal and that the C-terminal domain can physically interact with the Arm repeat region. These data suggest that the C-terminal domain plays a complex role in Wingless signaling and that Armadillo recruits the transcriptional machinery via multiple contact sites, which act in an additive fashion.

CELL-CELL signals and their attendant signal transduction pathways shape the fates of virtually all cells within the body, both during normal embryonic development and as a part of the physiology of the adult animal. Further, the inappropriate activation of these pathways is a contributing cause of many human cancers. It is thus important to understand in detail the mechanisms by which signals are transduced. In addition, many of these signaling pathways already existed in the common ancestor of most if not all multicellular animals. Identification of both the conserved features of these pathways and also the ways in which their deployment differs in different animals can help us understand the forces that shape evolutionary change.

We focus on the Wingless (Wg)-/Wnt-signaling pathway (reviewed in CADIGAN and NUSSE 1997). Members of the Wg/Wnt family of ligands direct a wide variety of cell fate decisions in all animals examined. This pathway mediates some of the earliest cell fate choices in both the vertebrate Xenopus and the nematode *Caenorhabditis elegans*, as well as directing fine-scale patterning in the embryonic ectoderm of Drosophila, the mammalian CNS, and fly and mammalian limbs. In many of these cases, the signal is transduced by a common set of components that have been identified by genetic screens in Drosophila, *C. elegans*, and mammals, as well as by biochemical approaches.

Drosophila Armadillo (Arm) and its vertebrate homolog β-catenin (βcat) are key effectors of Wg signal (reviewed in CADIGAN and NUSSE 1997). They also play additional roles in the cell; for example, they act as key components of cell-cell adherens junctions. These different roles are reflected in Arm/βcat's subcellular distribution. Arm/βcat accumulates in adherens junctions of most cells; in cells that do not receive Wg/Wnt signals, nonjunctional Arm/βcat is unstable and rapidly degraded by a multiprotein complex that includes Zeste white3 kinase (Zw3; vertebrate homolog is GSK-3β), APC, and Axin. Wg/Wnt signals act through a family of receptors related to the fruit fly Frizzled protein. Certain Frizzled family receptors activate the protein Dishevelled, leading to stabilization and thus accumulation of nonjunctional Arm/βcat via inactivation of the destruction machinery.

The data concerning the subsequent steps in the pathway have been interpreted in several ways. The data in Drosophila support a model in which Arm is stabilized by Wg signaling and thus enters the nucleus and binds to the HMG-class DNA-binding protein dTCF (also called Pangolin; BRUNNER *et al.* 1997; VAN DE WETERING *et al.* 1997). This complex is thought to act as a bipartite transcription factor that activates Wg-responsive genes, with dTCF contributing the DNA-binding domain and

Corresponding author: Mark Peifer, Department of Biology, CB#3280, Coker Hall, University of North Carolina, Chapel Hill, NC 27599-3280. E-mail: peifer@unc.edu

[1]These authors contributed equally to this work.

the proximal C terminus of Arm acting as a transcriptional activation domain. Several studies support this model: (1) mutations truncating the C terminus of Arm disrupt its ability to transduce Wg signaling *in vivo* (KLINGENSMITH *et al.* 1989; PEIFER *et al.* 1994a; ORSULIC and PEIFER 1996; WHITE *et al.* 1998), (2) Arm's C terminus acts as a transcription-activation domain in a simplified mammalian gene expression assay (VAN DE WETERING *et al.* 1997), and fusion of the Arm C terminus to TCF makes it an Arm independent activator (ROOSE *et al.* 1998; VLEMINCKX *et al.* 1999), and (3) mammalian βcat, the C terminus of which diverges from that of Arm, has reduced signaling ability in Drosophila (WHITE *et al.* 1998). However, these results contrast with data obtained in Xenopus. Overexpression of a βcat mutant encoding only the Arm repeat region (and thus lacking the C-terminal domain) activates Wnt signaling (FUNAYAMA *et al.* 1995), suggesting that in Xenopus βcat's C terminus is not essential for signaling. Wnt signaling is also activated by the Arm repeat region of plakoglobin, a βcat paralog (KARNOVSKY and KLYMKOWSKY 1995; RUBENSTEIN *et al.* 1997).

These latter data can be interpreted several ways. C-terminally truncated βcat should bind to components of the destruction machinery, such as APC or Axin. By doing so, it could shield the endogenous full-length β-catenin in frog embryos from destruction, allowing it to accumulate and thus to signal. This interpretation is consistent with the current model. Alternately, the current model may be wrong. We now realize that in the absence of Arm/βcat, TCF/LEF represses Wg/Wnt-responsive genes (BRANNON *et al.* 1997; RIESE *et al.* 1997; CAVALLO *et al.* 1998; ROOSE *et al.* 1998). Further, genetic data from *C. elegans* suggest that the TCF relative Pop-1 antagonizes Wnt signaling during early embryogenesis (ROCHELEAU *et al.* 1997; THORPE *et al.* 1997). This led to the suggestion that the only role of Arm/βcat might be to bind to and thus inhibit the repressor activity of TCF/LEFs, allowing the activation of Wg/Wnt-responsive genes (MERRIAM *et al.* 1997). C-terminally truncated Arm retains the dTCF-binding site (VAN DE WETERING *et al.* 1997) and thus could potentially inhibit TCFs.

The two models make different predictions about the signaling ability of C-terminally truncated Arm/βcat in the absence of endogenous wild-type Arm/βcat. If C-terminally truncated Arm/βcat acts only by stabilizing endogenous Arm/βcat, there should be no signaling in the absence of wild-type protein. In contrast, if Arm/βcat's C terminus is dispensable for signaling, the absence of endogenous protein should have no effect. In Drosophila we can remove the endogenous protein by mutation or replace it with mutated versions of the protein, retaining only certain functions. We thus carried out detailed tests of several C-terminally truncated versions of Arm, both in the presence and absence of wild-type endogenous Arm.

MATERIALS AND METHODS

Mutant constructs: The mutant genes created for use in this study encode different Arm domains. Arm-R (Arm repeats R1–13, encoding amino acids 127–719) and Arm-NR (the N-terminal domain plus Arm repeats 1–13, encoding amino acids 1–719) were subcloned from pBSArmR1–13 and pBSArmNR (PAI *et al.* 1996), respectively, either into pUAST (BRAND and PERRIMON 1993; Arm-R), or into pUAST-myc (Arm-Rmyc and Arm-NR), derived from pUAST by adding an initiator methionine and a single c-myc epitope immediately after the promoter. We also cloned full-length Xenopus β-*cat* into pUAST.

Biochemical analyses: Levels of protein expression and phosphorylation isoforms were analyzed by collecting embryos from crosses of individual transformant lines to *e22c*-GAL4/*CyO*, making and analyzing embryo extracts by SDS-PAGE and immunoblotting with anti-myc, followed by enhanced chemiluminescence (ECL; Amersham, Arlington Heights, IL) detection (for total levels) or detection with alkaline phosphatase-coupled secondary Ab, NBT, and BCIP (Promega, Madison, WI; for isoforms). Since ECL detection is not strictly linear, we examined several exposures of each blot and repeated individual experiments to confirm differences. For immunoblotting we used monoclonal anti-c-myc 9E10 culture supernatant directly. Other antibodies were diluted as follows: monoclonal anti-Arm 7A1 (PEIFER *et al.* 1994a; 1:500), monoclonal anti-BicD (SUTER and STEWARD 1991; 1:30). Membrane fractionation was as in PEIFER (1993).

Immunofluorescence and antibody staining: Embryos were collected and dechorionated as in COX *et al.* (1996), and antibody incubations and washes are described in PEIFER *et al.* (1993). For monoclonal Armadillo antibody 7A1 (1:200), embryos were fixed for 5 min in 37% formaldehyde, incubated in primary antibody for 1 hr at 25° or overnight at 4° in antibody wash (1% BSA in disc wash), and washed in antibody wash three times for 5 min each time. Secondary antibody incubation was as in COX *et al.* (1996).

Genetics: GAL4 stocks were provided by the Bloomington Drosophila Stock Center. The zygotic and maternal phenotypes of arm^{YD35}, $arm^{H8.6}$, and arm^{XM19} are described in PEIFER *et al.* (1993, 1994a) and PEIFER and WIESCHAUS (1990). All crosses were done at 25° with two or more independent lines of each mutant (mutant constructs, *UAS-arm-X*). For F_1 progeny, hatch rates were determined and cuticles of hatched larvae and unhatched embryos were prepared as in WIESCHAUS and NÜSSLEIN-VOLHARD (1986). We crossed *e22c*-GAL4/*CyO* females with *UAS-arm-X* homozygous males to look for dominant effects. We tested for rescue of animals with a maternal and zygotic contribution composed entirely of arm^{XM19}-mutant protein by generating females who were heterozygous for *e22c*-GAL4 and were carrying arm^{XM19} germline clones as in PEIFER *et al.* (1993). These females were mated to *UAS-arm-X* homozygous males.

Two-hybrid analysis: Two-hybrid experiments were carried out as described in PAI *et al.* (1996). Yeast cells were transformed with plasmids encoding portions of the Arm repeat region fused to the LexA DNA-binding domain, along with the GAL4 activation domain plasmid containing either the C-terminal region of Arm from isoleucine 451 in Arm repeat 10 to the C terminus or a control plasmid (pCK4) expressing only the Gal4p transcriptional activation domain. Values shown are averages from duplicate β-galactosidase assays performed on at least six independent transformants.

RESULTS

C-terminally truncated Arm signals less effectively than wild-type Arm: Arm protein can be divided into

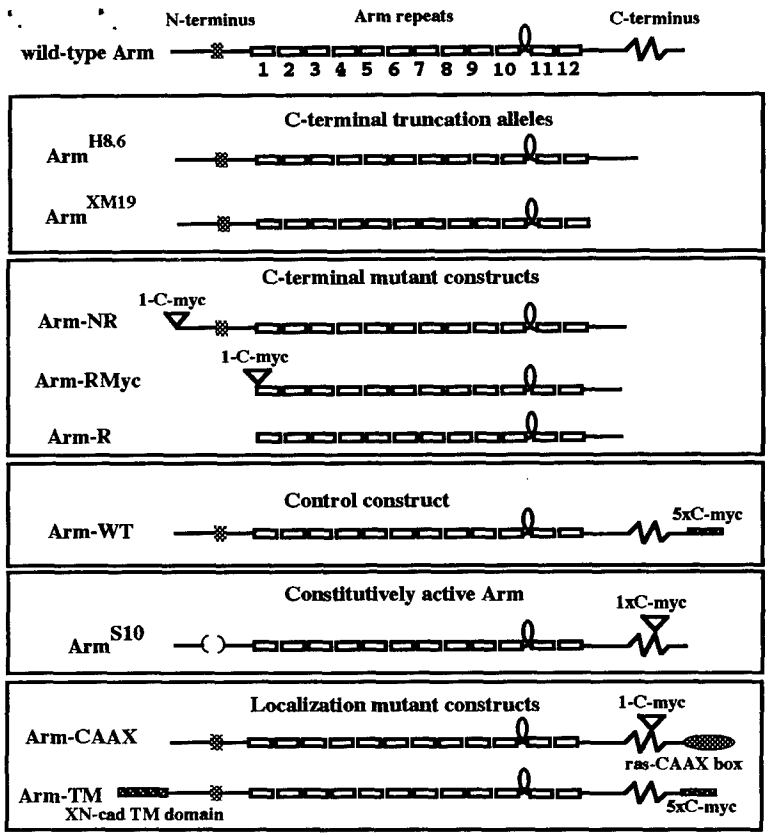

FIGURE 1.—*arm* mutants used in this study.

three "domains" (Figure 1), based on its sequence and on the crystal structure of the central portion of βcat (HUBER *et al.* 1997). The central two-thirds of Arm is composed of a series of Arm repeats, a structural motif present in Arm/βcat as well as numerous otherwise unrelated proteins. There are 125–150 amino acid regions both N-terminal and C-terminal to the Arm repeats. While we originally defined the boundary between the Arm repeats and the C-terminal domain at amino acid 707, we now suspect from the crystal structure that the C-terminal domain begins at amino acid 678, thus including what we originally viewed as Arm repeat 13. This repositioning of the boundary between the Arm repeats and the C-terminal domain means that the most proximal part of the C-terminal domain is quite well conserved between Arm and βcat, while the distal C terminus is less well conserved.

While Wg signaling determines the fate of cells in numerous tissues, we most often focus on its effect on anterior-posterior cell fate choices in the larval epidermis. The ventral epidermis is secreted by a dozen rows of cells along the anterior-posterior axis per embryonic segment; the anterior rows of cells secrete small hairs known as denticles, while posterior cells secrete naked cuticle (Figure 2A). Wg is secreted by the tenth row of cells and is required for proper cell fate choices. In *wg* mutants, all cells choose anterior fates and secrete denticles; in contrast, if one removes the negative regulator *zw3*, all cells choose posterior fates and secrete naked cuticle. The original mutagen-induced *arm* mutants form a natural truncation series, sequentially removing more and more protein from the C terminus (PEIFER and WIESCHAUS 1990). Some remove part (*arm*$^{H8.6}$; truncated after amino acid 725) or all (*arm*^{XM19}; truncated after amino acid 680) of the C-terminal domain (Figure 1), while others delete further, removing Arm repeats. *arm* mutations that reduce or remove the proximal C-terminal domain retain function in adherens junctions, but have severely reduced signaling function. At 25°, such embryos resemble *wg* null mutants both in cuticle phenotype (*e.g.*, Figure 2B is an *arm*^{XM19} maternal and zygotic mutant) and in the expression of Wg-responsive genes (KLINGENSMITH *et al.* 1989; PEIFER *et al.* 1991, 1994a; ORSULIC and PEIFER 1996). Mutations that delete further, removing portions of the Arm repeat region, also abolish function in adherens junctions (COX *et al.* 1996), resulting in disruption of epithelial structures.

Our previous tests of the function of C-terminally truncated Arm proteins were done in the absence of endogenous wild-type Arm and thus suggested that the C terminus played an essential role in signaling. However, all of the truncated *arm* mutants produce protein at levels somewhat lower than that of wild-type (PEIFER and WIESCHAUS 1990), perhaps due to mRNA instability triggered by a premature stop codon (reviewed in RUIZ-ECHEVARRIA *et al.* 1996). Arm^{XM19} and Arm$^{H8.6}$ proteins accumulate to about 10 and 30% of the level of wild-

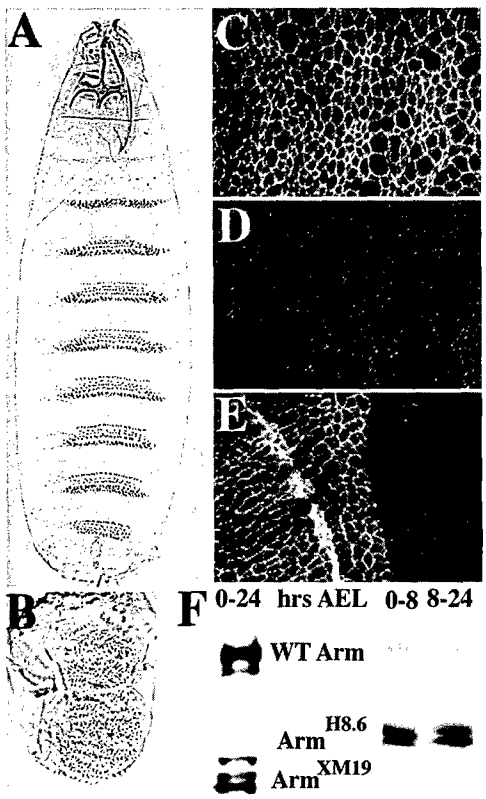

FIGURE 2.—C-terminal truncation of Arm dramatically reduces activity in Wg signaling. (A) Ventral view of the cuticle of a wild-type embryo at hatching. The body is divided into segments; on the ventral side anterior cells of each thoracic and abdominal segment secrete denticles and posterior cells secrete naked cuticle. (B) Cuticle of an arm^{XM19} maternal and zygotic mutant (a *wg* null mutant or an $arm^{H8.6}$ maternal and zygotic mutant would be essentially indistinguishable from this). Body size is dramatically reduced and all surviving ventral cells secrete denticles. (C–E) Embryos stained with anti-Arm antibody. (C) Zygotically wild-type sibling. Note stripes of cells accumulating cytoplasmic/nuclear Arm. (D) Embryo maternally and zygotically arm^{XM19} mutant. All cells accumulate Arm exclusively at the plasma membrane. (E) Side-by-side comparison of an embryo maternally and zygotically arm^{XM19} mutant (right) and a zygotically wild-type sibling (left), to show the difference in the intensity of Arm immunofluorescence. (F) Accumulation levels of C-terminally truncated proteins. Total cell extract was made from embryonic progeny of a cross of females with germlines homozygous for arm^{XM19} (left) or $arm^{H8.6}$ (right) to arm^{+}/Y males and immunoblotted with anti-Arm antibody. Age in hours after egg-laying (AEL) is indicated. (Left) Arm^{XM19} protein in arm^{XM19} maternally and zygotically mutant embryos accumulates at levels similar to that of wild-type Arm in their maternally mutant but zygotically wild-type siblings. (Right) $Arm^{H8.6}$ protein in $arm^{H8.6}$ maternally and zygotically mutant embryos accumulates at higher levels than wild-type protein in their maternally mutant but zygotically wild-type siblings.

type Arm protein in a wild-type embryo (PEIFER and WIESCHAUS 1990). This raised the possibility that the phenotype of Arm^{XM19} and $Arm^{H8.6}$ reflected their reduced level of accumulation and not a defect in signaling function.

To address this, we designed a strategy by which we could equalize the levels of wild-type and mutant proteins and then assess function. We did so by reducing the level of wild-type Arm by removing the wild-type maternal contribution. We crossed females with germlines homozygous for either $arm^{H8.6}$ or arm^{XM19} to wild-type males. The resulting progeny all have a maternal contribution composed exclusively of mutant protein. Because *arm* is on the X chromosome, half the progeny get a paternal Y chromosome and make only mutant protein zygotically; the other half of the embryos receive a paternal wild-type *arm* gene and thus produce wild-type Arm protein zygotically. We compared the level of wild-type protein in paternally rescued embryos to the level of mutant protein in maternally and zygotically mutant embryos (we measured levels of wild-type and mutant proteins in a mixed population of embryos, all of whom were maternally *arm* mutant and half of whom had received a paternal wild-type *arm* gene). Paternally rescued embryos have substantially reduced levels of wild-type protein compared to embryos with a wild-type maternal contribution (data not shown). The level of wild-type protein in maternally mutant but zygotically wild-type embryos is roughly equal to the level of Arm^{XM19} protein in arm^{XM19} maternally and zygotically mutant embryos (Figure 2F) and is only about 25% of the level of $Arm^{H8.6}$ protein in $arm^{H8.6}$ maternally and zygotically mutant embryos (Figure 2F; note that the nonlinearity of ECL detection may mean that the absolute differences may vary somewhat from our quantitated levels). Levels remain equivalent from early embryogenesis (0–8 hr), when the maternally contributed mutant proteins might be predominant, through later stages of embryogenesis (8–24 hr) when zygotic wild-type and mutant genes have come on to their full levels (Figure 2F).

This allows us to further interpret our previous phenotypic studies. Maternally and zygotically $arm^{H8.6}$- or arm^{XM19}-mutant embryos are null for Wg signaling as measured either by cuticle phenotype or by gene expression (KLINGENSMITH *et al.* 1989; PEIFER *et al.* 1994a; when assayed at 25°—$arm^{H8.6}$ has a slightly weaker phenotype at 18°). In contrast, maternally mutant embryos that receive a paternal wild-type *arm* gene are wild-type in phenotype and survive to adulthood. Thus wild-type Arm can transduce Wg signal even when its levels are reduced to levels equal to or lower than those of the C-terminally truncated mutants. This allows us to conclude that C-terminal truncation of Arm substantially impairs its ability to signal; this is not due solely to reduced levels of mutant protein.

These results do not, however, rule out the possibility that the reduced level of accumulation of mutant protein may influence its ability to signal. We previously observed that the signaling ability of Arm can be influenced by its subcellular localization. Thus, for example, when levels of wild-type Arm are low, DE-cadherin can serve as a sink, such that all remaining Arm in the cell

is sequestered in the cadherin-bound pool (Cox *et al.* 1996), leaving none available for signaling. We thus reexamined the subcellular distribution of Arm^{XM19} protein and compared it to the subcellular distribution of wild-type protein in the zygotically rescued siblings (we previously explored this in PEIFER *et al.* 1994a). As we previously noted, in embryos in which all maternal and zygotic protein was Arm^{XM19}, virtually all of the mutant Arm was found at the cell surface, even in cells receiving Wg signal (Figure 2, C *vs.* D).

Taken alone, these data suggest that Arm^{XM19} is synthesized at such low levels that all is sequestered in the cadherin-associated pool, leaving none available for signaling. By this model, however, there should be a similar sequestration of wild-type Arm at the junctions of zygotically rescued siblings, since wild-type Arm and Arm^{XM19} accumulate at equivalent levels (Figure 2F). This is not the case: in zygotically rescued embryos Arm accumulated both in the cadherin-associated pool at the plasma membrane and in the cytoplasm of cells that receive Wg signal (Figure 2C). Thus Wg signal can stabilize wild-type Arm but cannot stabilize Arm^{XM19}. These data are further reinforced by our previous observations on the ability of mutations in *zw3*, a component of the destruction machinery, to alter Arm accumulation. Mutation of *zw3* dramatically elevates the levels of wild-type Arm while *zw3* mutations have no effect on levels of Arm^{XM19} protein (PEIFER *et al.* 1994a,b). Together, these data suggest that C-terminally truncated Arm cannot be stabilized by Wg signal and that its destruction is independent of Zw3 activity.

We should note an apparent discrepancy between the levels of Arm^{XM19} as measured by immunoblotting, where Arm^{XM19} protein accumulated to levels similar to or higher than that of wild type, and the levels of Arm^{XM19} as measured by immunofluorescence, where levels of Arm^{XM19} protein appear significantly lower than those of wild-type protein (Figure 2E). Our antibody, which is directed against the N-terminal domain, may access wild-type and mutant protein equally on an immunoblot, where both proteins have been denatured, but not *in situ*, perhaps because the conformations of wild-type and mutant proteins differ in a way that alters accessibility to the antibody epitope.

Design and expression of different C-terminally truncated Arm mutants: To complement these experiments, we set out to examine the effect of elevating the level of C-terminally truncated Arm to fully wild-type levels, to see if this might partially rescue the reduction in signaling function observed in $arm^{H8.6}$ or arm^{XM19}. These experiments were designed to match more closely the experiments in Xenopus, where C-terminally truncated βcat was expressed at levels that met or exceeded those of the wild-type endogenous βcat. We designed a series of mutants that altered the termini of Arm protein, focusing on the role of the C terminus (Figure 1). In Arm-N terminus plus repeats (Arm-NR) the C terminus beyond amino acid 719 was removed, and an N-terminal myc-epitope tag was added; this truncation was thus intermediate in extent between $arm^{H8.6}$ or arm^{XM19}. However, as this mutation does not generate an mRNA with coding sequence flanking a premature stop codon, we expected the mRNA to be stable and thus encode normal levels of protein (we show in Figure 6 below that this is the case). The second set of mutants, Arm-Repeats (Arm-R) and Arm-Repeats plus myc (Arm-Rmyc), contain only the Arm repeat region and thus lack both N and C termini; Arm-Rmyc also carries an N-terminal myc-tag. Since Arm-R and Arm-Rmyc were identical in their phenotypic effects, we refer to both as Arm-R unless otherwise noted. Arm-R mimics the "repeat only" mutants of βcat that activate Wnt signaling when injected into wild-type Xenopus embryos (FUNAYAMA *et al.* 1995). We also generated a construct encoding full-length Xenopus β-*catenin*; while Arm and βcat are 71% identical in protein sequence overall, the divergence in the C-terminal region is much more substantial. All of these proteins were expressed under the control of the GAL4-UAS system (BRAND and PERRIMON 1993), in which the gene of interest is cloned downstream of a minimal promoter and a series of GAL4-binding sites. The gene of interest can be introduced in a silent state into flies lacking GAL4 and activated by crossing these flies to flies expressing GAL4 in the desired temporal and spatial pattern. We used the *e22c*-GAL4 driver, which is expressed essentially ubiquitously in the ectoderm beginning late in embryonic stage 9 (Cox *et al.* 1999).

The Arm repeats alone activate Wg signaling in a wild-type background: To look for dominant effects, we first expressed our mutant proteins in a wild-type background. Fly embryos are not sensitive to slight elevation in the level of expression of wild-type Arm. Increasing Arm levels using a chromosomal duplication, a wild-type transgene (ORSULIC and PEIFER 1996), or by overexpression of Arm-WT using *e22c*-GAL4 (PAI *et al.* 1997; data not shown) has no effect on the embryonic pattern. Likewise, when we expressed Arm-NR in wild-type embryos, it also did not have any dominant effects; in fact, animals expressing Arm-NR survived to adulthood (data not shown; Arm-NR was expressed at wild-type levels, unlike the C-terminally truncated mutants; see Figure 6 below). Expression of Xenopus βcat also had no dominant effects (data not shown).

In contrast, when we used *e22c*-GAL4 to express Arm-R, containing only the Arm repeat region, in the presence of wild-type endogenous Arm, we saw activation of Wg signaling (Figure 3, B and C). Expression of Arm-R led to a partial conversion of anterior epidermal cells to a posterior naked cuticle fate, suggesting uniform activation of Wg signaling. We previously observed a similar dominant phenotype when, using the same GAL4 driver, we expressed Arm^{S10} (Figure 3D), a mutant Arm protein retaining the C terminus but also

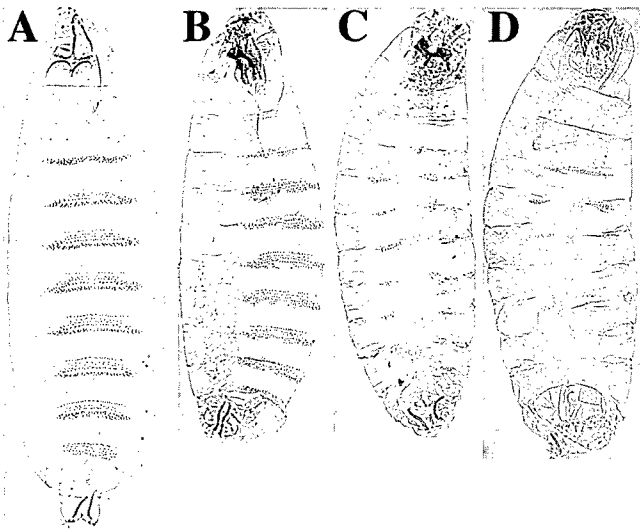

FIGURE 3.—Arm-R expression in a wild-type background activates Wg signaling. (A) Wild-type embryo. (B and C) Different lines expressing Arm-Rmyc (B and C) in an otherwise wild-type background, showing the range of dominant effects from a nearly wild-type pattern (B) to a strong conversion of denticles to naked cuticle (C). (D) For comparison, the very strong phenotype resulting from expressing Arm^{S10} (PAI *et al.* 1997), which retains the Arm repeats and C terminus but has a deletion in the N-terminal region, in an otherwise wild-type background.

missing the N-terminal region that downregulates protein stability (PAI *et al.* 1997). The dominant phenotypes induced by Arm-R were, on average, less severe than those induced by Arm^{S10}, suggesting that the C-terminal domain is required for full signaling activity. The difference between Arm-R and Arm-NR in their effect on the wild-type pattern likely reflects the fact that, like Arm^{S10}, Arm-R lacks the N-terminal stability-regulating domain, which is retained by Arm-NR.

The dominant phenotype of Arm-R in the wild-type background could be due to signaling by Arm-R itself. Alternatively, Arm-R might displace wild-type Arm from adherens junctions and also block the destruction machinery, allowing endogenous Arm to accumulate outside junctions and signal. To determine whether Arm-R exerts its dominant effects by stabilizing wild-type endogenous Arm, we examined the levels and localization of wild-type Arm in embryos expressing either Arm-R or Arm-NR (Figure 4). To do so, we used our N-terminal anti-Arm monoclonal, which recognizes wild-type Arm and Arm-NR but not Arm-R. Consistent with the failure of Arm-NR to affect normal development, the localization of Arm-NR plus wild-type Arm resembled that of wild-type Arm in a nontransgenic embryo (Figure 4, A and E *vs.* C). In contrast, Arm-R dramatically altered the accumulation of wild-type Arm (Figure 4, B and F). These differences were first seen at stage 11, when the levels of Arm-R driven by *e22c*-GAL4 begin to rise (see below). While levels of wild-type endogenous Arm at the plasma membrane remained stable or dropped, levels of wild-type Arm inside cells rose dramatically, so that all cells resembled cells receiving Wg signal (Figure 4, B *vs.* C). This stabilization of cytoplasmic wild-type Arm is very similar to that seen in a *zw3* mutant (PEIFER *et al.* 1994a) and thus could easily account for the dominant effects of Arm-R. The elevation in the level of intracellular Arm by Arm-R continues throughout the rest of embryonic development (Figure 4F). Despite the significant increase in intracellular Arm caused by Arm-R expression, the total levels of endogenous wild-type Arm were not increased, as assayed either by immunofluorescence or immunoblotting (Figures 4D and 8B).

C-terminally truncated Arm retains significant signaling activity when expressed at wild-type levels: To assess

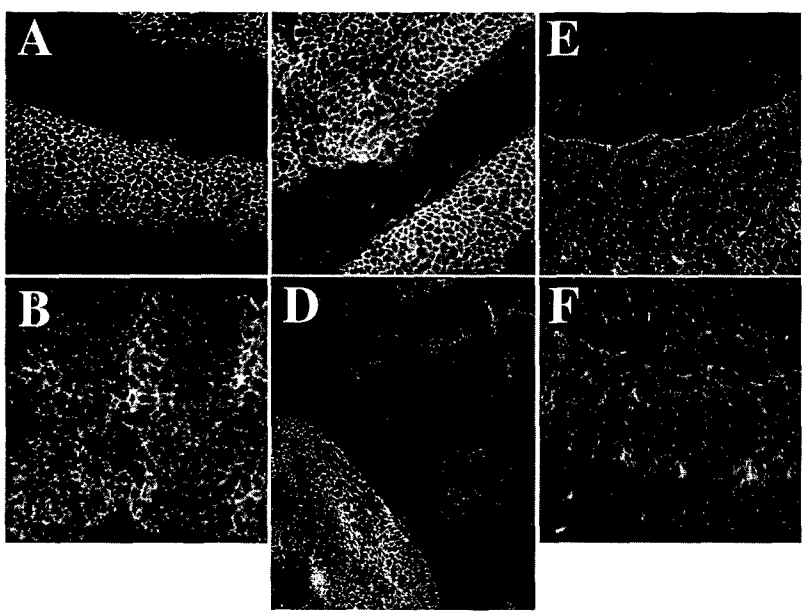

FIGURE 4.—Arm-R expression elevates the level of endogenous wild-type Arm in the cytoplasm and depresses its accumulation at the membrane. All embryos were stained with anti-Arm antibody, which recognizes endogenous Arm and Arm-NR, but not Arm-R. (A–D) Stage 11 embryos. (A) Arm-NR expression does not alter the level or localization of endogenous Arm, and its own localization resembles that of the endogenous protein. (B) In contrast, Arm-R expression results in the accumulation of elevated levels of endogenous wild-type Arm in the cytoplasm relative to the plasma membrane. (C) Nontransgenic sibling for comparison. (D) The total level of endogenous Arm in a Arm-R-expressing embryo (top) is not elevated relative to a nontransgenic sibling; in fact the levels seem lower. (E) Stage 13 embryo expressing Arm-NR. The pattern of Arm accumulation is unaltered from wild-type. (F) Stage 12 embryo expressing Arm-R, with elevated levels of intracellular Arm.

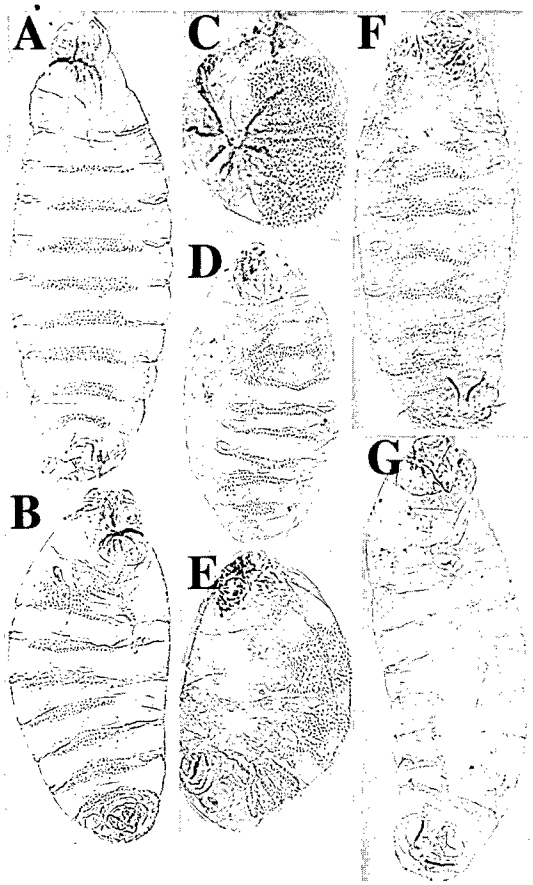

FIGURE 5.—Expression of wild-type levels of C-terminally truncated Arm can partially rescue signaling. (A and B) Two lines expressing Arm-WT in an arm^{XM19} background. The segment polarity phenotype is either completely (A) or substantially (B) rescued, with no gain of function effects on pattern. (C) Embryo maternally and zygotically mutant for arm^{XM19}. (D) Embryo expressing Arm-NR in an arm^{XM19} background. The segment polarity phenotype is partially rescued, but to a lesser extent than by Arm-WT. (E and F) Different lines expressing either Arm-Rmyc (E) or Arm-R (F) in an arm^{XM19} background. The segment polarity phenotype is rescued to varying degrees; in the embryos with the strongest rescue, vestiges of the dominant phenotype are observed as ablation of denticles along the ventral midline. Rescue by Arm-R is noticeably less than that by Arm-WT. (G) Embryo expressing Arm^{S10} in an arm^{XM19} background. Note the completely penetrant dominant phenotype.

the signaling ability of C-terminally truncated Arm when expressed at wild-type levels, we expressed Arm-R and Arm-NR in an *arm*-mutant background in the absence of endogenous wild-type Arm. As discussed above, $arm^{H8.6}$ and arm^{XM19} encode proteins partially or completely lacking the C-terminal domain, respectively. Embryos maternally and zygotically mutant for either $arm^{H8.6}$ or arm^{XM19} are null for Wg signaling at 25° (KLINGENSMITH *et al.* 1989; PEIFER *et al.* 1991, 1994a). $arm^{H8.6}$ retains intrinsic signaling activity, however, as revealed by the weaker phenotypes of $arm^{H8.6}$ at 18° (KLINGENSMITH *et al.* 1989) and of $arm^{H8.6}zw3$ double mutants, in which levels of $Arm^{H8.6}$ protein are elevated by reducing its degradation (PEIFER *et al.* 1994a,b). In contrast, neither reduction in temperature nor simultaneous mutation of *zw3* leads to any rescue of arm^{XM19}. We thus used arm^{XM19} as a background we expected to be null for Wg signaling.

To create embryos expressing C-terminally truncated protein at wild-type levels, we expressed Arm-NR, which lacks the distal C terminus (it is six amino acids shorter than $Arm^{H8.6}$; Figure 1), in embryos maternally and zygotically arm^{XM19} mutant. We expected that as Arm-NR lacks most of the C-terminal domain, it would not rescue signaling. Instead, we found that Arm-NR substantially rescued the Wg-signaling defects of arm^{XM19} mutants (embryos were restored to a more normal size and the segment polarity phenotype was substantially but not completely rescued, as fusions of denticle belts were often observed; Figure 5D). Arm-NR was diminished in signaling ability, however, as it rescued the phenotype less completely than did Arm-WT (Figure 5, A and B). Expression of Xenopus βcat also led to substantial but not complete rescue of signaling, to an extent essentially identical to that of Arm-NR (data not shown). Since Arm and βcat diverge substantially in sequence in the C-terminal region, the βcat C terminus may not function effectively in flies. Together these data suggest that removing Arm's C terminus diminishes, but does not eliminate its signaling function. WHITE *et al.* (1998) recently reported similar experiments with βcat and C-terminally truncated Arm; in their experiments, however, the signaling ability of C-terminally truncated Arm was less than what we observed, perhaps due to differences in the constructs and the means through which they were expressed.

Expression of Arm-R, containing the Arm repeats alone, at wild-type levels also substantially rescued the Wg-signaling defect of arm^{XM19} mutants (Figure 5, E and F). The extent of rescue was on average greater than that conferred by Arm-NR (Figure 5D), but less than that conferred by Arm-WT (Figure 5, A and B). Arm-R expression in an arm^{XM19} mutant also sometimes resulted in a dominant activated Wg-signaling phenotype similar to, but weaker than, that induced by Arm-R in a wild-type background (Figure 5F). The dominant activated phenotype predominated along the ventral midline, leading to partial ablation of the denticle belt. However, extra denticles were observed at the lateral margins, suggesting failure to completely rescue Wg signaling. The dominant effects of Arm-R in the arm^{XM19}-mutant background were substantially weaker than those of Arm^{S10} (Figure 5G), which also lacks the critical regulatory region in the N terminus but which retains the C terminus. Together, these data suggest that Arm proteins lacking the distal C-terminal domain retain reduced but still significant intrinsic signaling ability.

Arm-R accumulates to higher levels than wild-type Arm, partially explaining its activated phenotype: Arm-R was significantly more potent than Arm-NR: Arm-R was bet-

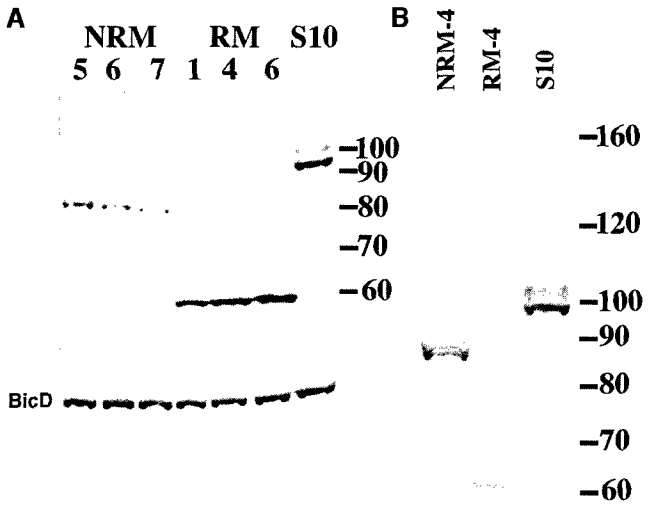

FIGURE 6.—Accumulation levels of Arm mutant proteins. Flies carrying UAS-Arm constructs as indicated were crossed to flies carrying the GAL4 driver *e22c*-GAL4. Embryo extracts were immunoblotted with anti-myc epitope antibody. MW markers are indicated at right. (A) Levels of expression of different Arm-NR (NRM) and Arm-Rmyc (RM) transgene insertion lines (three lines of each are presented, indicated by the line number below the label). They are compared to Arm^{S10} (S10), which accumulates to higher levels than wild-type (PAI *et al.* 1997). Arm-Rmyc lines accumulate high levels of protein, while Arm-NR lines accumulate levels of protein more similar to wild-type. The samples represent 0 to 19-hr-old embryos. (B) Phosphorylation of mutant Arm proteins. Arm^{S10} (S10) shows a set of phosphorylated isoforms similar to those of wild-type Arm. In contrast, only two isoforms of Arm-NR (line NRM-4) and one or two isoforms of Arm-Rmyc (line RM-4) are detectable.

ter at rescuing the signaling defect of arm^{XM19}, and Arm-R expression caused a dominant activated phenotype. We previously found that removal of part of the N-terminal domain of Arm (creating the mutant Arm^{S10}) stabilizes the mutant protein and thus renders it constitutively active in Wg signaling (PAI *et al.* 1997). This region is absent in Arm-R but present in Arm-NR, and thus the difference in their biological activities might be accounted for in part by differences in their level of accumulation. Neither Arm-R nor Arm-Rmyc is recognized by anti-Arm antibody, as they lack its N-terminal epitope. Arm-Rmyc and Arm-NR were both myc tagged, however, and thus we compared their level of expression with each other and with other myc-tagged Arm proteins. Arm-Rmyc accumulated to high levels (Figure 6A); the elevated levels of Arm-Rmyc, lacking the entire N and C termini, were similar to those attained by Arm^{S10} (Figure 6A), which lacks the key regulatory region in the N terminus (PAI *et al.* 1997). In contrast, Arm-NR, which retains both the N terminus and the repeats, accumulated at levels more similar to wild-type Arm (Figure 6A; data not shown). In the course of examining protein levels, we also looked at phosphorylation. Arm is phosphorylated on both Ser/Thr and Tyr residues (PEIFER *et al.* 1994b). Ser/Thr phosphorylation alters Arm's mobility on SDS-PAGE; we can use this to roughly estimate whether different mutant proteins are normally phosphorylated. Neither Arm-NR nor Arm-Rmyc has a full set of phosphorylation isoforms. Arm-NR, which lacks the C terminus, has only two visible isoforms (Figure 6B); this resembles the phosphorylation state of Arm^{XM19} (PEIFER *et al.* 1994b). Arm-Rmyc showed only a single isoform (Figure 6B). Thus at least some of the phosphorylation sites that alter Arm mobility are likely to be in the N and C termini; these proteins may remain phosphorylated on sites that do not alter the mobility of the protein, however.

Arm^{XM19} retains residual signaling ability: The data above suggest that Arm-R and $Arm^{H8.6}$, both of which lack the distal C-terminal region but retain the proximal conserved domain, retain some ability to signal, albeit less than wild-type Arm. Arm^{XM19} lacks the entire C-terminal domain, retaining only three amino acids past the end of the Arm repeats. In all of our previous experiments, Arm^{XM19} behaved as if it were null for signaling. However, in the course of other experiments (Cox *et al.* 1999), we identified circumstances that revealed that even Arm^{XM19} retains signaling activity. This activity was revealed by use of a membrane-tethered form of Arm, Arm-CAAX, which is tethered to the membrane using the lipid modification signal of mammalian K-ras. Arm-CAAX cannot signal on its own—when it is expressed in an animal lacking essentially all endogenous Arm (an embryo maternally and zygotically mutant for the near-null allele arm^{XP33}), Arm-CAAX rescues Arm's function in adherens junctions but has no signaling activity (Cox *et al.* 1999). However, when Arm-CAAX was expressed in embryos maternally and zygotically mutant for arm^{XM19}, these embryos were rescued to a nearly wild-type pattern (Figure 7, C and D). As Arm-CAAX cannot signal on its own (Cox *et al.* 1999), this suggested that Arm^{XM19} retains residual signaling activity, which is somehow promoted by Arm-CAAX coexpression.

We were surprised that Arm-CAAX had such a strong effect. One possible explanation is that Arm-CAAX binds to and blocks the destruction machinery, allowing Arm^{XM19} protein to accumulate to higher levels. We tested this. Arm-CAAX coexpression does not detectably increase the total level of Arm^{XM19} (Figure 8A, left) or the level of wild-type Arm in sibling embryos; in fact, levels of wild-type Arm slightly decrease (Figure 8A; likewise, Arm-WT, Arm-TM, and Arm-R coexpression does not elevate total levels of Arm^{XM19}; Figure 8B).

Arm-CAAX localizes to the plasma membrane in complex with DE-cadherin and α-catenin and retains full function in adherens junctions as tested genetically (Cox *et al.* 1999). By binding to DE-cadherin, Arm-CAAX could displace Arm^{XM19} from adherens junctions (most Arm in embryos is found in the junctional pool; PEIFER 1993). Even without elevating the total pool of

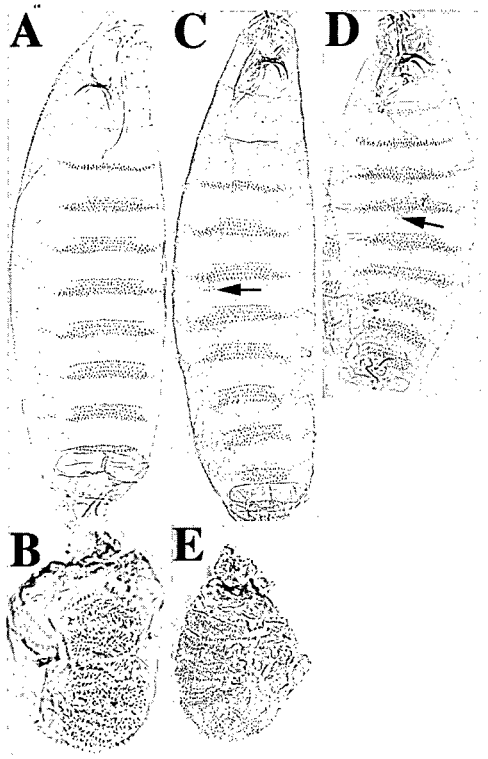

FIGURE 7.—Arm-CAAX substantially rescues the signaling defect of arm^{XM19}. (A) Wild-type embryo. (B) Embryo maternally and zygotically mutant for arm^{XM19}. (C and D) Unhatched and hatched embryos maternally and zygotically mutant for arm^{XM19} and also expressing Arm-CAAX. The segment polarity phenotype is almost totally rescued, leaving only a few denticles in the naked cuticle region. (E) Embryo maternally and zygotically mutant for arm^{XM19} and also expressing Arm-TM. Arm-TM has little rescuing ability.

Arm^{XM19}, Arm-CAAX could thus substantially elevate the pool of Arm^{XM19} available for signaling. To address this possibility, we fractionated cells derived from embryos maternally mutant for arm^{XM19} and isolated a membrane fraction. We found that expression of Arm-CAAX reduced the levels of both wild-type Arm and of Arm^{XM19} protein in the membrane fraction (Figure 8A, right). Quantitation of these blots followed by normalization for loading suggested that wild-type Arm in the membrane fraction was reduced more than threefold while levels of Arm^{XM19} protein in the membrane fraction were reduced more than fourfold (note that potential nonlinearity of ECL signal may affect the absolute levels, but should not alter conclusions about relative levels). Since total levels of Arm^{XM19} protein remained unaffected by Arm-CAAX coexpression (Figure 8A, left), this suggests that Arm-CAAX coexpression elevates levels of Arm^{XM19} protein in the cytoplasm (attempts to directly measure the levels of wild-type and mutant Arm in the soluble pool were prevented by limited quantities of material and the low level of Arm that is normally found in the soluble fraction). Further support for this model is provided by our previous observation that a different membrane-tethered form of Arm, Arm-TM, which carries the transmembrane domain of N-cadherin, did not significantly rescue embryos maternally and zygotically mutant for arm^{XM19} (Cox *et al.* 1999; Figure 7E). Arm-TM, unlike Arm-CAAX, does not localize to adherens junctions but instead appears to be trapped in the ER/Golgi (Cox *et al.* 1999) and thus may not be able to displace Arm^{XM19} into the signaling pool.

The C-terminal region of Arm can interact with the Arm repeat region: The crystal structure of the Arm repeat region of β-catenin revealed that the Arm repeats form a folded domain (HUBER *et al.* 1997). The structure of the N- and C-terminal regions remains unknown, as these were absent in the crystal; however, protease resistance studies (HUBER *et al.* 1997) and the ability of small fragments of the N-terminal domain to interact with α-catenin (ABERLE *et al.* 1996; PAI *et al.* 1996) suggest that these regions may not form independently folded domains and could exist as extended peptides or individual α-helices. If this model is correct, such peptides might be able to fold back into the groove formed by the Arm repeats of Arm/βcat. In the course of a two-hybrid screen for novel Arm interactors using most of the Arm repeat region as bait, we found that one interactor was a piece of Arm itself. This fragment of Arm extends from isoleucine 451 in Arm repeat 10 to the C terminus. We further mapped the interacting region using the two-hybrid system (Figure 9). The minimal piece of Arm with which the C-terminal fragment can strongly interact is Arm repeats 3–8; this is the same binding site occupied by DE-cadherin (PAI *et al.* 1996), dTCF (VAN DE WETERING *et al.* 1997), and dAPC (C. KIRKPATRICK and M. PEIFER, unpublished data). Very weak interactions were also detected with other more amino terminal fragments (Arm repeats 1–7, 1–6, and 1–4) but these βgal levels were much closer to the background levels in the absence of the C-terminal fragment.

DISCUSSION

Redefining the C-terminal domain: Arm protein has a modular structure. Its most prominent feature is the Arm repeats that make up the central two-thirds of the protein and serve as docking sites for a number of protein partners, including DE-cadherin, dAPC, and dTCF. On the basis of sequence alignment, we originally proposed that there were 13 Arm repeats, ending at amino acid 707, and thus the C-terminal domain began at this point. The Arm repeats came into sharper focus recently with the solution of the X-ray crystal structure of the Arm repeat region of βcat (HUBER *et al.* 1997). This allowed us to revise our model of Arm structure (Figure 10A); it is likely that there are only 12 Arm repeats, suggesting that the C-terminal domain begins at amino acid 678. This fits well with the biology, which suggests that the C terminus, as defined by its action in transcriptional activation, begins at this position.

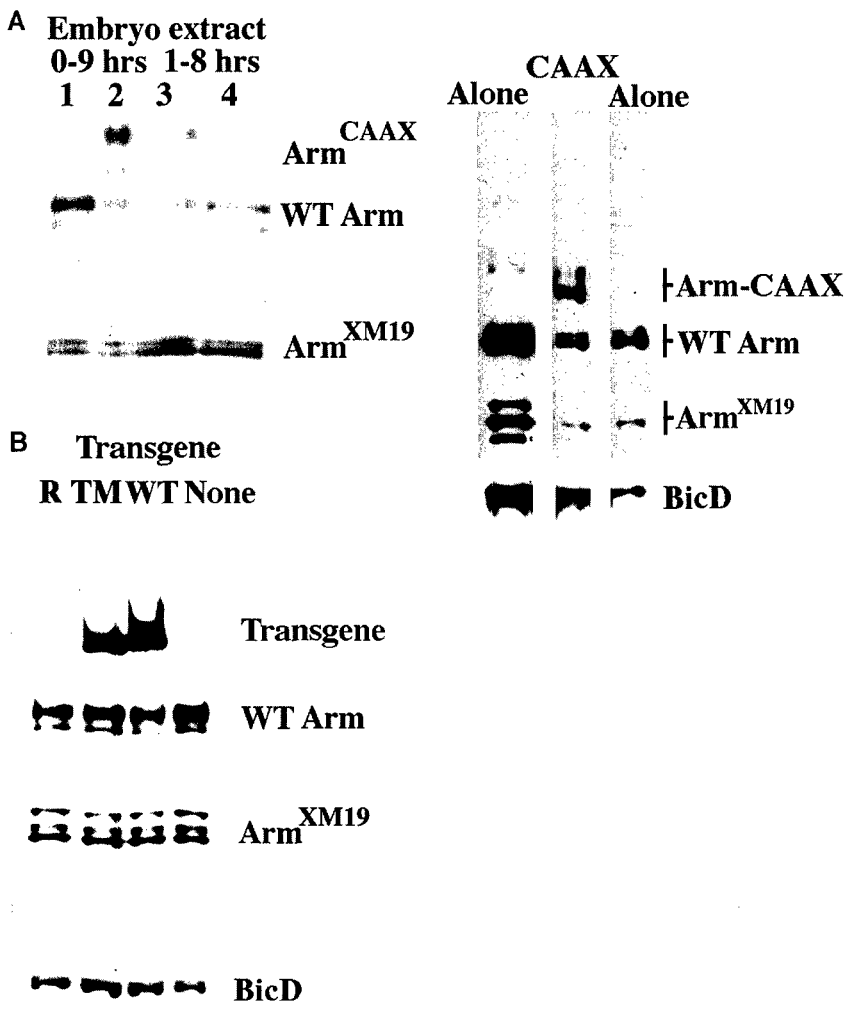

FIGURE 8.—Arm-CAAX does not raise total levels of Arm^{XM19} protein, but does lower its levels in the membrane-bound fraction. (A) Left: Coexpression of Arm-CAAX does not detectably elevate levels of total Arm^{XM19} protein in *arm^{XM19}*-mutant embryos. Females with germlines homozygous for *arm^{XM19}* were crossed to *arm^{+}/Y* males, expressing (lanes 2 and 3) or not expressing (lanes 1 and 4) Arm-CAAX. Total cell extracts were made from embryonic progeny of indicated ages after fertilization and immunoblotted with anti-Arm. Right: Coexpression of Arm-CAAX reduces levels of Arm^{XM19} protein in the membrane fraction. Females with germlines homozygous for *arm^{XM19}* were crossed to *arm^{+}/Y* males, expressing (middle lane) or not expressing (outside lanes) Arm-CAAX. Cell extracts were made from embryonic progeny and fractionated into membrane (P100) and soluble fractions. The membrane fraction was immunoblotted with anti-Arm. Due to the extremely limited number of embryos available, the entire sample was loaded in each case, and as a result, loading levels are not equal. BicD served as a loading standard. While the right lane has substantially less total protein than the central lane, the levels of Arm^{XM19} protein are equal. The left lane has only slightly more total protein than the central lane, but has substantially more Arm^{XM19} protein. (B) Coexpression of Arm-R (R), Arm-TM (TM), and Arm-WT (WT) does not elevate total levels of Arm^{XM19} protein and appears to decrease levels of endogenous wild-type Arm (WT Arm). Females with germlines homozygous for *arm^{XM19}* were crossed to *arm^{+}/Y* males expressing the indicated transgene. Total cell extracts were made and immunoblotted with anti-Arm. The blot was reprobed with BicD to control for loading differences.

Armadillo's C terminus can be divided into several regions that together play a complex role in Wg signaling: Our previous work led us to suggest that the proximal C terminus of Arm plays an essential role in Wg signal transduction by acting as a transcriptional activation domain. Inconsistent with this model, however, βcat mutants lacking the C terminus activate Wnt signaling when misexpressed in Xenopus (FUNAYAMA *et al.* 1995). To address this issue, we further characterized mutant Arm proteins lacking the C terminus. This analysis confirmed that the Arm C terminus potentiates signaling. We equalized the expression levels of wild-type and C-terminally truncated Arm by reducing wild-type Arm levels. Wild-type Arm remains fully functional in signaling when expressed at this reduced level. In contrast, Arm^{XM19}, lacking the entire C terminus, is null for Wg signaling at these levels of expression (PEIFER *et al.* 1991, 1994a; Figure 2).

However, our analysis also revealed that C-terminally truncated Arm retained significant signaling function and reinforced the idea that different C-terminally truncated mutants differ in their signaling ability (Figure 10B). Arm$^{H8.6}$ and Arm-NR, which have 40–50 amino acids of the C-terminal domain intact, retain substantially more signaling ability than Arm^{XM19}, which lacks the entire C-terminal domain. The contrast is most striking when comparing Arm$^{H8.6}$ and Arm^{XM19}. Arm$^{H8.6}$ retains clear residual signaling activity, as revealed by its weaker phenotype at lower temperatures and by the weaker phenotype seen when Arm degradation was decreased in an *arm$^{H8.6}$zw3* double mutant (KLINGENSMITH *et al.* 1989; PEIFER *et al.* 1994a). In contrast, there is no rescue of the signaling ability of Arm^{XM19} either by reduction of the temperature or by simultaneous mutation of *zw3* (PEIFER *et al.* 1994a). Full-length vertebrate βcat, when expressed in Drosophila, signals about as well as Arm-NR. Consistent with this, while βcat is highly related to Arm in the N terminus, the Arm repeats, and the proximal C terminus (retained in Arm-NR), βcat diverges extensively in the distal C terminus (missing

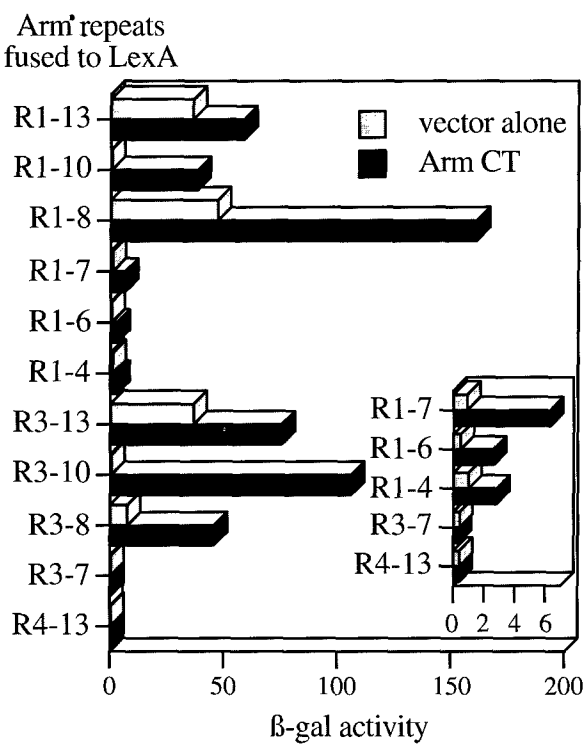

FIGURE 9.—The Arm C-terminal region can physically interact with Arm's central Arm repeats. A fusion protein containing a C-terminal portion of Arm fused to the GAL4 activation domain, originally isolated in a two-hybrid screen using Arm repeats 1–10 of Arm as bait, was tested for interaction with different portions of the Arm repeat region of Arm fused to the LexA DNA-binding domain (constructs as in PAI *et al.* 1996). β-Galactosidase levels were determined as in MATERIALS AND METHODS; cells carrying the activation domain vector alone (pCK4) show the background levels of β-galactosidase activity from the different Arm repeat fragments. The inset shows the data for weakly interacting or noninteracting fragments at higher resolution.

in Arm-NR). WHITE *et al.* (1998) previously demonstrated the reduced signaling ability of βcat in Drosophila; in their experiments it had even less signaling function.

Together, our current experiments and previous data suggest that the C terminus consists of at least three functional regions, two of which contribute to activation of Wg-responsive genes in an additive fashion (Figure 10). The C terminus distal to amino acid 757 is dispensable for Wg signaling, as demonstrated by the wild-type phenotype of the truncation mutant Arm^{S8}, which lacks this region (ORSULIC and PEIFER 1996). The region between amino acids 710 and 757 stimulates the ability of Arm to signal but is not essential, as demonstrated by the partial signaling ability of mutants such as Arm-NR or $Arm^{H8.6}$, which lack this region. Finally, the region of the C terminus from amino acids 678–710 plays a critical role in full signaling ability, as revealed by the further reduction in signaling function of Arm^{XM19}, which lacks this region. This latter region of the C terminus (amino acids 678–710) was recently revealed to contain the binding site for Drosophila Teashirt protein (GALLET *et al.* 1999), a zinc-finger transcription factor that binds Arm and helps mediate the late response to Wingless signaling (GALLET *et al.* 1998). Thus the difference in signaling ability between Arm^{XM19} and Arm-NR or $Arm^{H8.6}$ may reflect the fact that only the latter two are likely to bind Teashirt. These differences in signaling assayed *in vivo* are also reflected in the *in vitro* gene activation assay, which assesses the ability of Arm and dTCF to activate expression of a reporter construct with several dTCF-binding sites upstream. In this assay, Arm^{S8} behaves indistinguishably from wild type, $Arm^{H8.6}$ retains strong ability to coactivate the reporter, and the coactivation ability of Arm^{XM19} is sharply reduced but not completely eliminated (VAN DE WETERING *et al.* 1997; M. VAN DE WETERING and H. CLEVERS, personal communication).

The C terminus also appears to play a second function: regulating Arm stability. Nonjunctional Arm is normally unstable, but is stabilized by Wg signal. We found that while embryos maternally and zygotically arm^{XM19} mutant have levels of total Arm similar to those of their wild-type paternally rescued siblings, wild-type Arm accumulates in the cytoplasm/nuclei of cells receiving Wg signal, while Arm^{XM19} protein does not (PEIFER *et al.* 1994a; Figure 2). Further, we previously found that mutations in *zw3* greatly stabilize wild-type Arm but do not substantially stabilize Arm^{XM19} and only slightly stabilize $Arm^{H8.6}$ (PEIFER *et al.* 1994b). These latter data may help explain the fact that mutations in *zw3* have no effect on the phenotype of an arm^{XM19} mutant, while they slightly suppress the phenotype of an $arm^{H8.6}$ mutant (PEIFER *et al.* 1994a). Together these data suggest that C-terminally truncated Arm cannot be stabilized by Wg signaling. This idea was independently suggested by WHITE *et al.* (1998), who misexpressed mammalian plakoglobin and βcat in flies. βcat was stabilized in cells receiving Wg signal, while plakoglobin was not. They suggested that this might result from the divergence in C-terminal domains of Arm and plakoglobin and, thus, that the C terminus might regulate stability. The mechanism by which this occurs remains unknown.

In addition to these roles in transcriptional activation and in regulating stability, our data suggest a possible additional function for the C-terminal domain: it can bind, at least in two-hybrid experiments, to the central-most Arm repeats of Arm itself. Such an interaction could be either intermolecular, via Arm proteins forming homodimers, or intramolecular, with the tail folding back upon the Arm repeats of the same protein. Previous data failed to provide any support for the presence of Arm dimers (ORSULIC and PEIFER 1996; PAI *et al.* 1997), so if this interaction occurs *in vivo* it seems more likely to be intramolecular. Such an interaction would provide interesting possibilities for regulation. The C terminus could provide a competitor for other Arm partners such as cadherin or dTCF, allowing regulation

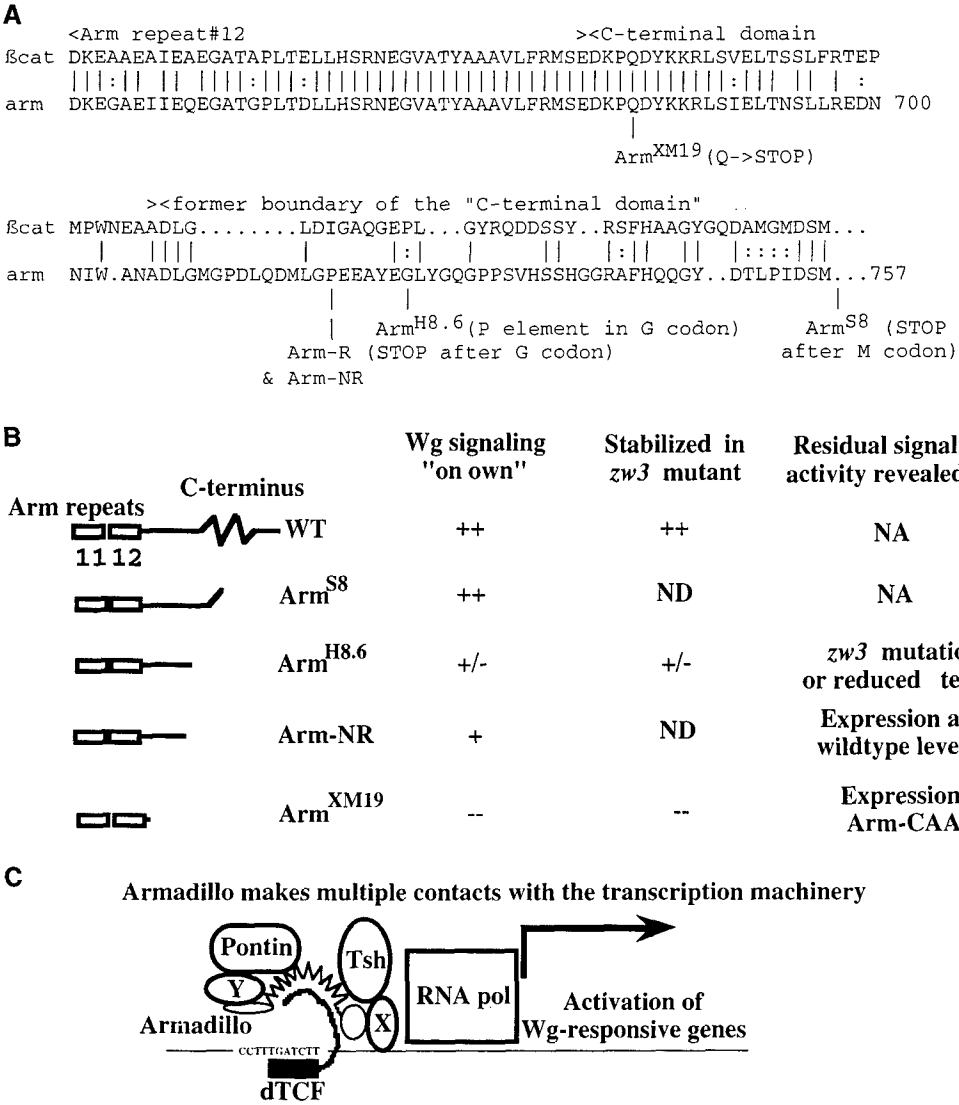

FIGURE 10.—Signaling and the C terminus. (A) Comparison of the proximal C-terminal domains of Arm and βcat, displaying the old and new boundaries of the C-terminal domain and the positions of the truncations in different Arm mutants. (B) Summary of the signaling activities of different C-terminally truncated mutant Arm proteins. NA, not applicable; ND, not determined. (C) Model in which Arm contacts the transcriptional machinery via multiple additive contacts.

of their binding by modulation of the affinity of the interaction of the C terminus *vs.* that of other heterologous partners. Such competition might even help explain the effect of the C terminus on stability discussed above—by competing for Arm interaction with cadherins and/or APC, the C terminus could regulate Arm stability, and its removal might thus alter the stability of Arm.

Arm protein lacking the entire C-terminal domain retains residual signaling ability: While previous work suggested that $Arm^{H8.6}$ might retain some signaling function, we were quite surprised to learn that Arm^{XM19}, lacking the entire C-terminal domain, retains detectable activity in Wg signaling. This was revealed by expression of membrane-tethered Arm-CAAX in an *arm*^{XM19} background. Arm-CAAX retains no signaling ability of its own (Cox *et al.* 1999), and thus the ability of Arm-CAAX to strongly stimulate signaling by Arm^{XM19} demonstrates that Arm^{XM19} retains residual activity in Wg signaling.

This raises the question of how membrane-tethered Arm promotes signaling by Arm^{XM19}. We first examined whether Arm-CAAX blocks the machinery that normally targets free Arm for destruction (as does tethered βcat in Xenopus; MILLER and MOON 1997). Arm-CAAX coexpression did not noticeably stabilize total Arm^{XM19}. Instead, we suspect that the major effect of Arm-CAAX is mediated by its ability to displace Arm^{XM19} from adherens junctions. Arm-CAAX retains function in adherens junctions and binds both DE-cadherin and α-catenin (Cox *et al.* 1999); as it is tethered to the membrane it may outcompete Arm^{XM19} for the available cadherin binding sites. Consistent with this, Arm-CAAX expression reduced the levels of Arm^{XM19} in the membrane-bound pool. Thus, Arm-CAAX may displace Arm^{XM19} into the soluble pool, where it would be available for signaling. Consistent with this model for the effect of Arm-CAAX, a different form of membrane-tethered Arm, Arm-TM, which does not localize to adherens junctions, does not significantly augment signaling by Arm^{XM19}.

Our data reinforce the idea that small changes in total Arm levels can produce large changes in signaling. A twofold increase in maternal *arm* (WIESCHAUS and

Noell 1986) or slight changes in cadherin dosage, which alter free Arm levels (Cox *et al.* 1996; Sanson *et al.* 1996), significantly stimulate signaling. In Xenopus, twofold or less differences in βcat levels on the dorsal *vs.* ventral sides trigger dorsal axis formation (Larabell *et al.* 1997). Several factors are likely to contribute to this threshold effect. Most important, the multiplicity of Arm partners and their differences in affinity for Arm mean that one partner can serve as a sink for active Arm. In a normal cell, most Arm is bound to cadherin; signaling-active dTCF-bound Arm is likely only a small fraction of the total Arm present. Once cadherins are saturated with Arm, small increases in total Arm lead to large increases in Arm available to interact with dTCF. Arm^{XM19} protein, present at lower levels than normal wild-type protein, may be particularly susceptible to such sequestration.

Theoretically, C-terminally truncated Arm, which retains the ability to bind dTCF (van de Wetering *et al.* 1997), could also promote signaling by titrating dTCF, preventing it from acting as a repressor (Cavallo *et al.* 1998). A comparison of the phenotypes of different mutants, however, suggests that this is not the case. *wg* null mutants have a very strong segment polarity phenotype, reflecting the lack of activation of Wg-responsive genes by Arm/dTCF complexes, but they retain repression mediated by dTCF/Groucho complexes (Cavallo *et al.* 1998). In contrast, embryos that are null for zygotic dTCF have substantial reductions in both activator and repressor functions of dTCF and thus have a milder phenotype, intermediate between that of a wild-type embryo and a *wg* mutant, retaining residual expression of Wg-responsive genes (Cavallo *et al.* 1998). If C-terminally truncated Arm, by binding dTCF, abolished its ability to repress Wg-responsive genes, the phenotype of such a mutant should be like that of *dTCF*. Instead, embryos carrying only C-terminally truncated Arm resemble *wg* null mutants, consistent with a failure to effectively antagonize repression.

Armadillo is likely to contact the transcriptional machinery through several protein interfaces: Since Arm protein lacking the C terminus retains detectable function in signaling, other regions of Arm may also interact with the basal transcriptional machinery or with other transcription factors, supplementing the role of the C terminus (Figure 10C). One accessory signaling interface is likely to reside in the C-terminal half of the Arm repeat region, as assayed by genetic and functional experiments in both Drosophila (Peifer and Wieschaus 1990; Orsulic and Peifer 1996) and in Xenopus (Behrens *et al.* 1996; Fagatto *et al.* 1996; Rubenstein *et al.* 1997). A second contact site resides in the N-terminal Arm repeats (Arm repeats 2–5), where βcat has been shown to bind to Pontin52, which in turn binds TATA-box binding protein; βcat and Pontin52 can form a tripartite complex with LEF/TCF proteins (Bauer *et al.* 1998). Finally, the N-terminal domain, while not essential for signaling *in vivo* (Orsulic and Peifer 1996; Pai *et al.* 1997), does contain sequences that can act as a transcriptional activation domain in cultured cells (Hsu *et al.* 1998). Together with the one or more binding sites for the transcriptional machinery present in the C-terminal domain, these multiple protein contacts may contribute in an additive or synergistic fashion to Arm transcriptional activation *in vivo*.

We thank Jennifer Fox and Mary Teachey for assistance with the two-hybrid experiments, Kathy Matthews and the Bloomington Drosophila Stock Center for providing fly stocks, and Jenny Adam, Bob Duronio, Amy Bejsovec, Mike Klymkowsky, Jeff Miller, and members of the Peifer lab for helpful discussions. This work was supported by grants from the National Institutes of Health (GM-47857) and the U.S. Army Breast Cancer Research Program (DAMD17-98-1-8223) to M.P., and a Pfizer Summer Undergraduate Research Fellowship and a Thompson Undergraduate Research Award to J.S. R.T.C. was supported in part by National Institutes of Health 5T32 GM-07092, C.K. was supported by the National Cancer Institute of Canada with funds from the Terry Fox Run, and M.P. was supported in part by a Career Development Award from the U.S. Army Breast Cancer Research Program.

LITERATURE CITED

Aberle, H., H. Schwartz, H. Hoschuetzky and R. Kemler, 1996 Single amino acid substitutions in proteins of the *armadillo* gene family abolish their binding to α-catenin. J. Biol. Chem. **271:** 1520–1526.

Bauer, A., O. Huber and R. Kemler, 1998 Pontin52, an interaction partner of beta-catenin, binds to the TATA box binding protein. Proc. Natl. Acad. Sci. USA **95:** 14787–14792.

Behrens, J., J. P. von Kries, M. Kühl, L. Bruhn, D. Wedlich *et al.*, 1996 Functional interaction of beta-catenin with the transcription factor LEF-1. Nature **382:** 638–642.

Brand, A. H., and N. Perrimon, 1993 Targeted gene expression as a means of altering cell fates and generating dominant phenotypes. Development **118:** 401–415.

Brannon, M., M. Gomperts, L. Sumoy, R. T. Moon and D. Kimelman, 1997 A beta-catenin/XTcf-3 complex binds to the siamois promoter to regulate dorsal axis specification in Xenopus. Genes Dev. **11:** 2359–2370.

Brunner, E., O. Peter, L. Schweizer and K. Basler, 1997 *pangolin* encodes a Lef-1 homolog that acts downstream of Armadillo to transduce the Wingless signal. Nature **385:** 829–833.

Cadigan, K. M., and R. Nusse, 1997 Wnt signaling: a common theme in animal development. Genes Dev. **11:** 3286–3305.

Cavallo, R. A., R. T. Cox, M. M. Moline, J. Roose, G. A. Polevoy *et al.*, 1998 *Drosophila* TCF and Groucho interact to repress Wingless signaling activity. Nature **395:** 604–608.

Cox, R. T., C. Kirkpatrick and M. Peifer, 1996 Armadillo is required for adherens junction assembly, cell polarity, and morphogenesis during *Drosophila* embryogenesis. J. Cell Biol. **134:** 133–148.

Cox, R. T., L.-M. Pai, J. M. Miller, S. Orsulic, J. Stein *et al.*, 1999 Membrane-tethered *Drosophila* Armadillo cannot transduce Wingless signal on its own. Development **126:** 1327–1335.

Fagatto, F., N. Funayama, U. Glück and B. M. Gumbiner, 1996 Binding to cadherins antagonizes the signaling activity of β-catenin during axis formation in Xenopus. J. Cell Biol. **132:** 1105–1114.

Funayama, N., F. Fagatto, P. McCrea and B. M. Gumbiner, 1995 Embryonic axis induction by the Armadillo repeat domain of β-catenin: evidence for intracellular signaling. J. Cell Biol. **128:** 959–968.

Gallet, A., A. Erkner, B. Charroux, L. Fasano and S. Kerridge, 1998 Trunk-specific modulation of Wingless signaling in *Drosophila* by Teashirt binding to Armadillo. Curr. Biol. **8:** 893–902.

Gallet, A., C. Angelats, A. Erkner, B. Charroux, L. Fasano *et al.*, 1999 The C-terminal domain of Armadillo binds to hypophos-

phorylated Teashirt to modulate Wingless signalling in Drosophila. EMBO J. **18:** 2208–2217.

HSU, S. C., J. GALCERAN and R. GROSSCHEDL, 1998 Modulation of transcriptional regulation by LEF-1 in response to Wnt-1 signaling and association with β-catenin. Mol. Cell. Biol. **18:** 4807–4818.

HUBER, A. H., W. J. NELSON and W. I. WEIS, 1997 Three-dimensional structure of the armadillo repeat region of β-catenin. Cell **90:** 871–882.

KARNOVSKY, A., and M. W. KLYMKOWSKY, 1995 Anterior axis duplication in Xenopus induced by the over-expression of the cadherin-binding protein plakoglobin. Proc. Natl. Acad. Sci. USA **92:** 4522–4526.

KLINGENSMITH, J., E. NOLL and N. PERRIMON, 1989 The segment polarity phenotype of *Drosophila* involves differential tendencies toward transformation and cell death. Dev. Biol. **134:** 130–145.

LARABELL, C., M. TORRES, B. A. ROWNING, C. YOST, J. R. MILLER *et al.*, 1997 Establishment of the dorso-ventral axis in *Xenopus* embryos is presaged by early asymmetries in β-catenin that are modulated by the Wnt signaling pathway. J. Cell Biol. **136:** 1123–1136.

MERRIAM, J. M., A. B. RUBENSTEIN and M. W. KLYMKOWSKY, 1997 Cytoplasmically anchored plakoglobin induces a Wnt-like phenotype in Xenopus. Dev. Biol. **185:** 67–81.

MILLER, J. R., and R. T. MOON, 1997 Analysis of the signaling activities of localization mutants of β-catenin during axis specification in *Xenopus*. J. Cell Biol. **139:** 229–243.

ORSULIC, S., and M. PEIFER, 1996 An in vivo structure-function analysis of armadillo, the β-catenin homologue, reveals both separate and overlapping regions of the protein required for cell adhesion and wingless signaling. J. Cell Biol. **134:** 1283–1301.

PAI, L.-M., C. KIRKPATRICK, J. BLANTON, H. ODA, M. TAKEICHI *et al.*, 1996 *Drosophila* α-catenin and E-cadherin bind to distinct regions of *Drosophila* Armadillo. J. Biol. Chem. **271:** 32411–32420.

PAI, L.-M., S. ORSULIC, A. BEJSOVEC and M. PEIFER, 1997 Negative regulation of Armadillo, a Wingless effector in *Drosophila*. Development **124:** 2255–2266.

PEIFER, M., 1993 The product of the *Drosophila* segment polarity gene *armadillo* is part of a multi-protein complex resembling the vertebrate adherens junction. J. Cell Sci. **105:** 993–1000.

PEIFER, M., and E. WIESCHAUS, 1990 The segment polarity gene *armadillo* encodes a functionally modular protein that is the *Drosophila* homolog of human plakoglobin. Cell **63:** 1167–1178.

PEIFER, M., C. RAUSKOLB, M. WILLIAMS, B. RIGGLEMAN and E. WIESCHAUS, 1991 The segment polarity gene *armadillo* affects the *wingless* signaling pathway in both embryonic and adult pattern formation. Development **111:** 1028–1043.

PEIFER, M., S. ORSULIC, D. SWEETON and E. WIESCHAUS, 1993 A role for the *Drosophila* segment polarity gene *armadillo* in cell adhesion and cytoskeletal integrity during oogenesis. Development **118:** 1191–1207.

PEIFER, M., D. SWEETON, M. CASEY and E. WIESCHAUS, 1994a *wingless* signal and Zeste-white 3 kinase trigger opposing changes in the intracellular distribution of Armadillo. Development **120:** 369–380.

PEIFER, M., L.-M. PAI and M. CASEY, 1994b Phosphorylation of the *Drosophila* adherens junction protein Armadillo: roles for Wingless signal and Zeste white-3 kinase. Dev. Biol. **166:** 543–556.

RIESE, J., X. YU, A. MUNNERLYN, S. ERESH, S.-C. HSU *et al.*, 1997 LEF-1, a nuclear factor coordinating signalling inputs from *wingless* and *decapentaplegic*. Cell **88:** 777–787.

ROCHELEAU, C. E., W. D. DOWNS, R. LIN, C. WITTMANN, Y. BEI *et al.*, 1997 Wnt signaling and an APC-related gene specify endoderm in early *C. elegans* embryos. Cell **90:** 707–716.

ROOSE, J., M. MOLENAAR, J. PETERSON, J. HURENKAMP, H. BRANTJES *et al.*, 1998 The Xenopus Wnt effector XTcf-3 interacts with Groucho-related transcriptional repressors. Nature **395:** 608–612.

RUBENSTEIN, A., J. MERRIAM and M. W. KLYMKOWSKY, 1997 Localizing the adhesive and signaling functions of plakoglobin. Dev. Genet. **20:** 91–102.

RUIZ-ECHEVARRIA, M. J., K. CZAPLINSKI and S. PELTZ, 1996 Making sense of nonsense in yeast. Trends Biochem. Sci. **21:** 433–438.

SANSON, B., P. WHITE and J.-P. VINCENT, 1996 Uncoupling cadherin-based adhesion from *wingless* signaling in *Drosophila*. Nature **383:** 627–630.

SUTER, B., and R. STEWARD, 1991 The role of the *Bicaudal-D* protein and its phosphorylation in *Drosophila* oocyte differentiation. Cell **67:** 917–926.

THORPE, C. J., A. SCHLESINGER, J. C. CARTER and B. BOWERMAN, 1997 Wnt signaling polarizes an early *C. elegans* blastomere to distinguish endoderm from mesoderm. Cell **90:** 695–705.

VAN DE WETERING, M., R. CAVALLO, D. DOOIJES, M. VAN BEEST, J. VAN ES *et al.*, 1997 Armadillo co-activates transcription driven by the product of the *Drosophila* segment polarity gene *dTCF*. Cell **88:** 789–799.

VLEMINCKX, K., R. KEMLER and A. HECHT, 1999 The C-terminal transactivation domain of β-catenin is necessary and sufficient for signaling by the LEF-1/βcatenin complex in *Xenopus laevis*. Mech. Dev. **81:** 65–74.

WHITE, P., H. ABERLE and J.-P. VINCENT, 1998 Signaling and adhesion activities of mammalian β-catenin and plakoglobin in *Drosophila*. J. Cell Biol. **140:** 183–195.

WIESCHAUS, E., and E. NOELL, 1986 Specificity of embryonic lethal mutations in *Drosophila* analyzed in germline clones. Roux's Arch. Dev. Biol. **195:** 63–73.

WIESCHAUS, E., and C. NÜSSLEIN-VOLHARD, 1986 Looking at embryos, pp. 199–228 in *Drosophila, A Practical Approach*, edited by D. B. ROBERTS. IRL Press, Oxford, England.

Communicating editor: V. G. FINNERTY

Cell Biology

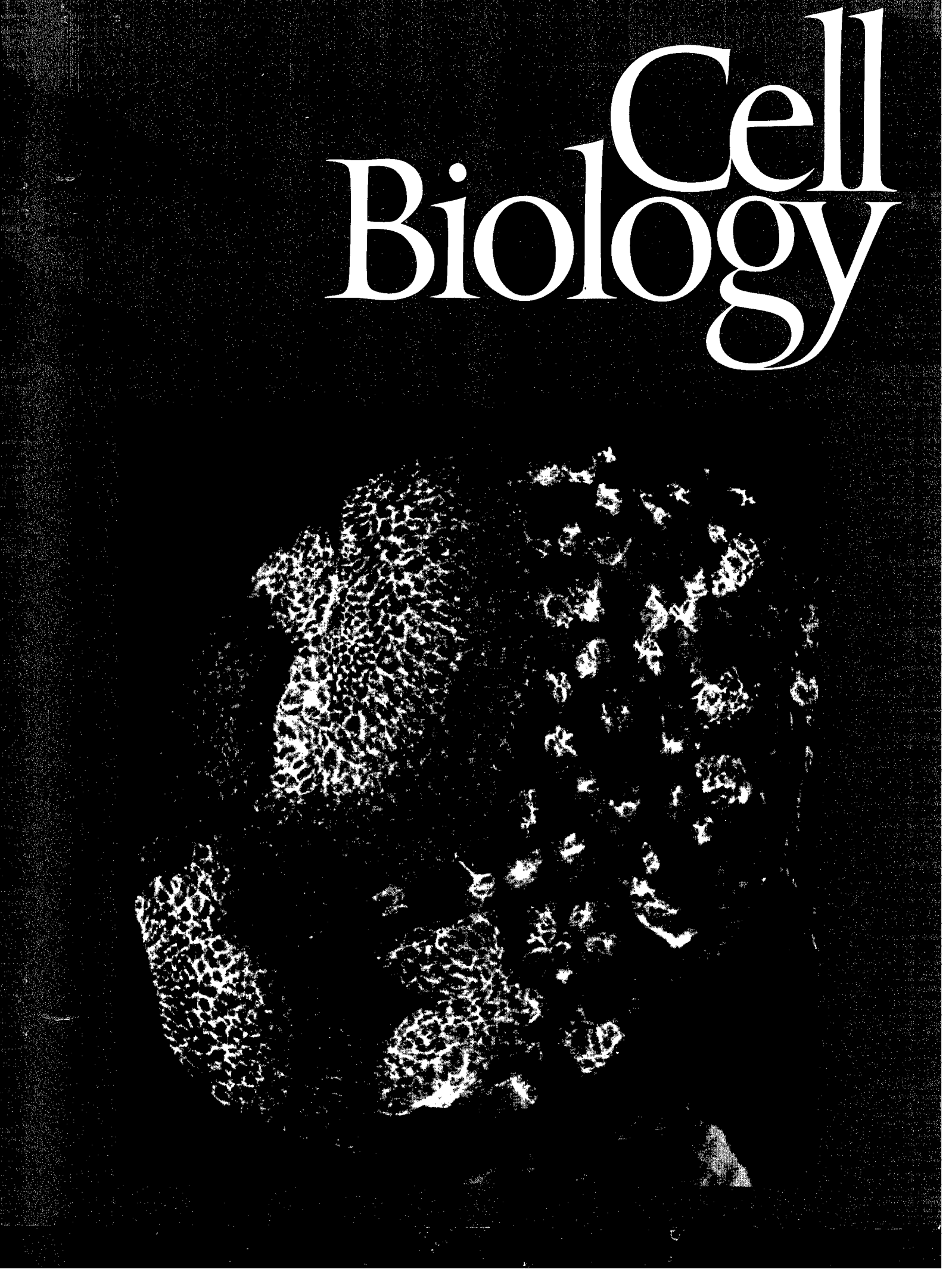

Drosophila APC2 Is a Cytoskeletally-associated Protein that Regulates Wingless Signaling in the Embryonic Epidermis

Brooke M. McCartney,* Herman A. Dierick,‡ Catherine Kirkpatrick,* Melissa M. Moline,‡ Annette Baas,* Mark Peifer,* and Amy Bejsovec‡

*Department of Biology, University of North Carolina at Chapel Hill, Chapel Hill, North Carolina 27599-3280; and
‡Department of Biochemistry, Molecular Biology, and Cell Biology, Northwestern University, Evanston, Illinois 60208-3500

Abstract. The tumor suppressor adenomatous polyposis coli (APC) negatively regulates Wingless (Wg)/Wnt signal transduction by helping target the Wnt effector β-catenin or its *Drosophila* homologue Armadillo (Arm) for destruction. In cultured mammalian cells, APC localizes to the cell cortex near the ends of microtubules. *Drosophila* APC (dAPC) negatively regulates Arm signaling, but only in a limited set of tissues. We describe a second fly APC, dAPC2, which binds Arm and is expressed in a broad spectrum of tissues. dAPC2's subcellular localization revealed colocalization with actin in many but not all cellular contexts, and also suggested a possible interaction with astral microtubules. For example, dAPC2 has a striking asymmetric distribution in neuroblasts, and dAPC2 colocalizes with assembling actin filaments at the base of developing larval denticles. We identified a *dAPC2* mutation, revealing that dAPC2 is a negative regulator of Wg signaling in the embryonic epidermis. This allele acts genetically downstream of *wg*, and upstream of *arm*, *dTCF*, and, surprisingly, *dishevelled*. We discuss the implications of our results for Wg signaling, and suggest a role for dAPC2 as a mediator of Wg effects on the cytoskeleton. We also speculate on more general roles that APCs may play in cytoskeletal dynamics.

Key words: *Drosophila* • adenomatous polyposis coli • Armadillo • β-catenin • Wingless

HUMAN β-catenin (βcat)[1] and its *Drosophila* homologue Armadillo (Arm) are key effectors of the conserved Wingless (Wg)/Wnt signal transduction pathway (for review see Gumbiner, 1998). In the absence of Wg signal, Arm in the cytoplasm is targeted for destruction by a multiprotein complex. Wg signal inactivates the destruction machinery, permitting accumulation of Arm in the cytoplasm and nucleus. Arm forms a complex with the DNA-binding protein, dTCF, to alter expression of Wg-responsive genes. Wnt signaling was implicated in colon cancer through the study of familial adenomatous polyposis, an inherited disease which results in early-onset colon cancer due to an increase in the frequency of benign colon polyps. These patients are heterozygous for a mutation in the adenomatous polyposis coli (APC) tumor suppressor; somatic disruption of the second copy of *APC* initiates polyp development (for review see Polakis, 1999). APC is part of the Arm/βcat destruction complex, along with Axin and the kinase Zeste-white 3 (Zw3)/glycogen synthase kinase 3β (GSK). In cells of a colon polyp, loss of APC function disables the destruction complex, leading to βcat accumulation, formation of βcat–TCF complexes, and activation of Wnt target genes such as the oncogene c-myc. APC is also important during normal development: mice homozygous for *APC* mutations die before gastrulation (Moser et al., 1995). A *Drosophila* homologue of APC, *dAPC* (Hayashi et al., 1997), acts as a negative regulator of Arm signaling in the photoreceptors of the developing adult eye (Ahmed et al., 1998).

APC's biochemical function in the destruction complex remains somewhat mysterious. It is thought to be a protein scaffold that binds numerous protein partners at distinct sites along its length (see Fig. 1) (for review see Polakis, 1999). APC was thought to facilitate interaction between βcat and GSK. However, Axin can also link βcat, GSK, and APC, raising questions about APC's role. Work in the nematode *Caenorhabditis elegans* suggests that APC's role

H.A. Dierick and C. Kirkpatrick contributed equally to this paper.

Address correspondence to Mark Peifer, Department of Biology, Coker Hall, CB#3280, University of North Carolina at Chapel Hill, Chapel Hill, NC 27599-3280. Tel.: (919) 962-2271. Fax: (919) 962-1625. E-mail: peifer@unc.edu; or Amy Bejsovec, Department of Biochemistry, Molecular Biology, and Cell Biology, Northwestern University, 2153 Sheridan Rd., Evanston, Illinois 60208-3500. Tel.: (847) 467-4042. Fax: (847) 467-1380. E-mail: bejsovec@nwu.edu

1. *Abbreviations used in this paper:* AEL, after egg laying; APC, adenomatous polyposis coli; Arm, Armadillo; βcat, β-catenin; BicD, Bicaudal D; Dsh, Dishevelled; dAPC, *Drosophila* APC; Fz, Frizzled; GSK, glycogen synthase kinase 3β; hAPC, human APC; Insc, Inscuteable; IP, immunoprecipitate; MT, microtubule; PP2A, protein phosphatase 2A; Wg, Wingless; Zw3, Zeste-white 3.

in Wnt signaling is more complex. Disruption of the closest nematode APC relative, *apr-1* (by double-stranded RNA interference), unexpectedly led to a phenotype similar to that of loss-of-function mutations in Wnt and Arm relatives, suggesting that APR-1 is a positive effector of Wnt signaling (for review see Han, 1997).

APC may also have additional cellular roles. When human APC (hAPC) is overexpressed in cultured cells, it decorates microtubules (MTs) and can bind and bundle MTs in vitro (Munemitsu et al., 1994; Smith et al., 1994). In cultured cells, APC localizes at the cell cortex in membrane puncta where bundles of MTs often terminate (Näthke et al., 1996). If one expresses a stabilized form of βcat (which cannot be phosphorylated by GSK) in MDCK cells, mutant βcat accumulates with APC in membrane puncta, and these cells display altered migratory behavior (for review see Barth et al., 1997). These data prompted the suggestion that APC may regulate cell migration via its interaction with MTs, and that this role is modulated by βcat. APC may also influence cytoskeletal dynamics by binding to EB1 (Su et al., 1995), which associates with the MT cytoskeleton in mammalian cells (Berrueta et al., 1998; Morrison et al., 1998). Yeast EB1 homologues contribute to MT function and may form part of a cytokinesis checkpoint (Beinhauer et al., 1997; Schwartz et al., 1997; Muhua et al., 1998). In addition to connections with MTs, APC may associate with the actin cytoskeleton via β- and α-catenin.

The actin and MT cytoskeletons are both targets of the Wg/Wnt pathway. Signaling by Wnt family members or by their Frizzled (Fz) receptors is required to orient certain cell divisions in both nematodes and flies. In *C. elegans*, Wnt signaling directs the orientation of mitotic spindles in specific early embryonic blastomeres and orients postembryonic asymmetric cell divisions (for review see Han, 1997), whereas in *Drosophila* Fz is required for orientation of the mitotic spindles of bristle precursor cells (Gho and Schweisguth, 1998). Fz also plays a key role in orienting the cytoskeleton during formation of hairs and bristles, polarized outgrowths of the cell membrane (for review see Shulman et al., 1998). Both the actin and MT cytoskeletons are required for hair positioning and growth (Wong and Adler, 1993; Turner and Adler, 1998).

Whereas dAPC regulates Arm signaling in the *Drosophila* larval photoreceptors (Ahmed et al., 1998), two features of dAPC were surprising given the widespread expression and essential function of mouse APC. Embryonic expression of dAPC is largely confined to the central nervous system (Hayashi et al., 1997), and null mutations in *dAPC* are viable and fertile, with strong effects only in the larval photoreceptors (Ahmed et al., 1998). These observations suggested the existence of a second APC gene in flies; a second mammalian APC has been identified (Nakagawa et al., 1998; van Es et al., 1999).

Materials and Methods

Biochemistry and Two-Hybrid Analysis

Extract preparation, immunoprecipitations (IPs), cell fractionation, and analysis of phosphorylation were as in Peifer (1993); anti-Arm IPs were at 1:40 and anti-dAPC2 IPs at 1:50. Samples were analyzed by 6% acrylamide SDS-PAGE, transferred to nitrocellulose, and immunoblotted with rat anti-dAPC2 (1:500), or mouse mAbs anti-Arm(7A1) at 1:500 (Peifer, 1993), anti–Bicaudal D (BicD) at 1:50, and anti–β-tubulin (Amersham Pharmacia Biotech) at 1:100, followed by ECL (Amersham Pharmacia Biotech) detection. Two-hybrid experiments were as in Pai et al. (1996). Yeast cells were transformed with plasmids encoding portions of the Arm repeat region fused to the LexA DNA binding domain and encoding fragments of dAPC or dAPC2 fused to the GAL4 activation domain; the control plasmid pCK4 expresses only the activation domain. Values are averages of duplicate β-galactosidase assays on more than six independent transformants.

Immunolocalization

Anti-dAPC2 antisera were raised in rats by Pocono Rabbit Farms against a GST-dAPC2 (amino acids 491–1061) fusion. Embryos were fixed in 37% formaldehyde/heptane (1:1) for 5 min (for anti–β-tubulin antibody, fix was 50 mM EGTA, pH 8, 33% formaldehyde). Larval tissues were fixed in 4% paraformaldehyde in PBS for 20 min. All were blocked and stained in PBS with 1% goat serum and 0.1% Triton X-100. Antibodies were used as follows: anti-dAPC2, 1:1,000; rabbit polyclonal antibody anti-Arm, 1:100; anti–β-tubulin (Amersham Pharmacia Biotech) 1:100; rhodamine phalloidin (Molecular Probes), 1:1,000; antiphosphohistone (Upstate Biotechnology), 1:200; anti-Prospero, 1:5 (kindly provided by C. Doe, University of Oregon, Eugene, OR).

Genetic Analysis

$dAPC2^{\Delta S}$ was induced by ethyl methanesulfonate (EMS) in a screen for suppressors of wg^{PE4}. $dAPC2^{\Delta S}$ also suppresses the null allele wg^{CX4}. Further analysis revealed that $dAPC2^{\Delta S}$ is a homozygous viable, temperature-sensitive maternal-effect lethal mutation mapping to 95E–F. Stocks for epistasis analysis were constructed at 18°C. Epistasis analysis was conducted at 25°C as in Table I. Antibody staining and RNA in situ hybridization were as in Dierick and Bejsovec (1998). Cuticle preparations were as in Wieschaus and Nüsslein-Volhard (1986). Genomic DNA from $dAPC2^{\Delta S}$ homozygotes, from the background chromosome, and from two wild-type stocks was subjected to PCR with overlapping sets of primers. PCR products were analyzed both by direct sequencing and by cloning into TA-vectors (Promega) and sequencing at least two independent clones.

Results

A Second Drosophila APC

10 expressed sequence tags from the Berkeley *Drosophila* Genome Project correspond to *dAPC2*; we obtained sequence of several cDNAs and the corresponding genomic region (we reported partial sequence in van Es et al., 1999; full sequence data available from EMBL/GenBank/DDBJ under accession no. AF091430). These predict a 1067 amino acid protein with striking similarity to other APC family members (Fig. 1) (for review of hAPC features see Polakis, 1999). All share an NH_2-terminal conserved domain, 6 Arm repeats, and a series of βcat binding (15 and 20 amino acid repeats) and Axin binding (SAMP repeats; Behrens et al., 1998) motifs. dAPC2 is shorter at its NH_2 and COOH termini than other APCs. dAPC2 lacks the COOH-terminal basic region (the putative MT binding site) found in hAPC and dAPC (Hayashi et al., 1997), as well as the hAPC region containing binding sites for Discs-large (DLG) and EB1. Substantial alternative splicing is unlikely, as there are only two small introns in coding sequences (63 and 197 nucleotides).

dAPC2 is most similar to other APC family members in the Arm repeats, where it most closely resembles dAPC; hAPC2 is more similar to hAPC (Fig. 1 B) (dAPC2 is 81% identical to dAPC and 57% identical to hAPC). Thus,

Table I. Drosophila Melanogaster Stocks Used in Epistasis Tests

Gene	Cross scheme	Results
wg	wg^{CX4}/CyO; $dAPC2^{\Delta S}$ females ×× males	All *wg* progeny show the suppressed phenotype ($n > 100$).
	wg^{CX4}/CyO; $dAPC2^{\Delta S}$/Df(3R)crb87-4 females ×× wg^{CX4}/+; +/Df(3R)crb87-4 males	1/3 of *wg* progeny show the suppressed phenotype ($n = 40$, *Df* homozygotes show *crumbs* phenotype).
arm	$arm^{H8.6}$/FM7/$dAPC2^{\Delta S}$ females ×× $dAPC2^{\Delta S}$ males	1/4 of the progeny show the *arm* zygotic phenotype (presumably $arm^{H8.6}$/Y; $dAPC2^{\Delta S}$ male embryos). 3/4 show excess naked cuticle like $dAPC2^{\Delta S}$ single mutants ($n > 200$).
dTCF	$dAPC2^{\Delta S}$; $dTCF^{3}$/ey^{D} females ×× males	1/4 of the progeny show the *dTCF* zygotic phenotype, and the remainder have excess naked cuticle ($n > 200$).
dsh	1. dsh^{75} FRT101/FM7; $dAPC2^{\Delta S}$/TM6 females ×× ovo^{D1} FRT101/Y; hsp-FLP(F38); $dAPC2^{\Delta S}$ males	Zygotic loss of *dsh* does not modify the $dAPC2^{\Delta S}$ mutant phenotype.
	2. Heat-shock progeny as third instar larvae twice to induce recombination	
	3. From among progeny cross: dsh^{75} FRT101/ovo^{D1} FRT101; $dAPC2^{\Delta S}$ females ×× 1. $dAPC2^{\Delta S}$ males, 2. $dAPC2^{\Delta S}$/Df(3R)crb87-4 males, or 3. Df(3R)crb87-4/TM3 males	In the first ($n > 30$) and second ($n = 23$) crosses, 1/2 the progeny show the *dsh* germline clone mutant phenotype (presumed to be the dsh^{75}/Y; $dAPC2^{\Delta S}$ male embryos) and 1/2 show a partially suppressed $dAPC2^{\Delta S}$ mutant phenotype, due to paternal rescue of *dsh* ($n > 30$). The partial suppression of the $dAPC2^{\Delta S}$ mutant phenotype is more dramatic ventrally, with most denticle belts fully formed; the dorsal surface is largely unrescued. In the cross to Df(3R)crb87-4/TM3 males, some progeny hatch (presumably those that are paternally wild-type), but dead embryos show phenotypes identical to those in the other crosses ($n = 19$).

there is no correspondence between individual human and fly proteins, even though both phyla show neural-enriched isoforms, dAPC and hAPC2, suggesting independent gene duplications. All APCs have six Arm repeats; a putative seventh Arm repeat is much more divergent and is not identifiable in dAPC2. The NH_2-terminal conserved region (61% identity to dAPC vs. 44% identity to hAPC) distantly resembles the Arm repeat consensus and may form one or two degenerate Arm repeats. APC family members also share similarity COOH-terminal to the Arm repeats. hAPC has two sets of repeated βcat binding sites, the 15 and 20 amino acid repeats (for review see Polakis, 1999; dAPC features are from Hayashi et al., 1997; hAPC2 lacks 15 amino acid repeats). dAPC2 shares two of the three 15 amino acid repeats of dAPC. dAPC and dAPC2 have five 20 amino acid repeats, among which are interspersed SAMP repeats (Fig. 1 C). dAPC has four SAMP repeats, whereas dAPC2 has two. dAPC2 ends 40 amino acids after the last SAMP repeat.

dAPC2 Protein

We generated antisera to a dAPC2 fusion protein (amino acids 491–1061); antisera from two independent rats immunized with this antigen both recognize a single set of protein isoforms of ~155–170 kD in embryonic extracts (Fig. 2 A) (they occasionally weakly cross-react with proteins of ~120 and > 200 kD). In contrast, the preimmune sera do not recognize any proteins on immunoblots of embryo extract, supporting the specificity of the antisera. Further, as we show below, the migration on SDS-PAGE of the putative dAPC2 protein is altered in a *dAPC2* mutant, consistent with these protein isoforms representing the genuine dAPC2 protein. The predicted molecular mass of dAPC2, 117 kD, is smaller than the observed molecular mass. However, an epitope-tagged version of the dAPC2 open reading frame expressed in human SW480 colon carcinoma cells also migrated at much higher apparent molecular mass than predicted from the sum of the predicted molecular mass of the dAPC2 coding sequence plus that of the epitope (Fig. 2 A). This suggests that the large apparent molecular mass of dAPC2 is a property of its migration on SDS-PAGE. We examined the developmental profile of dAPC2 expression during embryogenesis (Fig. 2 B). dAPC2 is present in the preblastoderm embryo (presumably maternally contributed), and levels remain relatively constant through the first half of embryogenesis, then drop sharply.

As hAPC is phosphorylated (e.g., Rubinfeld et al., 1996), we suspected that the dAPC2 isoforms might be phosphorylation variants. To test this, we immunoprecipitated (IPed) dAPC2 from embryos and treated the IPs with protein phosphatase 2A (PP2A), a serine/threonine-specific phosphatase. PP2A treatment reduced the apparent molecular mass of dAPC2; this effect was abolished if the PP2A inhibitor okadaic acid was included during incubation (Fig. 2 C, left panel). Further, if embryonic cells were dissociated and incubated in tissue culture medium, the apparent molecular mass of dAPC2 decreased (Fig. 2 C, right panel); this effect was also abolished by okadaic acid, suggesting that it is mediated by endogenous phosphatases. Parallel alterations in Arm phosphorylation support this hypothesis (Fig. 2 C, right panel) (Peifer, 1993). Taken together, these data suggest that the dAPC2 isoforms reflect, at least in part, differential phosphorylation.

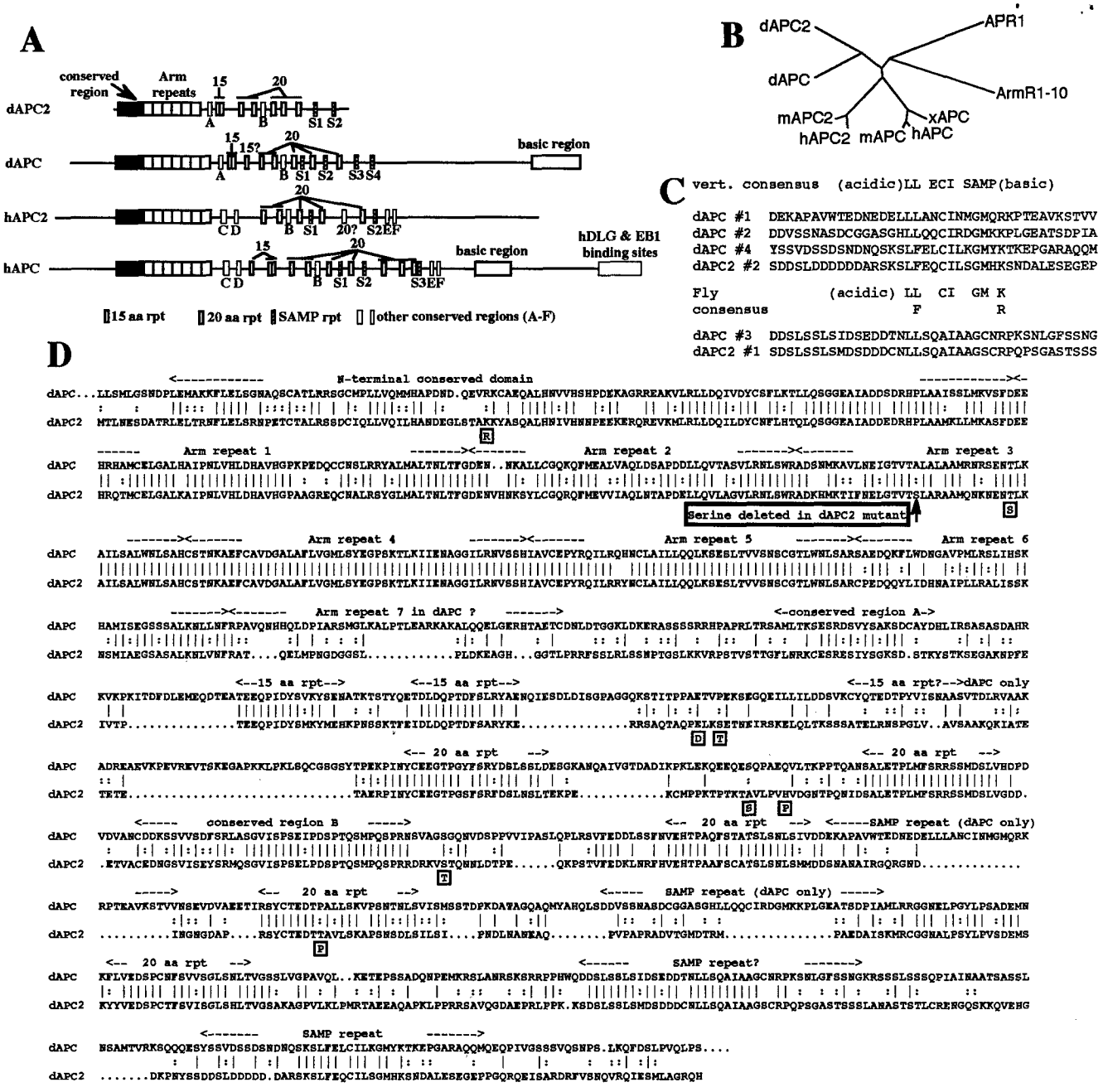

Figure 1. dAPC2. (A) Schematic diagrams of vertebrate and *Drosophila* APC proteins. Conserved sequence features are noted. A–F are conserved sequences of unknown function. The *dAPC2* start site was determined by the coincidence of the five longest Berkeley *Drosophila* Genome Project cDNAs and our 5′ rapid amplification of cDNA ends (RACE) cDNA products. (B) Unrooted tree showing relationships among the Arm repeats of APC family members from human, mouse, *Xenopus*, *Drosophila*, and *C. elegans*, as well as Arm repeats 1–10 of Arm. (C) Putative SAMP repeats of the *Drosophila* APCs. dAPC and dAPC2 share an additional sequence (bottom) which is a distant match to the SAMP motif. (D) Sequence comparison of dAPC and dAPC2, showing conserved domains. Below dAPC2 are listed polymorphisms on the background chromosome for $dAPC2^{\Delta S}$, and the position of the deleted serine in $dAPC2^{\Delta S}$. This residue is either serine or alanine in all APC family members, and this change is not found in five other wild-type strains.

dAPC2 Interacts Directly with Arm

hAPC and dAPC (Hayashi et al., 1997) bind to βcat and Arm, respectively. We tested whether dAPC2 also interacts with Arm in vivo. We immunoprecipitated Arm from embryonic extracts, and, in parallel, IPed proteins with a control mAb, anti-myc. dAPC2 specifically co-IPed with Arm from both early and older embryos (Fig. 2 D), but did not co-IP with the control anti-myc antibody. We were unable to detect Arm in anti-dAPC2 IPs (data not shown); because the antigen for the dAPC2 antisera includes the Arm binding region, these sera might not recognize a dAPC2–Arm complex. We also found that a dAPC2 fragment containing the putative βcat binding sites co-IPed with βcat when expressed in the human colorectal cancer cell line SW480 (data not shown).

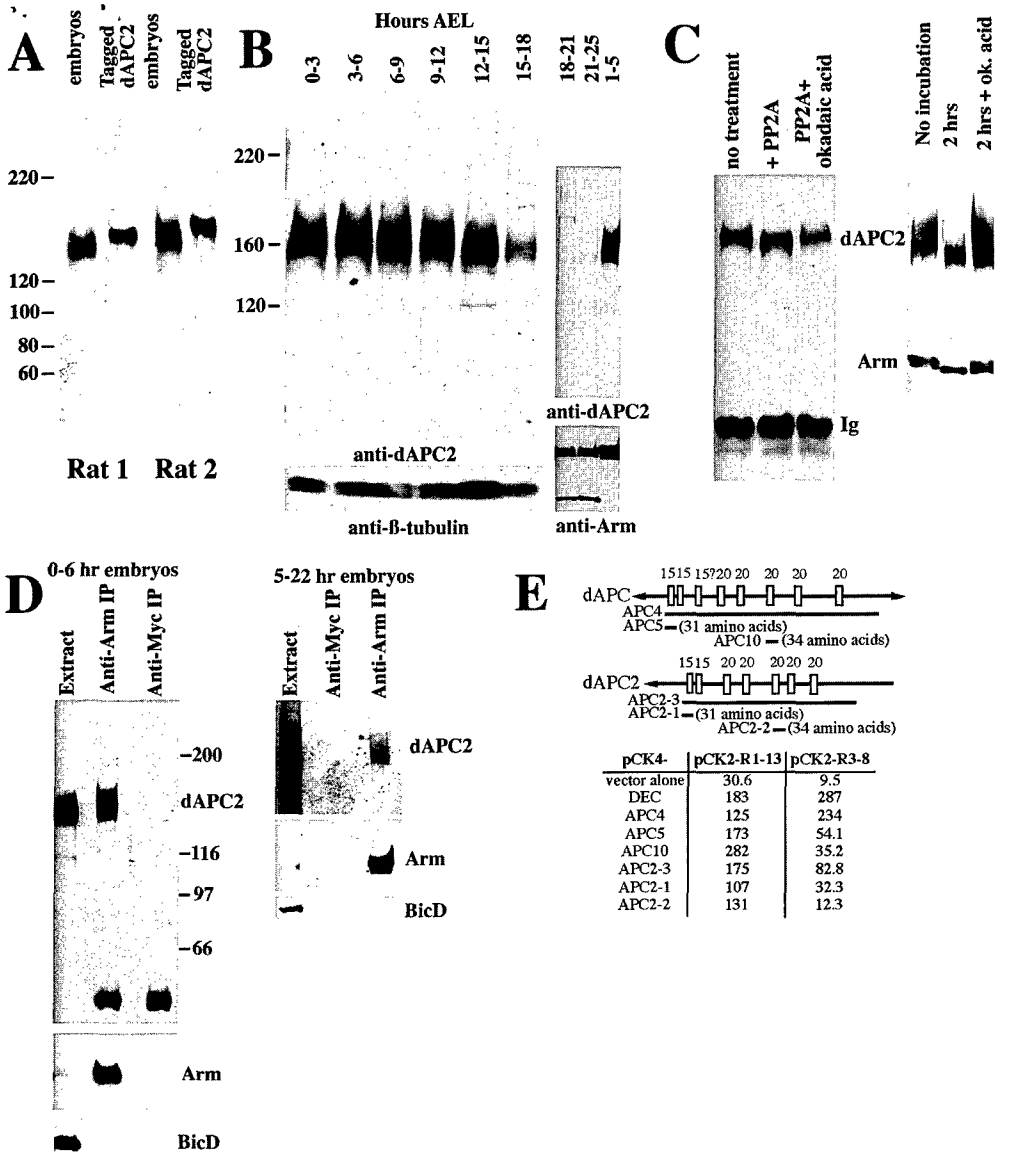

pCK4-	pCK2-R1-13	pCK2-R3-8
vector alone	30.6	9.5
DEC	183	287
APC4	125	234
APC5	173	54.1
APC10	282	35.2
APC2-3	175	82.8
APC2-1	107	32.3
APC2-2	131	12.3

Figure 2. dAPC2 protein properties. (A) dAPC2 protein. Extracts from 5–23-h *Drosophila* embryos and from human SW480 colon carcinoma cells expressing epitope-tagged dAPC2 coding sequences (the fusion protein includes a six-myc tag and additional amino acids at the fusion joint, raising its predicted molecular mass by 16 kD) were immunoblotted with anti-dAPC2 antisera from two independent rats immunized with our antigen. Most experiments in this paper were done with antisera from rat 2. (B) dAPC2 expression during embryogenesis. Extracts from embryos of the indicated ages AEL were immunoblotted with anti-dAPC2. β-Tubulin and Arm are loading controls. (C) dAPC2 is a phosphoprotein. (Left panel) Protein was immunoprecipitated from embryonic extracts with anti-dAPC2, left untreated, treated with PP2A, or treated with PP2A plus its inhibitor okadaic acid, and immunoblotted with anti-dAPC2. The apparent molecular mass of dAPC2 decreases upon phosphatase treatment. (Right panel) Dissociated gastrula stage embryonic cells were lysed immediately, or incubated in tissue culture medium for 2 h, in the absence or presence of the serine/threonine-specific phosphatase inhibitor okadaic acid. Extracts were immunoblotted with anti-dAPC2 or anti-Arm. During incubation, the apparent molecular mass of both dAPC2 and Arm is decreased; this is prevented by the phosphatase inhibitor. (D) dAPC2 associates with Arm in vivo. IPs with anti-Arm or anti-myc (a negative control) were done from embryonic extracts of 0–6-h (left panel) or 5–22-h (right panel) embryos. Extract and the IPs were immunoblotted with anti-dAPC2, anti-Arm, or anti-BicD (a negative control). dAPC2 specifically coimmunoprecipitated with anti-Arm. (E) dAPC2 binds Arm directly. β-Galactosidase activities were measured from yeast cells expressing the full Arm repeat region of Arm (pCK2-R1–13) or its centralmost Arm repeats (pCK2-R3–8) fused to a DNA-binding domain, together with various dAPC and dAPC2 fragments (diagrammed above) fused to a transcriptional activation domain. The empty vector and *Drosophila* E-cadherin (DEC) are negative and positive controls. Amino acid coordinates: APC4, APC5, and APC10 (751–1375, 751–781, and 1062–1095 of dAPC); APC2-3, APC2-1, and APC2-2 (491–991, 491–521, and 733–766 of dAPC2).

The hAPC–βcat interaction is direct, and is mediated by the 15 and 20 amino acid repeats of hAPC and the Arm repeats of βcat (for review see Polakis, 1999); the analogous region of dAPC binds Arm (Hayashi et al., 1997). To test whether dAPC2 directly interacts with Arm, we used the yeast two-hybrid system (Fig. 2 E), examining whether dAPC2's 15 and 20 amino acid repeats interact with the full set of Arm repeats of Arm (R1–13), or with the centralmost Arm repeats (R3–8; the binding site for *Drosophila* E-cadherin and dTCF). For comparison, we tested the 15 and 20 amino acid repeats of dAPC (Hayashi et al., 1997). The full 15 and 20 amino acid repeat regions of both dAPC and dAPC2 strongly interact with the entire Arm repeat region and with R3–8. We also tested 31–34 amino acid fragments carrying individual 15 or 20 amino acid repeats of dAPC and dAPC2 (selected as good matches to the consensus). Individual 15 amino acid repeats of either dAPC or dAPC2 interacted with both the entire Arm repeat region of Arm and with R3–8. An individual 20 amino acid repeat of dAPC also interacted with both Arm

fragments. A single 20 amino acid repeat of dAPC2 interacted strongly with Arm repeats 1–13; its interaction with R3–8 was much weaker.

dAPC2 Localization and the Actin and MT Cytoskeletons

To demonstrate that our anti-dAPC2 antisera are specific in situ, we determined that preimmune sera do not specifically stain any structures in *Drosophila* embryos, even at concentrations 10-fold higher than those we used below (data not shown). Our anti-dAPC2 sera also specifically stain mammalian cells engineered to express dAPC2 but not nontransfected cells (data not shown). The specificity of staining in situ is further supported by the change in intracellular localization seen in a dAPC2 mutant (see below), and by the fact that antisera from a second rat immunized with this antigen recognize a similar set of cellular structures (at least during midembryogenesis, the stage we examined).

Thus, we used our anti-dAPC2 antisera to characterize its expression and subcellular localization. During nuclear division cycles 10–13, which take place without cytokinesis in the peripheral cytoplasm of the embryo, dAPC2 shows dynamic changes in subcellular localization, coincident with those of actin (Fig. 3). Sequential changes in MT organization as nuclei proceed through mitosis direct reorganization of the cortical actin cytoskeleton (for review see Foe et al., 1993). Before nuclei migrate to the periphery, actin is found at the cortex in a random reticulum. When nuclei reach the periphery, actin condensations appear in interphase and prophase above each nucleus, forming an actin bud which overlays a cytoplasmic bud. This separates the mitotic apparatus of one nucleus from that of its neighbor. As division proceeds to metaphase, actin redistributes from the crown of the bud to its lateral cortex, forming an oblong ring around each spindle. During anaphase, actin redistributes into discs above each newly formed nucleus. Centrosomes and their associated MTs direct the changes in actin distribution, although the mechanism responsible for this interaction is not known.

In cycle 10–13 embryos, dAPC2 colocalizes with actin at all stages of mitosis (we could not test for colocalization with Arm, as its levels at these stages are too low to detect its localization). The dAPC2/actin colocalization is most prominent in the microvillar projections at the surface of the bud in interphase and prophase (Fig. 3, A–C). At metaphase and anaphase, dAPC2 and actin condensations are observed at the lateral cortex of the bud (Fig. 3, I–L); dAPC2 staining is somewhat less intense here relative to actin. Toward the base of the bud, condensations of actin and dAPC2 are also found in the region of the centrosome and asters (Fig. 3, E–H, arrows). These dAPC2 condensations occur within 0.3–0.5 μm of the surface of the embryo (data not shown), and thus are most prominent above the spindle apparatus; kinetochore MTs are not in uniform focus until ~1.25 μm from the surface of the embryo. The location of these dAPC2/actin condensations above the plane of the spindle places them in a position to interact with the astral MTs as they reach toward the cortex. During later nuclear cycles when pseudocleavage furrows are present, more defined dots of actin and dAPC2 staining are sometimes observed (Fig. 3, I–P, arrows) in the region of the centrosomes. In one of our wild-type stocks, which was infected with the bacterial endosymbiont *Wolbachia* (visible as small propidium iodide–positive bodies), we saw an additional APC2 localization. *Wolbachia* associate with astral MTs in *Drosophila* and thereby disperse into newly formed cells (Callaini et al., 1994; Kose and Karr, 1995). In infected embryos, dAPC2 localizes with the actin cytoskeleton as in uninfected stocks, and also associates with bacteria at the asters (Fig. 3 D). Another astral MT-associated protein, the kinesin-like protein KLP67A, is also reported to associate with bacteria (Pereira et al., 1997). EM studies have shown that the bacteria are encapsulated within a cytoplasmic vacuole attached to astral MTs via an electron-dense bridge, possibly composed of cellular MT-associated proteins (Callaini et al., 1994). dAPC2's localization to the aster region of noninfected embryos and its association with bacteria suggest that dAPC2 may contribute to the binding of the vacuole to the asters.

After cellularization, dAPC2 is still enriched in the region of MTs. Increased levels of cytoplasmic dAPC2 are observed in mitotic domains (groups of cells undergoing synchronous mitosis) (Fig. 4 D). Here, cytoplasmic condensations of dAPC2 are observed in the region of the spindle in metaphase and anaphase (Fig. 4, E and F, arrows), but are absent in prophase or telophase (the other cells in the mitotic domain in Fig. 4, E and F, are in prophase); serial sections revealed that these cytoplasmic condensations are most prominent within 2–4 μm of the cell apex. In mitotic domains of a *Wolbachia*-infected strain, we observed punctate condensations of dAPC2 near the spindle poles, presumably astrally associated bacteria (Fig. 4 G), consistent with dAPC2 localization to bacteria associated with preblastoderm asters.

dAPC2 is also expressed in dividing cells of the larval brain (Fig. 5). The optic lobes contain two proliferative regions, the inner and outer proliferative zones. dAPC2 is highly expressed in dividing cells of the proliferative zones and in their immediate progeny, but not in differentiated neurons (Fig. 5, A and C). In contrast, Arm is not enriched in the proliferative zones (Fig. 5, B and D) but is enriched in axons. In the ventral nerve cord, Arm is found in axons, whereas dAPC2 is found in midline glial cells (Fig. 5, C and D). In contrast, dAPC localizes to axons, at least in embryos (Hayashi et al., 1997).

However, in larval neuroblasts (neural stem cells) dAPC2 and Arm share a striking asymmetric distribution. Neuroblasts divide asymmetrically to produce a large neuroblast and a smaller ganglion mother cell, which will divide symmetrically to produce two neurons (for review see Fuerstenberg et al., 1998). The asymmetric division requires specific orientation of the mitotic spindle. Inscuteable (Insc), localized in a crescent opposite the future daughter cell during prophase and metaphase, is required for both spindle orientation and localization of the neural determinants Prospero and Numb (Kraut et al., 1996). In larval neuroblasts, both dAPC2 (Fig. 5 E, arrow) and Arm (Fig. 5 F, arrow) colocalize to a cortical crescent next to the future daughter cell; this crescent also includes the neural determinant Prospero (Fig. 5, H and I, arrow). In contrast to other asymmetric neuroblast components (for

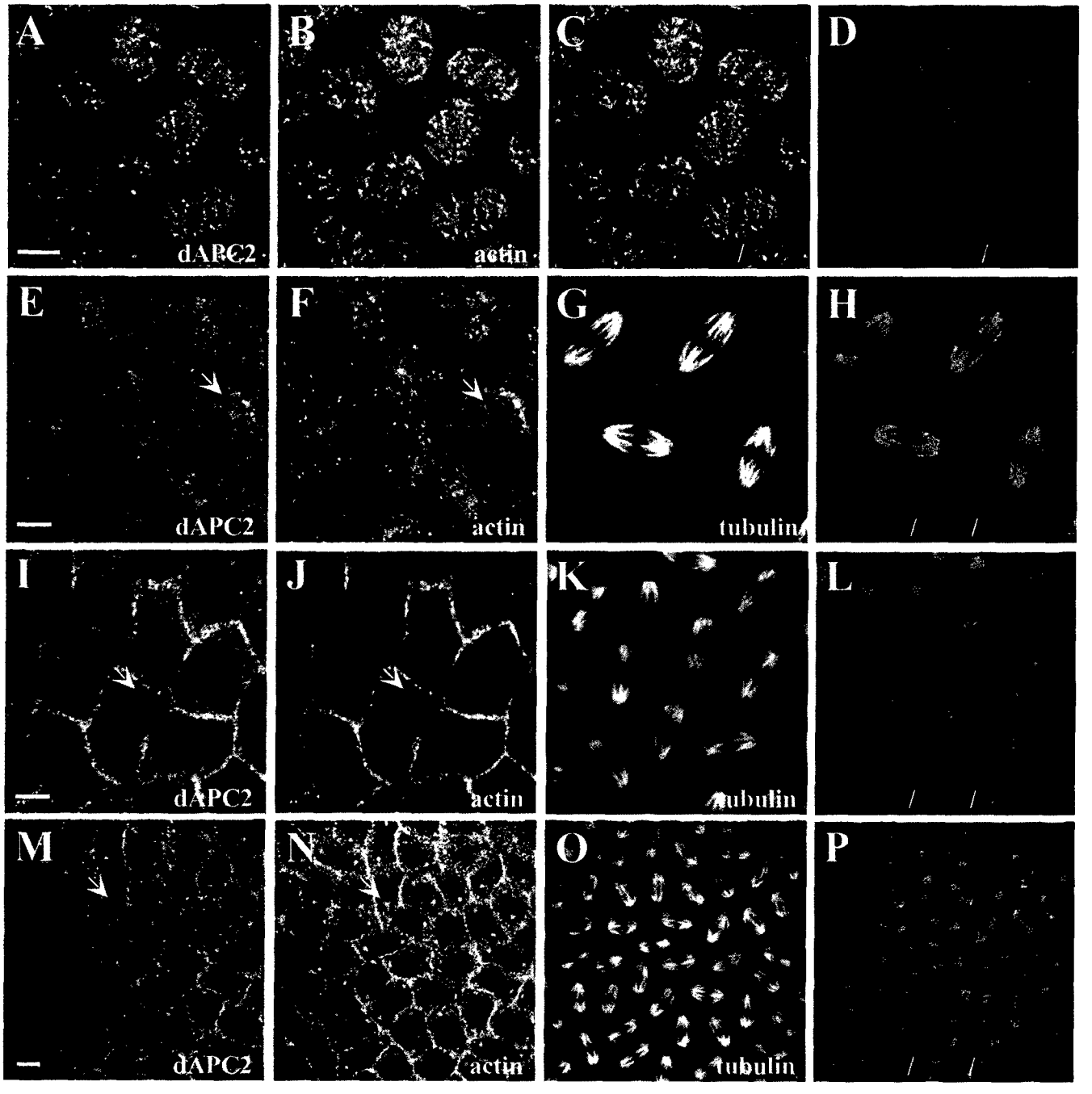

Figure 3. dAPC2 associates with actin in preblastoderm embryos. (A–C and E–P) Wild-type embryos labeled for dAPC2 (A, E, I, and M), actin (B, F, J, and N), and β-tubulin (G, K, and O). In the merged images of the triple-labeled wild-type embryos (H, L, and P), dAPC2 is blue, actin is red, and β-tubulin is green. (A–C) dAPC2 precisely colocalizes with actin in apical bud microvilli. (E–H) During cycle 10, dAPC2 and actin colocalize in halos in the region of the asters (arrows). (I–L) During cycle 11, dAPC2 and actin colocalize in the pseudocleavage furrows and in condensations at the centrosome (arrows). (M–P) During cycle 12, strong condensations of dAPC2 and actin were observed at the centrosome (arrows). (D) dAPC2 (red), β-tubulin (green). In embryos infected by *Wolbachia*, dAPC2 colocalizes with the bacteria at the asters. Bars: (A–H, M–P) 5 μm; (I–L) 7 μm.

review see Fuerstenberg et al., 1998), the dAPC2 and Arm crescents are present even at interphase (Fig. 5 E, lower neuroblast). In some neuroblasts, cortical actin also accumulates in a crescent with dAPC2 (Fig. 5, J and K, arrows), whereas in others this association is less apparent (Fig. 5, L and M, arrows). To examine the relationship between dAPC2 and the spindle, we triple-labeled neuroblasts with antibodies against phosphohistone, β-tubulin, and dAPC2 (Fig. 5, N–P). One pole of the spindle apparatus colocalizes with the dAPC2 crescent; dAPC2 is enriched at this point relative to the rest of the crescent (Fig. 5, O and P, arrows). We also observed low levels of dAPC2 at the opposite cortex at this stage of the cell cycle, the position of which often coincided with the other spin-

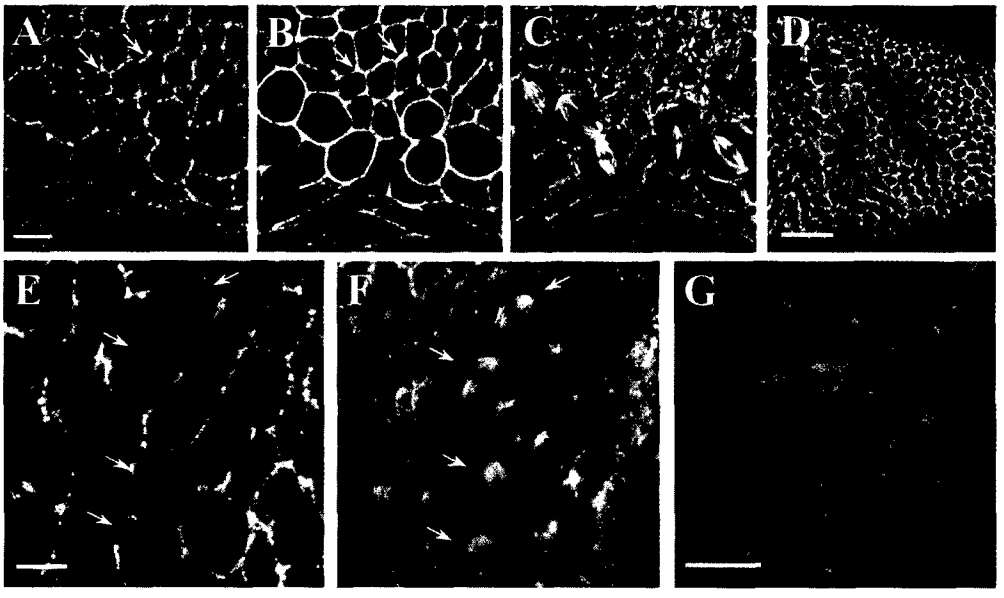

Figure 4. dAPC2 is associated with the cortex in cellularized embryos and with cytoplasmic condensations in dividing cells. (A–C) Wild-type embryos triple-labeled for dAPC2 (A), actin (B), and β-tubulin (C). dAPC2 is associated with the cortex in a punctate distribution corresponding to enrichments of actin (arrows). dAPC2 is not associated with actin at cleavage furrows. (D) Mitotic domain stained for dAPC2. Cytoplasmic dAPC2 is enhanced in dividing cells. (E and F) Wild-type mitotic domain stained for dAPC2 (E) and β-tubulin (F). Cytoplasmic condensations of dAPC2 were observed in the region of the spindle in dividing cells (arrows). (G) Mitotic domain in a *Wolbachia*-infected embryo stained for dAPC2 (red) and β-tubulin (green). dAPC2 is associated with bacteria in the region of the asters. Bars: (A–C, E–G) 5 μm; (D) 20 μm.

dle pole (Fig. 5, O and P, arrows). Whereas cortical dAPC2 associated with spindle poles, neuroblasts did not have cytoplasmic condensations of dAPC2 around the central spindle as were observed in epidermal cells. dAPC2 is also asymmetrically localized in embryonic neuroblasts (Fig. 5 G, arrows).

In nondividing cells, dAPC2 also associates with the cell cortex, and colocalizes with actin. In the embryo, dAPC2 is most strongly expressed in the epidermis and other epithelial cells. In the epidermis, dAPC2 is enriched at the cell cortex and is also found throughout the cytoplasm in a punctate distribution (Fig. 4 A). At the cortex, dAPC2 appears as numerous punctate condensations of protein (Fig. 4 A) which are most prevalent at the apical end of the lateral cell surface but are also found more basally. The most intense staining of dAPC2 appears at points of contact between multiple epidermal cells (Fig. 4 A, arrows). dAPC2 condensations often colocalize with condensations of actin (Fig. 4, A and B, arrows) and phosphotyrosine (data not shown), although actin and phosphotyrosine associate with the cortex more continuously. In fully polarized epithelial cells like the embryonic hindgut (Fig. 6, A and B) or the larval imaginal discs (Fig. 6, C and D), dAPC2 is enriched in adherens junctions, where it colocalizes with Arm; dAPC2 also accumulates on the apical plasma membrane (Fig. 6, A and C). The intracellular distribution of dAPC2 (Fig. 6 E), in contrast to that of Arm (Fig. 6 F), is not modulated in a segmental fashion. A strikingly different localization of dAPC2 occurs in the epidermis after stage 15. dAPC2 becomes organized into very large apical structures in segmentally repeated subsets of ventral epidermal cells (Fig. 6, G and H), just before the stage at which these cells initiate denticle formation. The dAPC2 structures occur specifically in anterior epidermal cells of each segment and colocalize with similar actin structures (Fig. 6, I–K), which likely represent larval denticle precursors.

Although dAPC2 colocalizes with actin in many tissues, it does not colocalize with actin in all contexts. For example, during cellularization, actin is prominent at the cellularization front, whereas dAPC2 is enriched at the apical cortex (data not shown). In addition, as we noted previously, at the cortex of epidermal cells actin is present at the membrane in a continuous fashion, whereas dAPC2 is restricted to regions of most intense actin staining. Finally, dAPC2 is not found with actin in cytokinesis furrows (Fig. 4, A and C). Thus, although dAPC2 associates with the actin cytoskeleton, the context-dependent nature of this association suggests that it is regulated.

Biochemical Properties of dAPC2

Biochemical analyses also suggest that dAPC2 associates with the cell cortex. When we fractionated 0–6-h-old embryos into soluble (S100) and membrane-associated (P100) fractions, dAPC2 partitioned almost equally into these two fractions (Fig. 7 A). In contrast, Arm was almost exclusively in the membrane fraction at this stage. The isoforms of dAPC2 in the membrane fraction migrated more rapidly on SDS-PAGE than those in either the soluble fraction or the total cell lysate (Fig. 7 A); because these isoforms are not detectable in total lysate, we suspect that they may arise during fractionation by dephosphorylation. To examine whether dAPC2 might associate with the membrane via a glycoprotein, we used Con A–Sepharose, which can be used to isolate membrane glycoproteins as well as proteins associated with them (e.g., Arm) (Peifer, 1993). A subset of dAPC2 specifically bound to Con A in extracts from 0–6-h embryos (Fig. 7 A; BicD was a negative control). Thus, dAPC2 may be anchored to the cortex via a transmembrane glycoprotein.

Identification of a dAPC2 Mutation

We mapped *dAPC2* to polytene region 95F1–2 on the

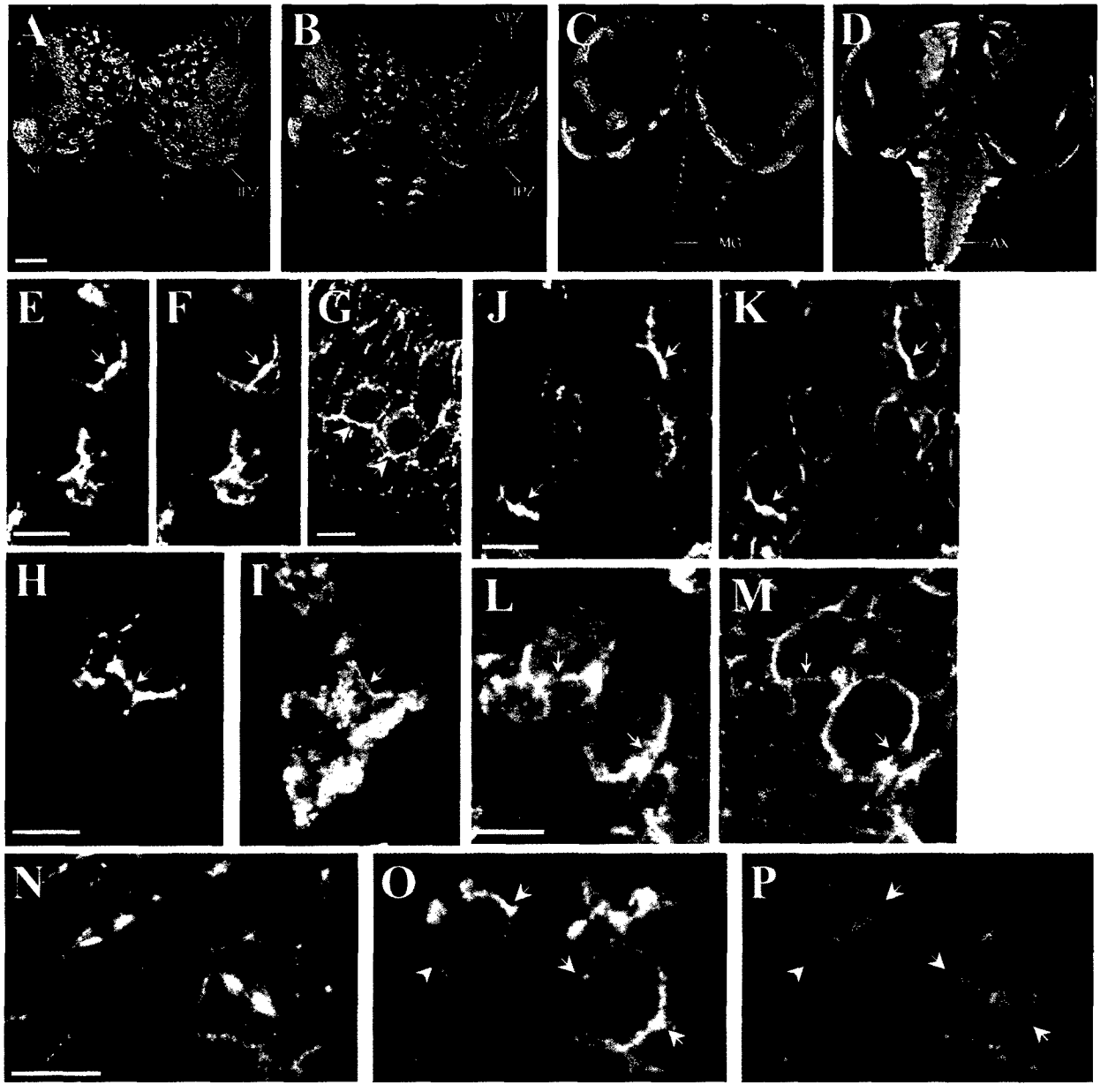

Figure 5. dAPC2 localization in dividing cells of the larval brain. (A–D) Third instar larval brain and ventral nerve cord double-labeled for dAPC2 (A and C) and Arm (B and D). OPZ, outer proliferative zone; IPZ, inner proliferative zone; NB, neuroblasts; MG, midline glia; AX, axons. (E, F, H, I, and J–M) Larval neuroblasts double-labeled for dAPC2 (E, H, J, and L), Arm (F), Prospero (I), and actin (K and M). dAPC2, Arm, and Prospero are asymmetrically localized at the cortex of neuroblasts. Actin is sometimes observed in crescents (K and M). (G) Embryonic neuroblasts labeled for dAPC2 reveal an asymmetric distribution (arrows). (N–P) Larval neuroblasts triple-labeled for β-tubulin (N and P, green), dAPC2 (O and P, red), and phosphohistone (P, blue). Condensations of dAPC2 occur in the region of the spindle poles (arrows). Bars: (A–D) 50 μm; (E–P) 10 μm.

third chromosome by in situ hybridization to wild-type and deficiency chromosomes. *dAPC2* is removed by *Df(3R)crb89-4* and *Df(3R)crb87-4* but not by *Df(3R) crb87-5* (data not shown). All three deficiencies remove *crumbs* and thus have a null *crumbs* phenotype (Tepass and Knust, 1990); thus, the severe epidermal fragmentation made examination of cuticular pattern impossible. During a genetic screen for suppressors of *wg*, we isolated a temperature-sensitive mutation which mapped to this genomic interval by complementation with the same deficiencies, and had a phenotype consistent with that of a negative regulator of Wg signaling (see below). Thus, we evaluated it as a candidate *dAPC2* mutation, sequencing *dAPC2* from the mutant and comparing its sequence to that of *dAPC2* in the parental stock from which the mutant was derived, and in several other wild-type stocks. The mutant and parental chromosomes share 33 polymorphisms relative to the wild-type Canton S; only 8 altered the protein, and most changes are conservative (Fig. 1 D). There is only a single difference between the parental chromosome and the mutant: deletion of three nucleotides, leading to deletion of serine 241. This serine residue

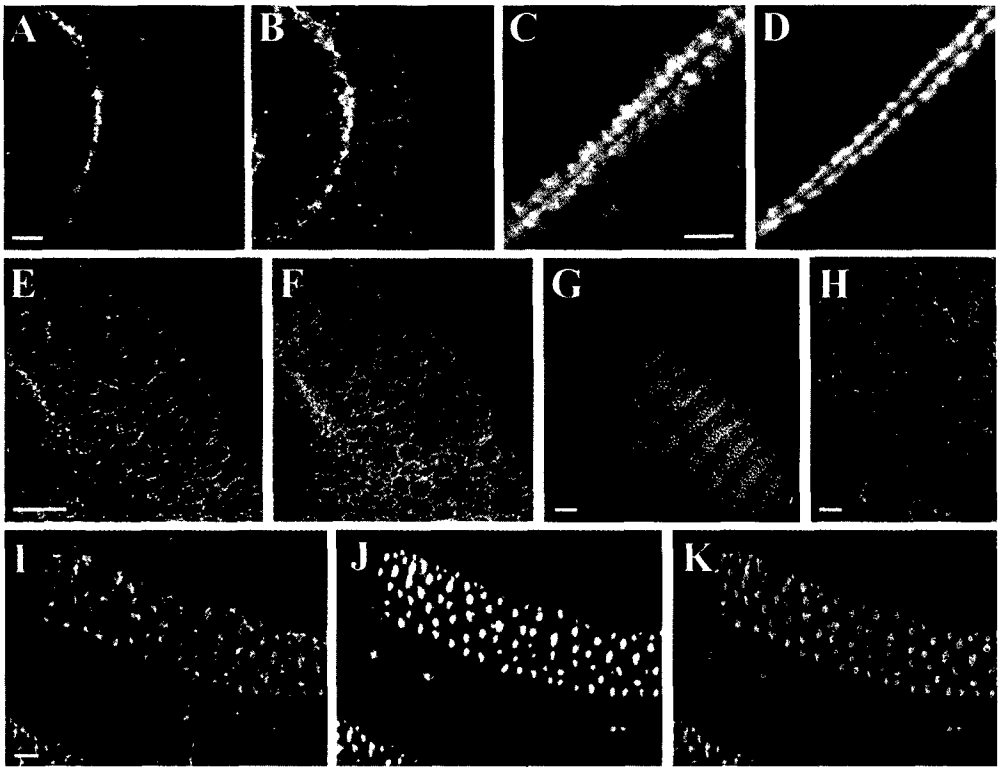

Figure 6. Localization of dAPC2 in epidermal and epithelial cells. The embryonic hindgut (A and B), wing imaginal disc (C and D), and early epidermis (E and F), double-labeled for dAPC2 (A, C, and E) and Arm (B, D, and F). (G) Stage 15 embryo labeled for dAPC2. Stripes of strong dAPC2 accumulation occur in the position of the developing denticles. (H) Stage 15 embryo double-labeled for dAPC2 (red) and Arm (green). Arm does not strongly colocalize with dAPC2 at the denticles. (I–K) Stage 15–16 embryo double-labeled for dAPC2 (I and K, red) and actin (J and K, green). They colocalize in the developing denticle. Bars: (A–D, H–K) 5 μm; (E–G) 25 μm.

falls within an alpha-helix in the third Arm repeat (by analogy to the Arm repeats of β-catenin) (Fig. 1 D). The length of this alpha-helix is invariant among APC family members, and this residue is either serine or alanine (a conservative change) in all APCs. Thus, we refer to this allele as *dAPC2*$^{\Delta S}$.

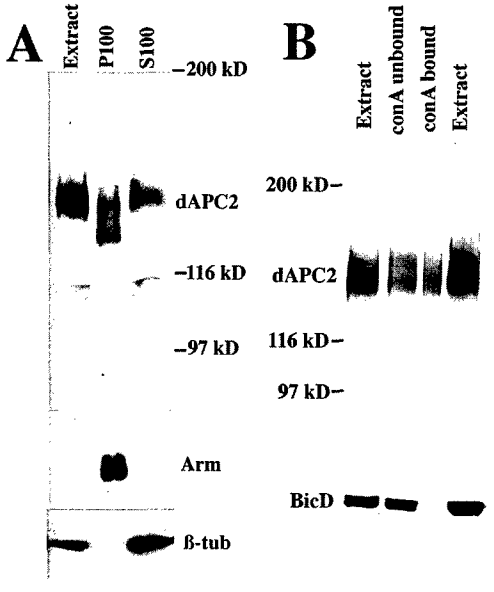

Figure 7. Biochemical properties of dAPC2. (A) dAPC2 is found in the membrane fraction. 0–6-h embryonic extract was fractionated into membrane (P100) and soluble (S100) fractions, and sequentially immunoblotted with anti-dAPC2, anti-Arm, and anti–β-tubulin. Arm and β-tubulin mark the different fractions. (B) A fraction of dAPC2 is bound to Con A. 0–6-h embryonic extract was fractionated using Con A–Sepharose, and sequentially immunoblotted with anti-dAPC2 and anti-BicD (a negative control).

Whereas homozygous mutant embryos accumulate normal levels of dAPC2, mutant dAPC2 migrates more rapidly on SDS-PAGE than wild-type protein (Fig. 8 M). A portion of dAPC2 in heterozygous mutants, which are wild-type in phenotype, also migrates abnormally (data not shown), suggesting that this is an intrinsic property of mutant dAPC2 rather than a consequence of the mutant phenotype. The subcellular localization of dAPC2 in *dAPC2*$^{\Delta S}$ mutants was dramatically altered at both the permissive (18°C) and restrictive (25°C) temperatures. At the restrictive temperature, dAPC2 association with the cell cortex is essentially abolished, rendering the protein almost completely cytoplasmic (Fig. 8 A vs. Fig. 8 D). At the permissive temperature, some cortical dAPC2 remains (Fig. 8 C). In heterozygotes, dAPC2 protein localization is intermediate between mutant and wild-type, as if mutant protein localizes incorrectly despite the presence of wild-type protein (Fig. 8 B). The loss of phosphorylated dAPC2 isoforms observed above (Fig. 8 M) may be a consequence of the loss of cortical association.

We also examined the localization of dAPC$^{\Delta S}$ mutant protein at the restrictive temperature in other tissues. Although dAPC$^{\Delta S}$ is found in apical buds in the preblastoderm embryo (Fig. 8, E and F), it no longer associates with actin structures as does the wild-type protein (Fig. 3, A–C). Furthermore, dAPC2$^{\Delta S}$ (Fig. 8 G) does not associate with the apical plasma membrane in the wing imaginal epithelia, marked by the presence of cortical actin (Fig. 8 H). In the larval neuroblasts, dAPC2$^{\Delta S}$ is largely cytoplasmic (Fig. 8, I and J), although an association with the cortex is sometimes observed (Fig. 8 I, arrow).

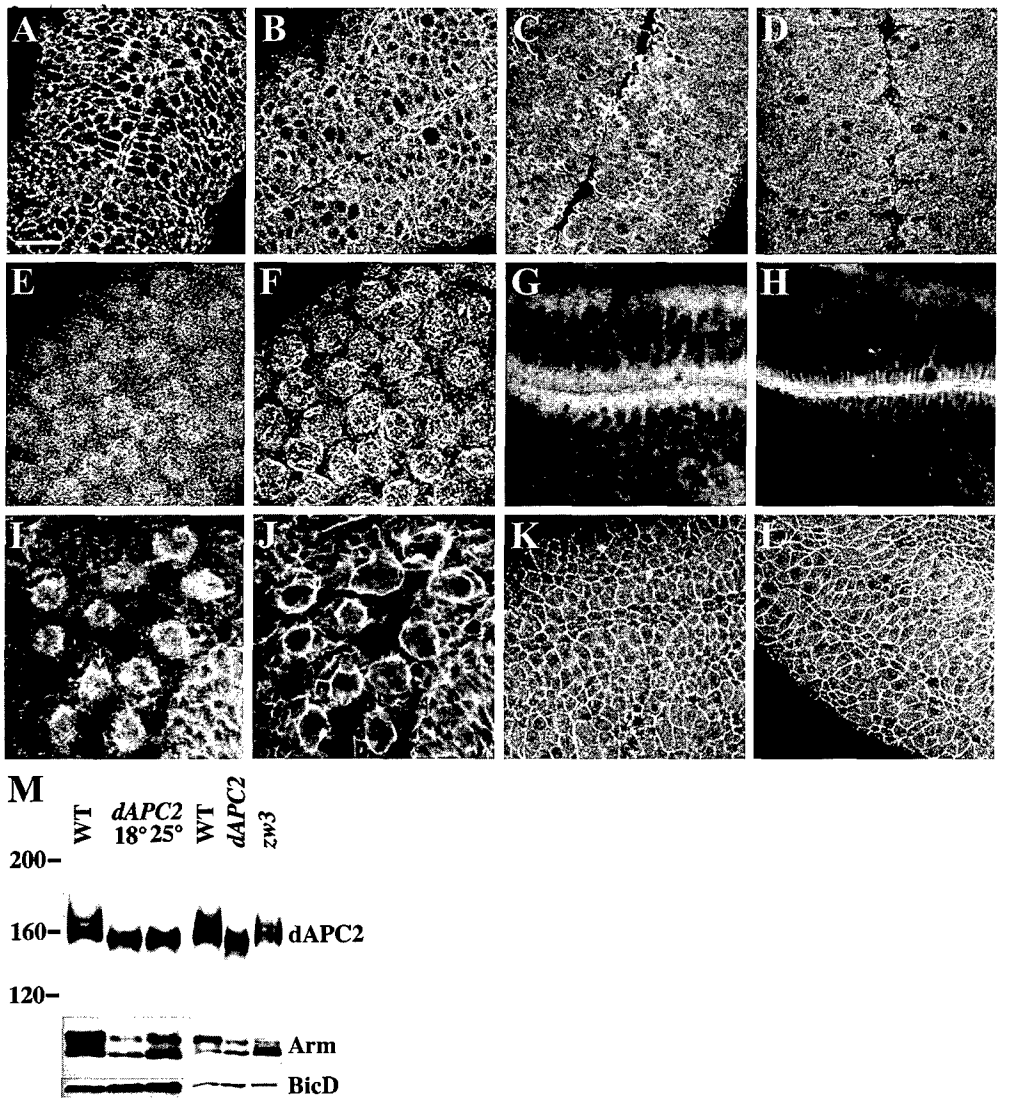

Figure 8. $dAPC2^{\Delta S}$ mutant protein is mislocalized. Embryos in A–D, K, and L are stage 9 of development. (A) Wild-type embryo labeled for dAPC2. dAPC2 is localized to the cell cortex and the cytoplasm. (B) $dAPC2^{\Delta S}$/+ embryo displays less cortical and more cytoplasmic dAPC2. (C and D) In embryos homozygous for $dAPC2^{\Delta S}$ cortical association of dAPC2 is largely abolished. This phenotype is more severe at the restrictive temperature (D, 25°C) than at the permissive temperature (C, 18°C). $dAPC2^{\Delta S}$ is found in apical buds (E) but is not associated with actin (F) in preblastoderm embryos. In the wing imaginal epithelium, $dAPC2^{\Delta S}$ (G) is not found in the adherens junction with actin (H). $dAPC2^{\Delta S}$ is localized to the cytoplasm in larval neuroblasts (I), although some cortical $dAPC2^{\Delta S}$ is observed (I, arrow). The neuroblast membranes are labeled with actin (J). (K–L) The localization of dAPC2 is unchanged in embryos ubiquitously expressing Wg (L) compared with wild-type (K). (M) dAPC2 and Arm proteins accumulate as lower molecular weight isoforms in $dAPC2^{\Delta S}$ homozygotes at both the permissive and restrictive temperatures. In *zw3* mutants, dAPC2 protein isoforms are unchanged, whereas the hypophosphorylated isoform of Arm accumulates. BicD is a loading control. Bars: (A–D, I–L) 20 μm; (E and F) 7 μm; (G and H) 10 μm.

dAPC2 Is a Negative Regulator of Wg Signaling in the Embryonic Epidermis

$dAPC2^{\Delta S}$ is viable and fertile at the permissive temperature (18°C). At the restrictive temperature (25°C), $dAPC2^{\Delta S}$ homozygous mutants derived from heterozygous mothers are viable, indicating that maternal contribution of dAPC2 is sufficient for embryonic development. Heterozygous embryos derived from homozygous mutant mothers are wild-type and survive to adulthood, suggesting that zygotic function is also sufficient. Mutant embryos derived from mutant mothers (referred to below as $dAPC2^{\Delta S}$ maternal/zygotic mutants) have severe abnormalities in their embryonic body plan. On the ventral surface, wild-type embryos show segmentally repeated denticle belts interspersed with naked cuticle (Fig. 9 A). In $dAPC2^{\Delta S}$ maternal/zygotic mutants, denticle belts are replaced with an almost uniform expanse of naked cuticle (Fig. 9 B), as is observed when *wg* is ubiquitously expressed (Fig. 9 D). The dorsal surface also has an array of pattern elements marking specific cell fates (Fig. 9 E); cells receiving Wg signal secrete fine hairs. On the dorsal surface of $dAPC2^{\Delta S}$ maternal/zygotic mutants, many more cells secrete fine hairs (Fig. 9 F), as they do when *wg* is ubiquitously expressed (data not shown). Thus, maternal/zygotic loss of *dAPC2* function activates Wg signal transduction both dorsally and ventrally, suggesting that wild-type dAPC2 helps negatively regulate this pathway.

Perturbing *dAPC2* function at defined developmental time points supports this hypothesis. At the permissive temperature, *dAPC2* mutant embryos develop normally into adults and a homozygous mutant stock can be maintained. When we shifted homozygous mutant embryos up to the restrictive temperature at 4 h after egg laying (AEL), they secreted uniform naked cuticle, like animals at the restrictive temperature throughout development. Progressively later upshifts result in intermediate cuticle defects, with increasing numbers of denticles secreted, until by 10 h AEL the pattern is essentially wild-type (data

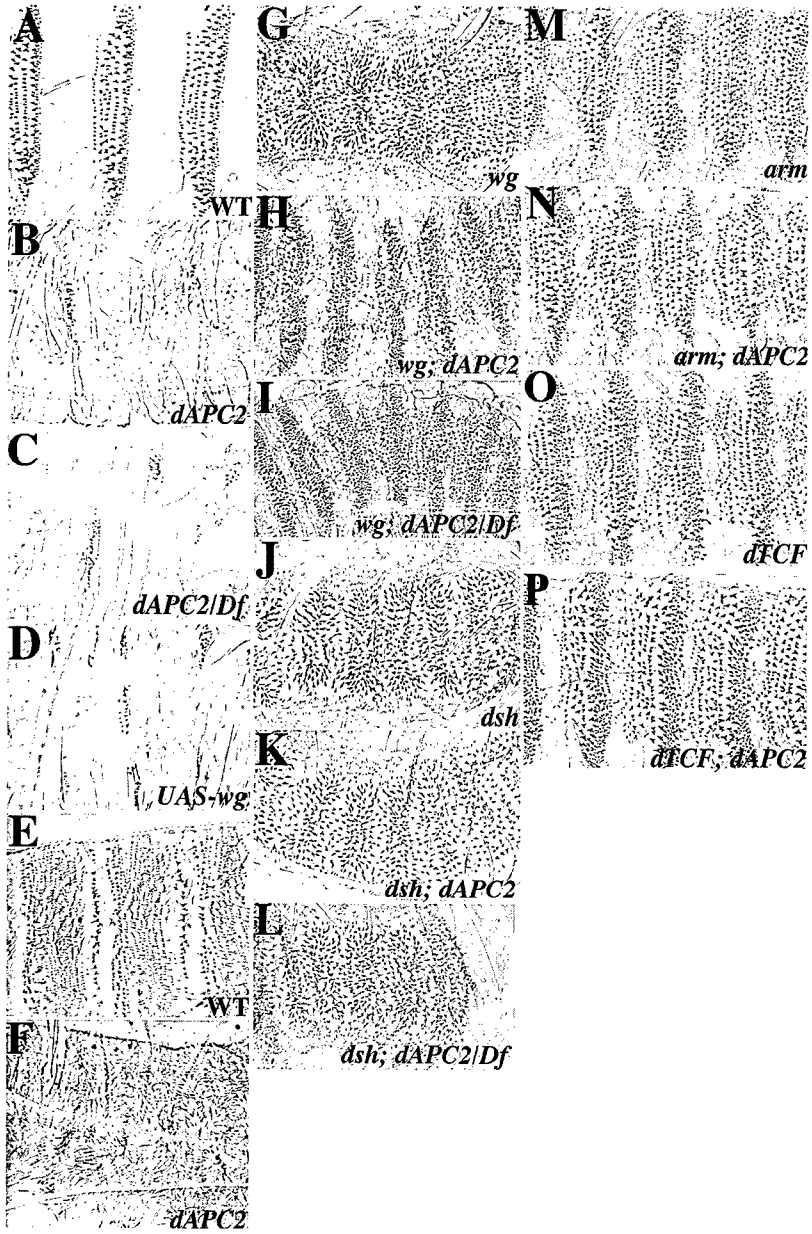

Figure 9. dAPC2 is a negative regulator of Wg signaling. (A) Wild-type cuticle pattern with alternating denticle belts and naked cuticle. (B) $dAPC2^{\Delta S}$ maternal/zygotic mutants show excess naked cuticle. (C) $dAPC2^{\Delta S}/Df(3)crb87\text{-}4$ embryos derived from $dAPC2^{\Delta S}/Df(3)crb87\text{-}4$ mothers are indistinguishable from $dAPC2^{\Delta S}$ homozygotes. (D) Embryo ubiquitously expressing upstream activation sequence (UAS)-Wg via the *e22c-GAL4* driver. (E) Dorsal surface of a wild-type embryo. (F) Dorsal surface of a $dAPC2^{\Delta S}$ maternal/zygotic mutant, covered with a uniform lawn of fine hairs. (G) wg^{CX4} (null) with a lawn of uniform denticles. (H and I) wg^{CX4}; $dAPC2^{\Delta S}$ homozygote (H) and wg^{CX4}; $dAPC2^{\Delta S}/Df(3R)crb87\text{-}4$ mutant (I) derived from $dAPC2^{\Delta S}$ mutant mother. The pattern is substantially but not completely rescued. (J, K, and L) dsh^{75} maternal/zygotic mutants (J), dsh^{75}; $dAPC2^{\Delta S}$ maternal/zygotic double mutants (K), and dsh^{75}; $dAPC2^{\Delta S}$ maternal/dsh^{75}/Y; $dAPC2^{\Delta S}/Df(3R)crb87\text{-}4$ zygotic mutants (L) are indistinguishable, with a *wg*-null–like phenotype. (M and N) $arm^{H8.6}$ homozygotes (M) and $arm^{H8.6}$; $dAPC2^{\Delta S}$ homozygous embryos derived from $dAPC2^{\Delta S}$ mutant mothers (N) are indistinguishable, with a weak *wg*-like phenotype. (O and P) $dTCF^{3}$ homozygotes (O) and $dAPC2^{\Delta S}$; $dTCF^{3}$ homozygous embryos from $dAPC2^{\Delta S}$ mutant mothers (P) are indistinguishable, with a weak *wg*-like phenotype.

not shown). Conversely, shifts from the restrictive temperature down to the permissive temperature at 4 h AEL fully rescue the pattern, whereas progressively later downshifts result in more and more naked cuticle replacing the ventral denticle belts. Thus, *dAPC2* activity is required between 4–10 h AEL, the same time window during which *wg* acts (Bejsovec and Martinez-Arias, 1991; Heemskerk et al., 1991). Somewhat surprisingly, *dAPC2* function may be dispensable for adult patterning; mutant embryos shifted up to the restrictive temperature after 10 h and cultured continuously at this temperature develop into apparently normal adults. This could be the result of partial activity of the $dAPC2^{\Delta S}$ allele. However, we suspect that $dAPC2^{\Delta S}$ is at least a strong hypomorph, as placing this allele over a deficiency for the region both in the mother and the zygote, does not increase the severity of the embryonic mutant phenotype at restrictive temperature (Fig. 9 C).

We carried out epistasis analysis to position *dAPC2* with respect to other components of the signal transduction pathway. *wg;* $dAPC2^{\Delta S}$ double mutant embryos (with $dAPC2^{\Delta S}$ mutant mothers) show a partial rescue of the *wg* phenotype, with restoration of the normal diversity of cuticular pattern elements and small expanses of naked cuticle (Fig. 9, G and H), suggesting that *dAPC2* is downstream of *wg*. There are two possible explanations for the fact that the double mutant does not show the same phenotype as the *dAPC2* single mutant: either $dAPC2^{\Delta S}$ is not null, or the negative regulatory machinery remains partially active in the absence of dAPC2. If $dAPC2^{\Delta S}$ is not null, we reasoned that repeating the epistasis test with $dAPC2^{\Delta S}$ in trans to a deficiency removing *dAPC2 (Df(3R)crb87-4)* might further reduce dAPC2 function, producing a double mutant phenotype more similar to that of $dAPC2^{\Delta S}$ alone. However, when we did this, there was no change in the double mutant phenotype (Fig. 9 I), sug-

gesting that $dAPC2^{\Delta S}$ may be genetically null for this function. Other components of the Wg signal transduction pathway act downstream of *dAPC2*. Embryos maternally and zygotically mutant for both *dishevelled* (*dsh*) and *dAPC2* (Fig. 9 K) show a phenotype indistinguishable from the *dsh* single mutant (Fig. 9 J), as do embryos maternally mutant for both *dsh* and *dAPC2* that are zygotically *dsh/Y; dAPC2*$^{\Delta S}$*/Df(3R)crb87-4* (Fig. 9 L). Likewise, *arm; dAPC2* and *dAPC2; dTCF* double mutants (derived from dAPC2 homozygous mothers) (Fig. 9, N and P) are indistinguishable from *arm* or *dTCF* single mutants (Fig. 9, M and O). Thus, *dsh*, *arm*, and *dTCF* all act genetically downstream of *dAPC2*; this was expected for *arm* and *dTCF*, but was surprising for *dsh*.

Loss of *dAPC2* also leads to ectopic activation of Wg-responsive genes. One target is *wg* itself. If the Wg pathway is constitutively activated by removing *zw3* function (Siegfried et al., 1992) or by expressing constitutively active Arm (Pai et al., 1997), an ectopic stripe of *wg* RNA is induced in each segment. A similar ectopic stripe of *wg* RNA is seen in $dAPC2^{\Delta S}$ maternal/zygotic mutants (Fig. 10, A and B). Similarly, the domain of expression of a second Wg target gene, *engrailed* (*en*), is expanded relative to wild-type (Fig. 10, G and H), as it is in *zw3* mutants or in the presence of activated Arm. In addition, a novel phenotype was observed. In $dAPC2^{\Delta S}$ maternal/zygotic mutants (Fig. 10, D and E), the levels of Wg protein are higher and Wg extends more cell diameters away from *wg*-expressing cells than in wild-type (Fig. 10 C). These effects on Wg protein do not appear to be accounted for solely by ectopic activation of *wg* RNA, as they are detected beginning at stage 9 before induction of ectopic *wg*, and they are not observed in embryos expressing activated Arm (Fig. 10 F). Thus, the efficiency of Wg protein transport (Dierick and Bejsovec, 1998) appears to be enhanced in *dAPC2* mutants.

dAPC2 mutant embryos still respond to Wg signaling, as segmental stripes of stabilized Arm remain (Fig. 10, I and J). In $dAPC2^{\Delta S}$ maternal/zygotic mutants, levels of cytoplasmic Arm in all cells are elevated, but cells receiving Wg signal continue to accumulate more Arm than their neighbors (Fig. 10 J). In contrast, *zw3* loss of function results in uniform accumulation of cytoplasmic Arm in all cells, eliminating the Arm stripes (Peifer et al., 1994). Immunoblot analysis of Arm protein from $dAPC2^{\Delta S}$ maternal/zygotic mutants revealed an accumulation of hypophosphorylated Arm (Fig. 8 M). This effect was not as dramatic as that seen in a *zw3* mutant (Fig. 8 M), but was similar to that seen upon ubiquitous expression of Wg using the *e22c-GAL4* driver (data not shown). Thus, the effect of $dAPC2^{\Delta S}$ on Arm levels is intermediate between that of wild-type and that of *zw3* loss of function, suggesting that negative regulation of Arm is reduced but not completely abolished in $dAPC2^{\Delta S}$.

As $dAPC2^{\Delta S}$ activates Wg signaling, we examined whether the change in its localization was simply a consequence of pathway activation. When we activated Wg signaling by ubiquitous Wg expression (via the *e22c-GAL4* driver) or by removing *zw3* function, the localization of dAPC2 was essentially unchanged, suggesting that pathway activation is not sufficient to eliminate cortical dAPC2 (Fig.8, K and L; data not shown). There was also

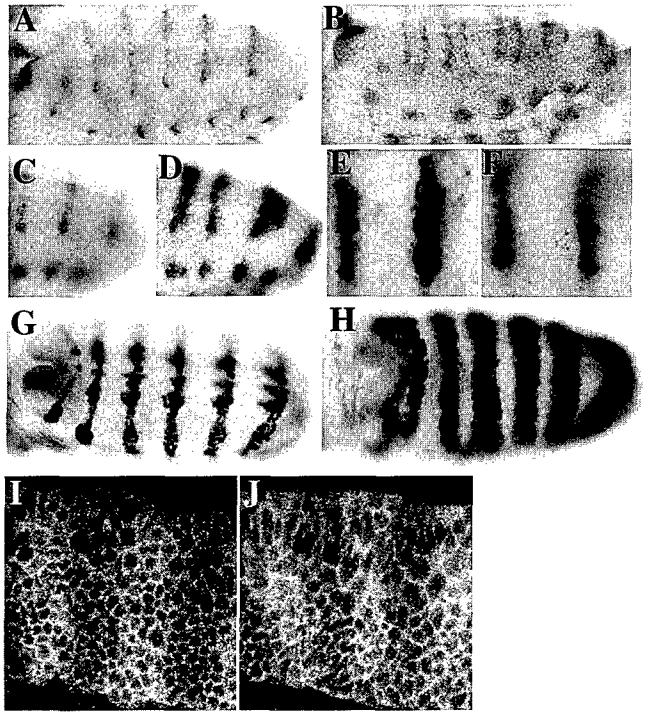

Figure 10. Molecular responses in $dAPC2^{\Delta S}$ mutants mimic Wg hyperactivity. (A) Wild-type *wg* RNA is expressed in one row of cells per segment. (B) In $dAPC2^{\Delta S}$ maternal/zygotic mutants, an ectopic stripe of *wg* is induced. (C) In wild-type embryos, Wg protein can be detected several cell diameters beyond the mRNA expression domain. (D) Wg is distributed over a greater distance in a $dAPC2^{\Delta S}$ maternal/zygotic mutant. (E) Close-up of Wg in $dAPC2^{\Delta S}$. (F) Wg in an embryo expressing activated Arm. (G) Wild-type Engrailed expression. (H) Engrailed expression is dramatically expanded in $dAPC2^{\Delta S}$ maternal/zygotic mutants. (I) In wild-type embryos, Arm protein is stabilized in cells receiving Wg signal, thus accumulating in broad stripes. (J) In $dAPC2^{\Delta S}$ maternal/zygotic mutants, Arm levels rise in both stripe and interstripe cells, but cells receiving Wg still accumulate more Arm.

no apparent change in dAPC2 protein levels or isoforms in *zw3* mutants relative to wild-type (Fig. 8 M); this was somewhat surprising as GSK phosphorylates hAPC (Rubinfeld et al., 1996), and suggests that dAPC2 can be phosphorylated by another kinase.

Discussion

dAPC2 and Wg Signaling

The current model for hAPC function suggests that it is part of the destruction machinery for βcat and thus, negatively regulates Wnt signaling. dAPC negatively regulates the Wg pathway in the *Drosophila* eye (Ahmed et al., 1998), although surprisingly not in other tissues. We examined the function of dAPC2, which shows a broader pattern of expression. dAPC2 interacts directly with Arm and negatively regulates Wg signaling in the embryonic epidermis, helping trigger Arm destruction. *dAPC2* mutant embryos resemble *zw3* mutants in cuticle phenotype and in ectopic activation of Wg target genes. One novel pheno-

type of $dAPC2^{\Delta S}$ is a broadening of the stripes of Wg protein, suggesting an effect on Wg transport (Dierick and Bejsovec, 1998). This is not observed when Wg signaling was activated by other means, suggesting that dAPC2 may have novel roles in Wg signaling.

In *zw3* mutants, cytoplasmic Arm levels rise sharply (Peifer et al., 1994). The effect of the $dAPC2^{\Delta S}$ mutation on Arm was similar but less severe. The current model for the destruction machinery is that Zw3, Axin, and APC function as a complex, facilitating Arm phosphorylation by Zw3 and thus targeting it for destruction (for review see Polakis, 1999). Axin can bind GSK/Zw3 and βcat/Arm independently of APC. Perhaps in the absence of dAPC2, Zw3 may still phosphorylate Arm, but not as effectively, explaining why loss of dAPC2 affects Arm stability less severely than does loss of Zw3. However, this conclusion is tempered by the fact that $dAPC2^{\Delta S}$ is not a protein-null, and in addition, other APC family members may play redundant roles.

Our epistasis tests between *dAPC2* and other components of the Wg pathway generally conform to earlier models of APC function, but also suggest further complexity. As expected, *dAPC2* acts downstream of *wg* and upstream of *arm* and *dTCF*. However, the suppression of *wg* by $dAPC2^{\Delta S}$ is incomplete. As above, this may be because $dAPC2^{\Delta S}$ is not null, because dAPC2 is not completely essential for Arm downregulation, or because of redundancy. In contrast to *zw3* (Siegfried et al., 1992), $dAPC2^{\Delta S}$ is genetically upstream of *dsh*. However, the relative positioning of dAPC2 and Dsh will not be definitive until a protein-null allele of *dAPC2* is available. Most current models place Dsh upstream of the destruction machinery, but the recent discovery that Dsh, along with Axin, APC, and Zw3/GSK, is a component of the destruction complex (Fagotto et al., 1999; Kishida et al., 1999; Smalley et al., 1999) reveals that these proteins may function as a network rather than as a linear series, making the results of epistasis tests more difficult to interpret. For example, the epistasis relationships might be explained if dAPC2 regulated assembly of Dsh into the destruction complex. In the absence of dAPC2, Dsh might constitutively turn off the destruction complex, activating signaling; thus, loss of dAPC2 would have no effect if Dsh is also absent.

The localization of dAPC2 to large membrane-associated structures is intriguing. Axin and Dsh also accumulate in large punctate, often cortical structures when overexpressed in vertebrate cells, and like dAPC2, a fraction of Axin associates with a glycoprotein (Axelrod et al., 1998; Fagotto et al., 1999; Kishida et al., 1999; Smalley et al., 1999). Colocalization experiments will reveal whether cortical dAPC2 puncta contain other components of the destruction machinery. In light of these data, the inability of $dAPC2^{\Delta S}$ to associate with the plasma membrane may be informative. Loss of serine 241 likely affects the secondary structure of the Arm repeats, which may affect dAPC2 binding to a protein partner at the membrane. A membrane-bound localization of the destruction complex, perhaps via dAPC2, could be essential for optimal function of the Wg pathway. Both mislocalization of mutant $dAPC2^{\Delta S}$ protein and the slight residual activity of the destruction complex in these mutants could be explained if Arm destruction continues, albeit at greatly reduced levels, in the cytosol. These speculative ideas can be tested in the future by examining colocalization of dAPC2 and other components of the destruction complex in wild-type embryos and in the various mutant backgrounds.

Although dAPC (Ahmed et al., 1998) and dAPC2 clearly negatively regulate the Wg pathway, misexpression of APC in *Xenopus* suggested an apparent positive role in Wnt signaling (Vleminckx et al., 1997). APR-1, the closest *C. elegans* APC relative, also appears to be a positive effector of Wnt signaling (Rocheleau et al., 1997). However, APR-1 is very distantly related to the APC family. APR-1's Arm repeats are only slightly more similar to those of APC than to the Arm repeats of Arm (Fig. 1 B). Whereas APR-1 has two highly divergent SAMP repeats (Rocheleau et al., 1997), it does not contain the conserved NH_2-terminal region or recognizable 15 or 20 amino acid repeats. Perhaps APR-1 is not an APC homologue, but instead plays a distinct role in the pathway.

$dAPC2^{\Delta S}$ adults are viable and morphologically normal, suggesting that dAPC2 may not be required for critical functions such as patterning imaginal discs. Since the phenotypic severity of $dAPC2^{\Delta S}$ homozygotes is similar to that of $dAPC2^{\Delta S}$/*Deficiency*, this allele is likely to be at least a strong hypomorph for Wg signaling in the embryonic epidermis. Although it is possible dAPC2 only functions there, its widespread expression at other stages suggests otherwise. Whether or not $dAPC2^{\Delta S}$ is a null, dAPC2 may still serve other functions. The specific effects of *dAPC2* (these data) and *dAPC* (Ahmed et al., 1998) mutations suggest that in some contexts they may be redundant. The possible other functions of dAPC2 remain to be tested by examining the effect of *dAPC2* mutations on processes such as neuroblast divisions, and by characterizing *dAPC dAPC2* double mutants.

dAPC2 and the Cytoskeleton

Previous studies of APC in vertebrate cultured cells revealed that APC localizes to the membrane and cytoplasm (e.g., Näthke et al., 1996), where it can associate with MTs (Munemitsu et al., 1994; Smith et al., 1994; Näthke et al., 1996). Our biochemical and localization studies of dAPC2 reveal a complex relationship between dAPC2 and the actin and MT cytoskeletons, suggesting potential functions for dAPC2 in regulation of the cytoskeleton.

dAPC2 colocalizes with actin in many but not all cell types, suggesting a regulated interaction. The association between the actin cytoskeleton and dAPC2 may occur via Arm and α-catenin, although in some places where dAPC2 and actin colocalize, there is little or no detectable Arm. The colocalization of dAPC2 and actin is intriguing given the effects of Wnt/Fz signaling on planar polarity in *Drosophila* (for review see Shulman et al., 1998; for possible effects of Wg see Tomlinson et al., 1997). In the wing, the best studied example, Fz signaling triggers asymmetric polymerization of actin, leading to development of an actin-based wing hair in the distal vertex of each hexagonal wing cell (Wong and Adler, 1993). The colocalization of actin and dAPC2 during the onset of denticle formation was particularly striking in this context, because the process of denticle formation is very similar to that of wing hair formation in the nature of the structure, its strict ori-

entation in the plane of the tissue, and in its cell biological and genetic bases. This raises the possibility that Wg/Wnt signaling directly affects the actin cytoskeleton and thus tissue polarity, using dAPC2 as an effector.

Although dAPC2 does not contain the basic region thought to mediate MT association of hAPC, our data are consistent with the possibility that dAPC2, like hAPC (Munemitsu et al., 1994; Smith et al., 1994; Näthke et al., 1996), may associate with MTs under certain circumstances. The data for a microtubule association of dAPC2 are less robust than those suggesting association with actin. Whereas dAPC2 does not prominently localize to most microtubule-based structures (nor does hAPC, unless overexpressed), dAPC2 localized to several places consistent with a role in anchoring microtubules. In preblastoderm embryos, when actin is essential for tethering the spindle to the membrane (for review see Foe et al., 1993), dAPC2 colocalizes with cortical actin and subcortical actin puncta. Subcortical dAPC2 is concentrated just above the spindle, placing it in a position to interact with astral MTs as they reach toward the cortex. Both dAPC2 and actin also localize to a dot-like structure which may be the centrosome. In postblastoderm embryos, dAPC2 is subtly enriched in the vicinity of the spindle.

The asymmetric localization of dAPC2 in dividing neuroblasts is also consistent with a possible role for dAPC2 in linking the spindle to the cortex. During neuroblast mitosis, the spindle is specifically oriented (for review see Fuerstenberg et al., 1998). Insc, which localizes to a crescent opposite the future daughter cell from late interphase through metaphase, coordinates the neuroblast asymmetric cell division (Kraut et al., 1996). Other proteins are likely to act in this process; e.g., Bazooka acts upstream of Insc (Kuchinke et al., 1998). In *C. elegans* (Waddle et al., 1994) and yeast (for review see Heil-Chapdelaine et al., 1999), actin or actin-associated proteins localize asymmetrically in cells in which spindle orientations are specified, suggesting a role for actin in this process. The position of actin in a crescent next to the future daughter cell in a subset of the neuroblasts suggests that actin may affect spindle orientation in *Drosophila* neuroblasts as well. dAPC2 may also play a role in this process. Within the crescent, dAPC2 localization was strongest in the region of the spindle pole. During later stages of mitosis, although dAPC2 remains enriched in a crescent next to the future daughter, dAPC2 also localizes to the cortex on the opposite side of the cell, often in the region of the other spindle pole. In contrast to other asymmetrically localized components of the neuroblast, dAPC2 localizes to a crescent during all stages of the cell cycle; in fact, the dAPC2 crescent was most apparent during interphase and prophase. dAPC2 and actin could also act as polarity markers for other proteins; actin is required for the asymmetric localization of Insc, Prospero, and Staufen (Broadus and Doe, 1997; Knoblich et al., 1997). We emphasize that the dAPC2/MT connection remains speculative. In the future we must directly test whether dAPC2 associates with MTs, whether it can affect spindle orientation, and whether dAPC2 and Arm function in the neuroblast asymmetric cell division.

We raise this issue in light of the influence of Wnt signaling on mitotic spindle orientation in both *C. elegans* embryos (Thorpe et al., 1997) and in *Drosophila* sensory cells (Gho and Schweisguth, 1998). In *C. elegans*, Wnt signaling controls spindle orientation independent of transcription (Schlesinger et al., 1999), suggesting that the Wnt pathway directly targets the cytoskeleton. Since dAPC2 regulates Wg/Wnt signal transduction and appears to have connections to the cytoskeleton, it is a candidate for a direct effector of this process. RNA interference studies of *C. elegans* relatives of Arm (WRM-1) and APC (APR-1) did not reveal defects in spindle orientation (Schlesinger et al., 1999), suggesting the existence of a branch to the cytoskeleton upstream of APC and Arm. However, because RNA interference may not completely remove gene function, and because of the divergence between APR-1 and the APC family noted above, the involvement of Arm and dAPC2 in the pathway remains plausible. These data are also intriguing in light of studies of the hAPC binding protein EB1 (Su et al., 1995), which colocalizes with the spindle, centrosome, and asters (Berrueta et al., 1998; Morrison et al., 1998). Budding and fission yeast EB1 homologues are required for spindle assembly and stability (Beinhauer et al., 1997; Schwartz et al., 1997; Muhua et al., 1998). However, it is worth noting that dAPC2 appears to lack the binding domain for EB1 identified in hAPC.

In summary, our results define a role for *Drosophila* APC2 in the negative regulation of Wg signaling in the embryonic epidermis, and raise the possibility that it may act upstream of Dsh. This supports the idea that different APC family members operate in different tissues. The localization of dAPC2 in vivo, together with previous studies of hAPC in cultured cells, raises the possibility that dAPC2 acts as an effector molecule through which Wnt signaling influences the cytoskeleton. Finally, because dAPC2 associates with the actin cytoskeleton in contexts where no Wg signaling is thought to occur, such as in preblastoderm embryos, dAPC2 may play more fundamental roles in cytoskeletal regulation. Such functions may be revealed by further genetic analyses of *dAPC* and *dAPC2*.

We thank S. Tiong, C. Southern, M. Teachey, and N. Vo for assistance; C. Doe, B. Duronio, T. Karr, P. Polakis, L. Rose, S. Selleck, and B. Theurkauf for tutorials and discussions; and S. Hayashi, E. Wieschaus, U. Tepass, P. Polakis, C. Doe, the Bloomington *Drosophila* Stock Center, the Berkeley *Drosophila* Genome Project, and R. Fehon and the Duke University Comprehensive Cancer Center's Shared Confocal Facility for essential reagents or equipment.

This work was funded by National Institutes of Health grant GM47857, a U.S. Army Breast Cancer Research Program Career Development Award and the Human Frontier Science Program (to M. Peifer), a National Science Foundation Career Award IBN-9734072 and National Science Foundation grant IBN 96-00539 (to A. Bejsovec), a National Research Service Award grant 1 F32 CA79172-01 (to B. McCartney), the National Cancer Institute of Canada (C. Kirkpatrick), and the Nederlandse Kankerbestrijding (A. Baas).

Submitted: 2 June 1999
Revised: 29 July 1999
Accepted: 9 August 1999

Note Added in Proof: While this manuscript was in review, a related work was published by Yu, X., L. Waltzer, and M. Bienz. 1999. *Nature Cell Biol.* 1:144–151.

References

Ahmed, Y., S. Hayashi, A. Levine, and E. Wieschaus. 1998. Regulation of Armadillo by a *Drosophila* APC inhibits neuronal apoptosis during retinal development. *Cell.* 93:1171–1182.

Axelrod, J.D., J.R. Miller, J.M. Shulman, R.T. Moon, and N. Perrimon. 1998. Differential recruitment of Dishevelled provides signaling specificity in the planar cell polarity and Wingless signaling pathways. *Genes Dev.* 12:2610–2622.

Barth, A.I., I.S. Nathke, and W.J. Nelson. 1997. Cadherins, catenins and APC protein: interplay between cytoskeletal complexes and signaling pathways. *Curr. Opin. Cell Biol.* 9:683–690.

Behrens, J., B.-A. Jerchow, M. Würtele, J. Grimm, C. Asbrand, R. Wirtz, M. Kühl, D. Wedlich, and W. Birchmeier. 1998. Functional interaction of an axin homolog, conductin, with β-catenin, APC, and GSK3β. *Science.* 280: 596–599.

Beinhauer, J.D., I.M. Hagan, J.H. Hegemann, and U. Fleig. 1997. Mal3, the fission yeast homologue of the human APC-interacting protein EB-1 is required for microtubule integrity and the maintenance of cell form. *J. Cell Biol.* 139:717–728.

Bejsovec, A., and A. Martinez-Arias. 1991. Roles of *wingless* in patterning the larval epidermis of *Drosophila. Development.* 113:471–485.

Berrueta, L., S.K. Kraeft, J.S. Tirnauer, S.C. Schuyler, L.B. Chen, D.E. Hill, D. Pellman, and B.E. Bierer. 1998. The adenomatous polyposis coli-binding protein EB1 is associated with cytoplasmic and spindle microtubules. *Proc. Natl. Acad. Sci. USA.* 95:10596–10601.

Broadus, J., and C.Q. Doe. 1997. Extrinsic cues, intrinsic cues and microfilaments regulate asymmetric protein localization in *Drosophila* neuroblasts. *Curr. Biol.* 7:827–835.

Callaini, G., G. Riparbelli, and R. Dallai. 1994. The distribution of cytoplasmic bacteria in the early *Drosophila* embryo is mediated by astral microtubules. *J. Cell Sci.* 107:673–682.

Dierick, H.A., and A. Bejsovec. 1998. Functional analysis of Wingless reveals a link between intercellular ligand transport and dorsal-cell-specific signaling. *Development.* 125:4729–4738.

Fagotto, F., E. Jho, L. Zeng, T. Kurth, T. Joos, C. Kaufmann, and F. Costantini. 1999. Domains of axin involved in protein–protein interactions, Wnt pathway inhibition, and intracellular localization. *J. Cell Biol.* 145:741–756.

Foe, V.E., G.M. Odell, and B.A. Edgar. 1993. Mitosis and morphogenesis in the *Drosophila* embryo: point and counterpoint. *In* The Development of *Drosophila.* M. Bate and A. Martinez-Arias, editors. Cold Spring Harbor Laboratory Press, Plainview, NY. 149–300.

Fuerstenberg, S., J. Broadus, and C.Q. Doe. 1998. Asymmetry and cell fate in the *Drosophila* embryonic CNS. *Int. J. Dev. Biol.* 42:379–383.

Gho, M., and F. Schweisguth. 1998. Frizzled signalling controls orientation of asymmetric sense organ precursor cell divisions in *Drosophila. Nature.* 393: 178–181.

Gumbiner, B.M. 1998. Propagation and localization of Wnt signaling. *Curr. Opin. Genet. Dev.* 8:430–435.

Han, M. 1997. Gut reaction to Wnt signaling in worms. *Cell.* 90:581–584.

Hayashi, S., B. Rubinfeld, B. Souza, P. Polakis, E. Wieschaus, and A. Levine. 1997. A *Drosophila* homolog of the tumor suppressor gene adenomatous polyposis coli down-regulates β-catenin but its zygotic expression is not essential for the regulation of Armadillo. *Proc. Nat. Acad. Sci. USA.* 94:242–247.

Heemskerk, J., S. DiNardo, R. Kostriken, and P.H. O'Farrell. 1991. Multiple modes of *engrailed* regulation in the progression towards cell fate determination. *Nature.* 352:404–410.

Heil-Chapdelaine, R.A., N.R. Adames, and J.A. Cooper. 1999. Formin' the connection between microtubules and the cell cortex. *J. Cell Biol.* 144:809–811.

Kishida, S., H. Yamamoto, S.I. Hino, S. Ikeda, M. Kishida, and A. Kikuchi. 1999. DIX domains of dvl and axin are necessary for protein interactions and their ability to regulate beta-catenin stability. *Mol. Cell. Biol.* 19:4414–4422.

Knoblich, J.A., L.Y. Jan, and Y.N. Jan. 1997. The N terminus of the *Drosophila* Numb protein directs membrane association and actin-dependent asymmetric localization. *Proc. Natl. Acad. Sci. USA.* 94:13005–13010.

Kose, H., and T.L. Karr. 1995. Organization of *Wolbachia pipientis* in the *Drosophila* fertilized egg and embryo revealed by an anti-*Wolbachia* monoclonal antibody. *Mech. Dev.* 51:275–288.

Kraut, R., W. Chia, L.Y. Jan, Y.N. Jan, and J.A. Knoblich. 1996. Role of inscuteable in orienting asymmetric cell divisions in *Drosophila. Nature.* 383: 50–55.

Kuchinke, U., F. Grawe, and E. Knust. 1998. Control of spindle orientation in *Drosophila* by the Par-3-related PDZ-domain protein Bazooka. *Curr. Biol.* 8:1357–1365.

Morrison, E.E., B.N. Wardleworth, J.M. Askham, A.F. Markham, and D.M. Meredith. 1998. EB1, a protein which interacts with the APC tumor suppressor, is associated with the microtubule cytoskeleton throughout the cell cycle. *Oncogene.* 17:3471–3477.

Moser, A.R., A.R. Shoemaker, C.S. Connelly, L. Clipson, K.A. Gould, C. Luongo, W. Dove, P.H. Siggers, and R.L. Gardner. 1995. Homozygosity for the Min allele of Apc results in disruption of mouse development prior to gastrulation. *Dev. Dyn.* 203:422–433.

Muhua, L., N.R. Adames, M.D. Murphy, C.R. Shields, and J.A. Cooper. 1998. A cytokinesis checkpoint requiring the yeast homologue of an APC-binding protein. *Nature.* 393:487–491.

Munemitsu, S., B. Souza, O. Müller, I. Albert, B. Rubinfeld, and P. Polakis. 1994. The APC gene product associates with microtubules in vivo and promotes their assembly in vitro. *Cancer Res.* 54:3676–3681.

Nakagawa, H., Y. Murata, K. Koyama, A. Fujiyama, Y. Miyoshi, M. Monden, T. Akiyama, and Y. Nakamura. 1998. Identification of a brain-specific APC homologue, APCL, and its interaction with beta-catenin. *Cancer Res.* 58: 5176–5181.

Näthke, I.S., C.L. Adams, P. Polakis, J.H. Sellin, and W.J. Nelson. 1996. The adenomatous polyposis coli (APC) tumor suppressor protein localizes to plasma membrane sites involved in active cell migration. *J. Cell Biol.* 134: 165–180.

Pai, L.-M., C. Kirkpatrick, J. Blanton, H. Oda, M. Takeichi, and M. Peifer. 1996. *Drosophila* α-catenin and E-cadherin bind to distinct regions of *Drosophila* Armadillo. *J. Biol. Chem.* 271:32411–32420.

Pai, L.-M., S. Orsulic, A. Bejsovec, and M. Peifer. 1997. Negative regulation of Armadillo, a Wingless effector in *Drosophila. Development.* 124:2255–2266.

Peifer, M. 1993. The product of the *Drosophila* segment polarity gene *armadillo* is part of a multi-protein complex resembling the vertebrate adherens junction. *J. Cell Sci.* 105:993–1000.

Peifer, M., D. Sweeton, M. Casey, and E. Wieschaus. 1994. *wingless* signal and Zeste-white 3 kinase trigger opposing changes in the intracellular distribution of Armadillo. *Development.* 120:369–380.

Pereira, A.J., B. Dalby, R.J. Stewart, S.J. Doxsey, and L.S. Goldstein. 1997. Mitochondrial association of a plus end-directed microtubule motor expressed during mitosis in *Drosophila. J. Cell Biol.* 136:1081–1090.

Polakis, P. 1999. The oncogenic activation of β-catenin. *Curr. Opin. Genet. Dev.* 9:15–21.

Rocheleau, C.E., W.D. Downs, R. Lin, C. Wittmann, Y. Bei, Y.-H. Cha, M. Ali, J.R. Priess, and C.C. Mello. 1997. Wnt signaling and an APC-related gene specify endoderm in early *C. elegans* embryos. *Cell.* 90:707–716.

Rubinfeld, B., I. Albert, E. Porfiri, C. Fiol, S. Munemitsu, and P. Polakis. 1996. Binding of GSK-β to the APC/β-catenin complex and regulation of complex assembly. *Science.* 272:1023–1026.

Schlesinger, A., C.A. Shelton, J.N. Maloof, M. Meneghini, and B. Bowerman. 1999. Wnt pathway components orient a mitotic spindle in the early *Caenorhabditis elegans* embryo without requiring gene transcription in the responding cell. *Genes Dev.* 13:2028–2038.

Schwartz, K., K. Richards, and D. Botstein. 1997. BIM1 encodes a microtubule-binding protein in yeast. *Mol. Biol. Cell.* 8:2677–2691.

Shulman, J.M., N. Perrimon, and J.D. Axelrod. 1998. Frizzled signaling and the developmental control of cell polarity. *Trends Genet.* 14:452–458.

Siegfried, E., T.-B. Chou, and N. Perrimon. 1992. *wingless* signaling acts through zeste-white 3, the *Drosophila* homolog of glycogen synthase kinase-3, to regulate *engrailed* and establish cell fate. *Cell.* 71:1167–1179.

Smalley, M.J., E. Sara, H. Paterson, S. Naylor, D. Cook, H. Jayatilake, L.G. Fryer, L. Hutchinson, M.J. Fry, and T.C. Dale. 1999. Interaction of axin and Dvl-2 proteins regulates Dvl-2-stimulated TCF-dependent transcription. *EMBO (Eur. Mol. Biol. Organ.) J.* 18:2823–2835.

Smith, K.J., D.B. Levy, P. Maupin, T.D. Pollard, B. Vogelstein, and K.W. Kinzler. 1994. Wild-type but not mutant APC associates with the microtubule cytoskeleton. *Cancer Res.* 54:3672–3675.

Su, L.K., M. Burrell, D.E. Hill, J. Gyuris, R. Brent, R. Wiltshire, J. Trent, B. Vogelstein, and K.W. Kinzler. 1995. APC binds to the novel protein EB1. *Cancer Res.* 55:2972–2977.

Tepass, U., and E. Knust. 1990. Phenotypic and developmental analysis of mutations at the *crumbs* locus, a gene required for the development of epithelia in *Drosophila melanogaster. Roux's Arch. Dev. Biol.* 199:189–206.

Thorpe, C.J., A. Schlesinger, J.C. Carter, and B. Bowerman. 1997. Wnt signaling polarizes an early *C. elegans* blastomere to distinguish endoderm from mesoderm. *Cell.* 90:695–705.

Tomlinson, A., W.R. Strapps, and J. Heemskerk. 1997. Linking Frizzled and Wnt signaling in *Drosophila* development. *Development.* 124:4515–4521.

Turner, C.M., and P.N. Adler. 1998. Distinct roles for the actin and microtubule cytoskeletons in the morphogenesis of epidermal hairs during wing development in *Drosophila. Mech. Dev.* 70:181–192.

van Es, J.H., C. Kirkpatrick, M. van de Wetering, M. Molenaar, A. Miles, J. Kuipers, O. Destrée, M. Peifer, and H. Clevers. 1999. Identification of APC2, a homologue of the adenomatous polyposis coli tumour suppressor. *Curr. Biol.* 9:105–108.

Vleminckx, K., E. Wong, K. Guger, B. Rubinfeld, P. Polakis, and B.M. Gumbiner. 1997. Adenomatous polyposis tumor suppressor protein has signaling activity in *Xenopus* embryos resulting in the induction of an ectopic dorsoanterior axis. *J. Cell Biol.* 136:411–420.

Waddle, J.A., J.A. Cooper, and R.H. Waterston. 1994. Transient localized accumulation of actin in *Caenorhabditis elegans* blastomeres with oriented asymmetric divisions. *Development.* 120:2317–2328.

Wieschaus, E., and C. Nüsslein-Volhard. 1986. Looking at embryos. *In Drosophila*, A Practical Approach. D.B. Roberts, editor. IRL Press, Oxford, UK. 199–228.

Wong, L.L., and P.N. Adler. 1993. Tissue polarity genes of *Drosophila* regulate the subcellular location for prehair initiation in pupal wing cells. *J. Cell Biol.* 123:209–221.

Reprint Series
3 March 2000, Volume 287, pp. 1606–1609

Science

Wnt Signaling in Oncogenesis and Embryogenesis—a Look Outside the Nucleus

Mark Peifer[1]* and Paul Polakis[2]

Wnt Signaling in Oncogenesis and Embryogenesis—a Look Outside the Nucleus

Mark Peifer[1]* and Paul Polakis[2]

The Wnt cell-cell signaling pathway plays a critical and evolutionarily conserved role in directing cell fates during embryogenesis. In addition, inappropriate activation of the Wnt signal transduction pathway plays a role in a variety of human cancers. Many recent studies of Wnt signaling have provided mechanistic insight into these dual roles. Here we focus on two areas of rapid advance: (i) the machinery that regulates the stability of the key signal transducer, β-catenin, and (ii) the effect of Wnt signaling on cellular targets outside the nucleus, the actin and microtubule cytoskeletons.

Some of the most profound questions in biology were first asked by ordinary people confronting events in their everyday lives. The miracle of a newborn baby raises questions about how an egg assembles itself into an animal. The tragedy of a cancer diagnosis leads to questions about how normal cells go wrong. Although seemingly distinct, biological processes like embryogenesis and carcinogenesis both rely on cell communication via identical signaling pathways. For example, in the larva of the fruit fly *Drosophila*, cells determine their position within each body segment by communicating with one another. One of the key signaling molecules is the secreted Wnt family protein Wingless (Wg), which acts as a "Be posterior" signal [reviewed in (*1*)]. Fate decisions require changes in gene expression; thus cells must transmit information from the cell surface to the nucleus.

Wnt signaling also regulates cell proliferation in adult tissues. The epithelial cells lining the colon provides an excellent illustration of this [reviewed in (*2*)]. Colonic cells proliferate at a rate that perfectly balances the death of cells due to attrition. Cells are sent signals to proliferate when appropriate, and when sufficient cell numbers are attained, proliferation is halted. Colon cancer, like other cancers, results in part from mutations that cause cells to receive a continuous signal to proliferate. Mutations can lock a signal transduction component in an ON position or can inactivate a protein that normally keeps the pathway in an OFF position. For example, in most colon cancers, a negative regulator of Wnt signal transduction, APC [the tumor suppressor protein encoded by the adenomatous polyposis coli (*APC*) gene], is inactivated, and the Wnt pathway is aberrantly turned on.

In this review we will summarize the current model for Wnt signal transduction and then discuss two particularly active areas of investigation: the critical role of regulated protein destruction in determining where the Wnt pathway is ON or OFF and cytoskeletal targets of the pathway. There are many other aspects of Wnt signaling that we will not cover; for a more comprehensive review see (*1*). Detailed information about Wnt signaling can also be found on the Wnt gene homepage (http://www.stanford.edu/~rnusse/wntwindow.html) and at the connections map at *Science*'s STKE Web site (http://www.stke.org).

A Model for Wnt Signaling

Wnt signaling is regulated by the presence or absence of the intracellular protein β-catenin [Fig. 1; reviewed in (*1*)]. A large multiprotein machine that includes proteins of the APC and Axin families normally facilitates the addition of phosphate groups to β-catenin by glycogen synthase kinase-3β (GSK3β). Phosphorylated β-catenin binds to a protein called βTrCP, and is then modified by the covalent addition of a small protein called ubiquitin. Proteins tagged with ubiquitin are degraded by the proteosome, the cell's protein-recycling center. When Wnt signal is absent, the signal transduction pathway is OFF because β-catenin is rapidly destroyed. When cells are exposed to Wnt, it binds to cell surface receptors of the Frizzled family. Receptor activation antagonizes the APC-Axin "destruction complex" by an unknown mechanism that requires Dishevelled protein. This blocks β-catenin phosphorylation and its subsequent ubiquitination. β-Catenin is thus diverted from the proteosome, and it accumulates and enters the nucleus, where it finds a partner, a DNA binding protein of the TCF/LEF family. Together, they activate new gene expression programs. In the embryonic skin of a fruit fly, Wg signal turns on genes conferring "posterior identity," whereas in human colon cancer cells, inappropriate activation of the Wnt pathway drives cell proliferation by turning on genes encoding oncoproteins and cell-cycle regulators. As discussed below, Wnt signals also regulate the polarity and function of both the actin and microtubule cytoskeletons.

The β-Catenin Destruction Complex

The tumor suppressor protein APC is a critical component of the β-catenin destruction machinery. APC is inactivated in most colorectal cancers, resulting in activation of the Wnt pathway. The Wnt pathway also plays a role in other cancers: for example, viral activation of *Wnt-1* causes mammary tumors in mice, and mutations that make β-catenin refractory to destruction are found in a variety of human tumors [reviewed in (*2*)]. Elucidation of the β-catenin destruction machinery may reveal how Wnt signaling regulates embryogenesis, and may uncover new oncogenes and tumor suppressors. Many proteins that work with APC in regulating β-catenin have been identified, including Axin, Dishevelled, GSK3β, β-TrCP, casein kinases 1ε and II, protein phosphatase-2A, and FRAT (frequently rearranged in advanced T cell lymphomas). These proteins all interact functionally or physically, but their specific roles in β-catenin regulation remain to be resolved.

A second key component of the destruction machinery is Axin [reviewed in (*2*)]. Mice lacking functional Axin have defects in development of the dorsal-ventral body axis similar to those elicited by Wnt overexpression in embryos of the frog, *Xenopus laevis*. In both *Xenopus* and mammalian cells, Axin and its paralog Conductin/Axil destabilize β-catenin, thus negatively regulating Wnt signaling (*3–6*). Axin and APC physically interact. The binding site in Axin is in its RGS (regulator of G protein signaling) domain. The RGS domain binds to three copies of a short protein motif in APC known as the SAMP repeat (*4*, *6*). The truncated APC proteins found in most colon cancers lack these SAMP repeats and thus cannot bind Axin.

[1]Department of Biology and Lineberger Comprehensive Cancer Center, University of North Carolina at Chapel Hill, Chapel Hill, NC 27599–3280, USA. [2]Genentech, 1 DNA Way, Mail Stop #40, S. San Francisco, CA 94080, USA.

*To whom correspondence should be addressed. E-mail: peifer@unc.edu

Likewise, APC protein fragments that destabilize β-catenin in cultured cells contain both β-catenin and Axin binding sites [reviewed in (*2*)]. It has been hypothesized that the truncation of APC observed in cancer may be driven by selection against Axin's ability to bind APC. Consistent with this idea, mice carrying truncating mutations in *APC* that remove the Axin binding sites develop colon tumors at a high frequency [reviewed in (*2*)], whereas mice carrying truncating *APC* mutations that retain an Axin binding site do not develop tumors (*7*).

Why is the physical interaction between APC and Axin so critical to β-catenin regulation? This issue is far from clear, as conflicting data have emerged from studies of different animal models. In *Xenopus*, Axin mutants lacking the RGS domain not only fail to inhibit Wnt signaling but they act positively, promoting dorsal axis duplication. This is consistent with an obligate role of APC binding in Axin-mediated destruction of β-catenin [reviewed in (*2*)]. In contrast, mammalian Axin mutants lacking the RGS domain still destabilize β-catenin in cultured cells (*4*–*6*, *8*, *9*). Similarly, *Drosophila* Axin lacking the RGS domain inhibits Wg signaling when ectopically expressed (*10*). One interpretation is that APC stimulates or localizes Axin by binding to its RGS domain; overexpression of Axin mutants lacking this domain might overcome the requirement for APC. The differences observed in *Xenopus* could relate to relative expression levels. Consistent with the hypothesis that APC family members localize the destruction complex, a mutation in *Drosophila* APC2 that disrupts its cortical localization also disrupts its function (*11*). Whereas most data suggest that APC negatively regulates Wnt signaling, experiments with *Xenopus* and the nematode *Caenorhabditis elegans* suggest that APC may also play an unexpected positive role in Wnt signaling [reviewed in (*2*)].

The APC-Axin complex is thought to modulate activity of the serine/threonine kinase GSK3β. Mutation of the GSK3β homolog in *Drosophila* and expression of dominant-negative GSK3β in *Xenopus* activate Wnt signaling [reviewed in (*1*)], suggesting that Wnt signaling inhibits GSK3β (Fig. 1). One substrate of GSK3β is β-catenin. The GSK3β phosphorylation sites of β-catenin are mutated in tumors; these mutations stabilize β-catenin [reviewed in (*2*)]. Although β-catenin is a poor GSK3β substrate in vitro, β-catenin phosphorylation is significantly enhanced when a fragment of Axin containing β-catenin and GSK3β binding sites is included in the reaction (*3*, *4*, *12*). Thus, Axin may serve as a scaffold on which both GSK3β and β-catenin reside, facilitating their interaction (Fig. 2). Both APC [reviewed in (*2*)] and Axin (*12*) are also GSK3β substrates and their ability to bind β-catenin in vitro is enhanced by phosphorylation. Wnt signaling in mammalian cells leads to Axin dephosphorylation, as does incubation of cells with LiCl, a GSK3β inhibitor (*12*, *13*). The mechanism by which Wnt signaling "turns off" GSK3β remains unclear. In fruit flies, at least, Dishevelled is critical for this. Recent demonstrations that Dishevelled is part of the "destruction complex" (*8*, *9*, *14*) and binds directly to Axin, may provide the first mechanistic clue. Other proteins such as FRAT, which binds GSK3β and Dishevelled and which antagonizes GSK3β function when ectopically expressed (*14*), may also play a role.

Phosphorylation by GSK3β is critical to β-catenin destruction. Other proteins are targeted for ubiquitination—and thus destruction—by phosphorylation. Sites for this phosphorylation have been mapped in some, such as the nuclear factor kappa B (NF-κB) regulator IκB. IκB and β-catenin share sequence similarity within the region required in both proteins for destruction. This is reminiscent of the situation in yeast, where the stability of certain proteins is regulated by E3 ubiquitin ligases that only recognize their substrates when phosphorylated. F-box proteins act as the recognition subunits. Mutation of the *Drosophila* F-box protein Slimb stabilizes the fruit fly β-catenin homolog (*15*), leading to speculation that Slimb and its human homolog β-TrCP form part of an F-box–containing ubiquitin ligase targeting phosphorylated β-catenin. This hypothesis has now been experimentally verified (*16*–*18*). β-Catenin binds β-TrCP only when phosphorylated by GSK3β, and oncogenic β-catenin mutants that lack GSK3β phosphorylation sites do not bind β-TrCP. Further, overexpression of a β-TrCP derivative lacking the F-box activates β-catenin–dependent gene expression. Studies with *Xenopus* embryos are also consistent with a role for β-TrCP as a negative regulator of β-catenin signaling (*19*). Thus β-TrCP is the penultimate stop on β-catenin's trip to the proteosome. These observations explain how oncogenic mutants of β-catenin avoid the proteosome and continue to signal.

Although this may seem complex enough, other protein players continue to be identified. Where there are kinases, there must be phosphatases. Wnt signal triggers Axin dephosphorylation, thus reducing its ability to bind β-catenin and trigger its destruction (*12*). The protein phosphatase PP2A dephosphorylates Axin in vitro, and the PP2A inhibitor okadaic acid blocks Wnt-mediated Axin dephosphorylation in mammalian cells, suggesting that PP2A may regulate β-catenin stability in response to Wnt signaling (*12*).

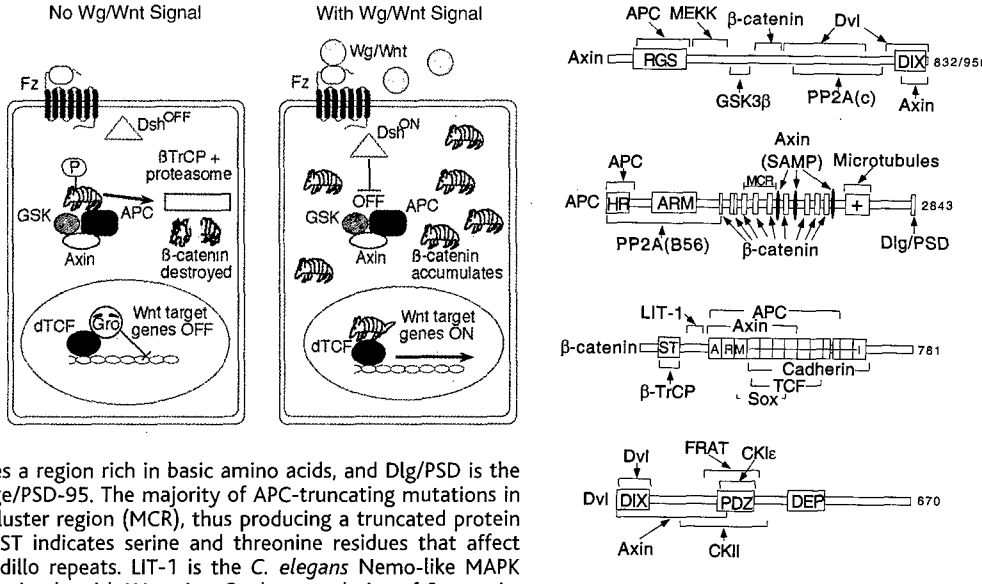

Fig. 1 (left). The Wingless/Wnt signaling pathway. Schematic summary of the response of a cell to Wg signal. See text for details. The icon for β-catenin, an armadillo, is based on the name of its fruit fly homolog. **Fig. 2 (right).** Linear representation of Axin, APC, β-catenin, and Dishevelled (Dvl), with the approximate locations of the binding sites for various protein partners indicated with arrows. The length of each polypeptide in amino acids is shown to the right. Two numbering conventions have been adopted for Axin, as the initiation codon has not been identified. In Axin, the DIX domain is a domain shared with Dishevelled. In APC, HR is heptad repeat, ARM indicates seven Armadillo repeats (a motif first found in the fruit fly β-catenin homolog Armadillo), + indicates a region rich in basic amino acids, and Dlg/PSD is the binding site for the PDZ protein Discs large/PSD-95. The majority of APC-truncating mutations in colon cancer occur within the mutation cluster region (MCR), thus producing a truncated protein lacking Axin binding sites. In β-catenin, ST indicates serine and threonine residues that affect protein stability; ARM indicates 12 Armadillo repeats. LIT-1 is the *C. elegans* Nemo-like MAPK homolog; its binding has been demonstrated only with Wrm-1, a *C. elegans* relative of β-catenin. Dishevelled has three recognizable domains: a DIX domain shared with Axin, a PDZ domain, and a DEP (Dishevelled, EGL-10, pleckstrin) domain.

PP2A's catalytic subunit binds directly to Axin; its B56 regulatory subunit interacts with APC (*20, 21*). Overexpression of the B56 subunit downregulates β-catenin protein levels and Wnt signaling (*21*). Finally, the Aβ regulatory subunit of PP2A is mutated in a subset of primary colon tumors (*22*). It remains problematic that PP2A's effect on Wnt-triggered Axin dephosphorylation is consistent with a positive role in regulating the Wnt pathway, whereas the downregulation of β-catenin by the B56 subunit is consistent with a negative role.

More recently, another serine/threonine kinase, casein kinase 1ε (CK1ε), entered the fray. CK1ε can stabilize β-catenin and thus activate Wnt-target genes, and dominant negative forms of CK1ε inhibit Wnt signaling (*23, 24*). CK1ε has been placed downstream of Dishevelled and upstream of GSK3β, although biochemical analysis suggests that it binds directly to Dishevelled's PDZ region (Fig. 2). Dishevelled is phosphorylated when coexpressed with CK1ε, implicating it as a possible target. Thus, CK1ε has the hallmarks of a Wnt signaling molecule and may represent a missing link between the Wnt receptor and β-catenin stabilization. Axin also binds a third serine/threonine kinase, the MAP kinase kinase MEKK1 [Fig. 2 (*25*)].

The APC-Axin Complex—Some Assembly Required

When considering the numerous interactions reported to occur within the APC-Axin complex (Fig. 2), one is confronted with many potential models for complex assembly and mechanisms of action. APC binds directly to itself, β-catenin [reviewed in (*2*)], Axin (*4, 6, 18, 26*), and the PP2A B56 subunit (*21*), whereas Axin binds directly to itself (*5, 8, 20*), APC, β-catenin, GSK3β (*3, 4, 6, 27*), the PP2A catalytic subunit (*20*), and Dishevelled (*8, 9, 14*). In turn, Dishevelled binds to itself (*8*), Axin, CK1ε (*23, 24*), and FRAT (*14*). Moreover, β-catenin can bind β-TrCP while associated with the APC-Axin complex (*16*). Given this complexity, it is clear that linear models for signaling are not appropriate.

How might things work? The binding of APC to the Axin-GSK3β complex could promote APC phosphorylation and thus increase its affinity for β-catenin. This might allow proper presentation of β-catenin to GSK3β, resulting in its efficient phosphorylation and subsequent binding to β-TrCP. Upon activation by Wnt, CK1ε might phosphorylate Dishevelled, resulting in the displacement of FRAT from Dishevelled, thereby positioning FRAT to inhibit the GSK3β that is associated with Axin. These models are consistent with the literature, but so are many others. There are also unsolved mysteries: for example, what is the link between the destruction machinery and Wnt receptors? Perhaps we are still missing a G protein. After all, Frizzled proteins distantly resemble G protein–coupled receptors, Axin harbors an RGS domain, and Dishevelled contains a DEP (Dishevelled, EGL-10, pleckstrin) domain, which is also present in certain RGS proteins. However, researchers looking for a G protein connection to Wnt-1 signaling have so far come up empty-handed, though Wnt-5A may utilize one. A related mystery is the intracellular localization of the destruction complex. Is it assembled adjacent to the Frizzled receptor? Finally, thus far only APC and β-catenin have been found mutated in primary human tumors. Mutations in other destruction complex components may also be uncovered in cancer.

All Roads Do Not Lead to the Nucleus

Extracellular signals clearly affect gene expression, and they also induce changes in cell shape, in cell-cell interactions, and in cell migration. Many of these effects are mediated by the cytoskeleton. Wnt signals affect both the actin and microtubule cytoskeletons. The effect on the actin cytoskeleton occurs in epithelial cells, which possess two sorts of cell polarity. Apical-basal polarity distinguishes the top and bottom surfaces of the cell sheet; planar polarity allows cells to determine directions in the plane of the sheet, providing compass coordinates as on a map. Wnt signaling regulates planar polarity (Fig. 3A) [reviewed in (*28*)]. For example, the hexagonal cells of a fruit fly wing each secrete a single hair, an actin-filled plasma membrane projection. All hairs extend distally from the distal cell vertex. Certain mutations disrupt planar polarity, so that cells polymerize actin at random locations, thereby randomizing the position and direction of wing hairs. Two planar polarity genes encode the most upstream known components of the Wg pathway: Frizzled, a Wg receptor, and Dishevelled, which acts just downstream.

An alternative signal pathway appears to mediate the effects of Wnts on planar polarity (Fig. 3C) [reviewed in (*29*)]. Genetic epistasis experiments suggest that the small guanosine triphosphatase Rho, and a kinase cascade including Misshapen (a Ste20 homolog), JNKK, and JNK (the JNK pathway) act downstream of Frizzled in planar polarity. Furthermore, Dishevelled can activate JNK (*30, 31*), suggesting that there is a branchpoint at Dishevelled, with one branch leading to the canonical Wg pathway and regulating cell fate, and the other leading to the JNK pathway and regulating planar polarity. The discovery that Axin overexpression stimulates JNK signaling (*25*) suggests that Dishevelled may work with Axin in this process. Loss-of-function mutations in JNKK and JNK do not affect planar polarity directly (*30*), suggesting that other MAPK proteins play a redundant role in the process. Candidate genes have been identified in *C. elegans*: one encodes a MAPKKK related to vertebrate TAK1, and the other encodes a divergent MAPK family member related to *Drosophila* Nemo (*32–35*). These kinases are required for Wnt signaling but are postulated to act in a pathway parallel to the traditional Wnt pathway. TAK1 and Nemo thus could be part of an alternative kinase pathway that operates in planar polarity.

In the simplest model, Frizzled receptors could activate the canonical Wnt pathway in some tissues and the JNK pathway in others. This could occur if different Frizzled family receptors used specific signal transduction pathways. However, *Drosophila* Frizzled, originally implicated in planar polarity, acts upstream of Armadillo, the β-catenin homolog, in the embryonic epidermis and central nervous system (*36–40*), implying that individual receptors can act through either

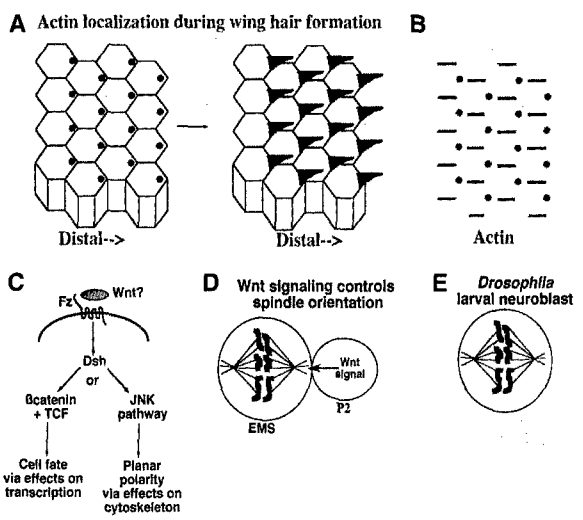

Fig. 3. Wingless/Wnt signaling directly regulates the cytoskeleton. (**A**) In tissue polarity, Wnt signaling directs polymerization of the actin cytoskeleton at particular positions on the cell cortex with respect to the animal's body axes. (**B**) Flamingo protein is enriched on particular sides of the cell and thus may mark the side of the cell where actin polymerization should be directed. (**C**) Model in which Dishevelled acts as a branchpoint, with different signal transduction pathways activated to modulate cell fate choices or to regulate planar polarity. (**D**) Wnt signaling directs the positioning of the cell's mitotic spindle in both early *C. elegans* embryos (this example) and *Drosophila* sensory cells. (**E**) dAPC2 localizes to a crescent in larval neuroblasts undergoing an asymmetric cell division. This crescent localizes with one pole of the spindle.

pathway. One remaining question is which Wnt, if any, is involved in planar polarity.

Other fruit fly proteins required for planar polarity are not obviously connected to Wg signaling. Most encode novel proteins with recognizable motifs but without homologs of known function: for example, Strabismus and Fuzzy are transmembrane proteins [reviewed in (*28*)], and Prickle has multiple Lim domains (*41*). These proteins may be the effector machinery activated by Wnt signaling to alter actin polymerization. The discovery of Flamingo (also known as Starry Night) (*42–44*) may reveal new insight. Flamingo's extracellular domain resembles that of the cadherins, a family of cell adhesion molecules, and Flamingo can mediate cell-cell adhesion in culture. COOH-terminal to Flamingo's cadherin repeats is an apparent G protein–coupled receptor domain, distantly resembling Frizzled family receptors. Perhaps most intriguing is Flamingo's subcellular localization. Before the initiation of planar polarity, it is found uniformly around the cell cortex. However, as planar polarity is being established, Flamingo becomes preferentially localized to the faces of the cell where actin polymerization will occur (Fig. 3B). It thus may mark those cell surfaces, distinguishing them from the others. Both genetic and cell biological tests suggest that Flamingo acts downstream of Frizzled. It could couple Wnt signal to cytoskeletal rearrangements, marking a site on the cell cortex where actin should polymerize.

Another possible effector that may couple Wnt signaling to actin rearrangement is the APC relative *Drosophila* APC2 (dAPC2). dAPC2 colocalizes with actin and is found in cell-cell adherens junctions of polarized cells (*11*, *45*). dAPC2 colocalizes with actin during assembly of the embryonic denticle (*11*), an actin-based structure similar to the developing wing hair. Thus dAPC2 is properly positioned to influence actin polymerization. However, a role for it or other APC proteins in planar polarity remains to be tested.

Wnt signaling also affects positioning of the mitotic spindle. Certain cells divide with a fixed orientation relative to the body axes of the animal, requiring that the mitotic spindle be properly oriented. In both *C. elegans* and *Drosophila* this process can be directed by Wnt signaling. During division of an early embryonic cell in *C. elegans* called EMS (Fig. 3D) [reviewed in (*46*)], the mitotic spindle is oriented by contact with a neighboring cell, P2, such that one pole is directed toward the signaling cell. The polarizing signal is thought to be a Wnt molecule acting via a Frizzled receptor. Wnt signaling directly affects the cytoskeleton (*47*): inhibition of transcription does not block spindle positioning, indicating that this effect does not require activation of Wnt target genes. In *C. elegans*, Frizzled and GSK3β homologs are essential for spindle orientation (*47*), whereas in fruit flies Frizzled and Dishevelled are essential (*48*). In contrast, double-stranded RNA inhibition of the *C. elegans* β-catenin relative Wrm-1 or of the distant APC relative APR-1 does not block spindle orientation, nor do mutations in the Wnt *mom-2* or the TCF relative *pop-1*. One interpretation of these data is that there is a branch in the pathway at GSK3β, with one pathway affecting gene regulation and the other influencing spindle orientation. However, differences in the genetic circuitry and divergence in the sequences of Wrm-1 and Apr-1 relative to their homologs suggest that the nematode pathway may be mechanistically different than that in mammals or fruit flies, so this may not apply to other animals. Regardless, because Dishevelled, GSK3β, and APC can all reside in the same protein complex (see above), output from this complex may affect signaling to both the nucleus and to the cytoskeleton.

The mechanism by which Wnt regulates spindle positioning remains to be determined. One possibility is that APC plays a role: mammalian APC binds and bundles microtubules in vitro, and in migrating cultured cells it localizes to spots at the plasma membrane where bundles of microtubules terminate [reviewed in (*49*)]. Further, in dividing stem cells of the *Drosophila* brain, dAPC2 localizes asymmetrically within the cell to a crescent adjacent to one spindle pole (*11*) (Fig. 3E). The functional significance of this localization remains to be tested. The cadherin-relative Flamingo is also required for spindle orientation in neural precursors (*43*), suggesting that it mediates the effects of Wnt signaling on both the actin and the microtubule cytoskeletons.

In summary, investigation of the Wnt signaling pathway has revealed insights into both embryogenesis and oncogenesis. Many challenges remain. We now have an outline of how this critical pathway operates, but fleshing out the precise mechanisms involved will occupy us for years to come.

References and Notes

1. A. Wodarz and R. Nusse, *Annu. Rev. Cell Dev. Biol.* **14**, 59 (1998).
2. P. Polakis, *Curr. Opin. Genet. Dev.* **9**, 15 (1999).
3. S. Ikeda *et al.*, *EMBO J.* **17**, 1371 (1998).
4. M. J. Hart, R. de los Santos, I. N. Albert, B. Rubinfeld, P. Polakis, *Curr. Biol.* **8**, 573 (1998).
5. C. Sakanaka and L. T. Williams, *J. Biol. Chem.* **274**, 14090 (1999).
6. J. Behrens *et al.*, *Science* **280**, 596 (1998).
7. R. Smits *et al.*, *Genes Dev.* **13**, 1309 (1999).
8. S. Kishida *et al.*, *Mol. Cell. Biol.* **19**, 4414 (1999).
9. M. J. Smalley *et al.*, *EMBO J.* **18**, 2823 (1999).
10. K. Willert, C. Y. Logan, A. Arora, M. Fish, R. Nusse, *Development* **126**, 4165 (1999).
11. B. M. McCartney *et al.*, *J. Cell Biol.* **146**, 1303 (1999).
12. K. Willert, S. Shibamoto, R. Nusse, *Genes Dev.* **13**, 1768 (1999).
13. H. Yamamoto *et al.*, *J. Biol. Chem.* **274**, 10681 (1999).
14. L. Li *et al.*, *EMBO J.* **18**, 4233 (1999).
15. J. Jiang and G. Struhl, *Nature* **391**, 493 (1998).
16. M. Hart *et al.*, *Curr. Biol.* **9**, 207 (1999).
17. M. Kitagawa *et al.*, *EMBO J.* **18**, 2401 (1999).
18. C. Liu *et al.*, *Proc. Natl. Acad. Sci. U.S.A.* **96**, 6273 (1999).
19. Y. Marikawa and R. P. Elinson, *Mech. Dev.* **77**, 75 (1998).
20. W. Hsu, L. Zeng, F. Costantini, *J. Biol. Chem.* **274**, 3439 (1999).
21. J. M. Seeling *et al.*, *Science* **283**, 2089 (1999).
22. S. S. Wang *et al.*, *Science* **282**, 284 (1998).
23. J. M. Peters, R. M. McKay, J. P. McKay, J. M. Graff, *Nature* **401**, 345 (1999).
24. C. Sakanaka, P. Leong, L. Xu, S. D. Harrison, L. T. Williams, *Proc. Natl. Acad. Sci. U.S.A.* **96**, 12548 (1999).
25. Y. Zhang, S. Y. Neo, X. Wang, J. Han, S. C. Lin, *J. Biol. Chem.* **274**, 35247 (1999).
26. S. Kishida *et al.*, *J. Biol. Chem.* **273**, 10823 (1998).
27. C. Sakanaka, J. B. Weiss, L. T. Williams, *Proc. Natl. Acad. Sci. U.S.A.* **95**, 3020 (1998).
28. J. M. Shulman, N. Perrimon, J. D. Axelrod, *Trends Genet.* **14**, 452 (1998).
29. M. Boutros and M. Mlodzik, *Mech. Dev.* **83**, 27 (1999).
30. M. Boutros, N. Paricio, D. I. Strutt, M. Mlodzik, *Cell* **94**, 109 (1998).
31. L. Li *et al.*, *J. Biol. Chem.* **274**, 129 (1999).
32. M. D. Meneghini *et al.*, *Nature* **399**, 793 (1999).
33. T. Ishitani *et al.*, *Nature* **399**, 798 (1999).
34. C. E. Rocheleau *et al.*, *Cell* **97**, 717 (1999).
35. T. H. Shin *et al.*, *Mol. Cell* **4**, 275 (1999).
36. K. M. Bhat, *Cell* **95**, 1027 (1998).
37. J. R. Kennerdell and R. W. Carthew, *Cell* **95**, 1017 (1998).
38. H. Muller, R. Samanta, E. Wieschaus, *Development* **126**, 577 (1999).
39. P. Bhanot *et al.*, *Development* **126**, 4175 (1999).
40. C. Chen and G. Struhl, *Development* **126**, 5441 (1999).
41. D. Gubb *et al.*, *Genes Dev.* **13**, 2315 (1999).
42. T. Usui *et al.*, *Cell* **98**, 585 (1999).
43. B. Lu, T. Usui, T. Uemura, L. Jan, Y. N. Jan, *Curr. Biol.* **9**, 1247 (1999).
44. J. Chae *et al.*, *Development* **126**, 5421 (1999).
45. X. Yu, L. Waltzer, M. Bienz, *Nature Cell Biol.* **1**, 144 (1999).
46. B. Bowerman, C. A. Shelton, *Curr. Opin. Genet. Dev.* **9**, 390 (1999).
47. A. Schlesinger, C. A. Shelton, J. N. Maloof, M. Meneghini, B. Bowerman, *Genes Dev.* **13**, 2028 (1999).
48. M. Gho and F. Schweisguth, *Nature* **393**, 178 (1998).
49. A. I. Barth, I. S. Nathke, W. J. Nelson, *Curr. Opin. Cell Biol.* **9**, 683 (1997).

50. Work in the Peifer lab is funded by the NIH, the Army Breast Cancer Research Program, and the Human Frontiers Science Program. We regret that editorial policy precluded us from providing a more comprehensive list of primary references.